University of Southern Denmark

Master's Thesis

Feasibility Study of Sustainable Jet Fuel Production on Funen

University	*University of Southern Denmark*
Faculty	*Faculty of Engineering*
Project Period	*1st of February - 3rd of June 2019*
Project Supervisors	*Henrik Wenzel and Anders Winther Mortensen*

Rune Dal Andersen

Exam number: 69092313

Date: 03/06-19

Rune Kvols Rasmussen

Exam number: 65008953

Date: 03/06-19

UNIVERSITY OF SOUTHERN DENMARK

Abstract

Feasibility Study of Sustainable Jet Fuel Production on Funen

This project analyzes a few potential pathways based on biogas for the production of sustainable jet fuel, and a case study of the feasibility of implementing one of them for the production of sustainable jet fuel on Funen, Denmark. The main pathways which are analyzed are the Fischer-Tropsch pathway, the methanol pathway and a pathway based on the Oxidative Coupling of Methane. The project includes a screening of the technology options available in each of the unique process segments of the pathways, where their advantages and disadvantages are discussed. Additionally, Sankey diagrams with energy flows of the potential pathways are constructed, and differences between central and decentral jet fuel production are discussed. Based on the aforementioned analysis, the central low-temperature Fischer-Tropsh pathway with an iron-based catalyst is chosen for the case study of jet fuel production on Funen, Denmark. In this pathway, 15 PJ of biogas is converted to 6.04 PJ of jet fuel and 3.63 PJ of gasoline, as well as additional co-products. For the case study three scenarios for the GTL plant are established. In one of the scenarios the biogas is unsubsidized making the biomethane input price 146.9 DKK/GJ for the GTL plant. With this biomethane price the plant is not feasible, with an NPV result of -5.68 billion DKK. In two other scenarios where the biogas is subsidized, the biomethane input prices are 54.4 DKK/GJ and 82.3 DKK/GJ, and the GTL plant turns out to be feasible with NPVs of 6.36 billion DKK and 2.95 billion DKK respectively. The highest biomethane input price for a feasible GTL plant is found to be 106.4 DKK/GJ. At this input price, the biogas would need to be subsidized by 40.5 DKK/GJ. Furthermore the necessary jet fuel sales price for a scenario with no subsidies on biogas is found to be 348.7 DKK/GJ for the plant to become feasible.

Contents

List of Figures

List of Tables

Nomenclature

List of Abbreviations

Co-LTFT	A Low Temperature Fischer-Tropsch Process with a Cobalt-based Catalyst
CTL	Coal-to-Liquid
DEA	Danish Energy Agency
DME	Dimethyl Ether
Fe-HTFT	A High Temperature Fischer-Tropsch Process with an Iron-based Catalyst
Fe-LTFT	A Low Temperature Fischer-Tropsch Process with an Iron-based Catalyst
FT	Fischer-Tropsch
GTL	Gas-to-Liquid
HTFT	High-Temperature Fischer-Tropsch
LNG	Liquified Natural Gas
LPG	Liquified Petroleum Gas
LTFT	Low-Temperature Fischer-Tropsch
MOGD	Mobil Olefin to Gasoline and Distillate
MTG	Methanol-to-Gasoline
MTO	Methanol-to-Olefin
NPV	Net Present Value
PSA	Pressure Swing Adsorption
SNG	Synthetic Natural Gas
syncrude	Synthetic Crude Oil
syngas	Synthesis Gas
TIGAS	Topsoe Improved Gasoline Synthesis
XTL	X-to-Liquid
ZSM	Zeolite Socony Mobil

Chapter 1

Introduction

With an increased global recognition of climate change being a consequence of greenhouse gas emissions from human activities, many governments worldwide have committed themselves to emission reduction goals in an attempt to limit the climate impacts. The European Union has a goal of reducing its internal greenhouse gas emissions by 40% compared to 1990 before 2030, while Denmark has a national goal of being entirely independent of fossil fuels in 2050 (The Ministry of Energy, Utilities and Climate 2019).

Achieving such a goal calls for a restructuring of large parts of the Danish energy system, as everything has been built with a focus on fossil fuels as the major energy source. The main idea for restructuring the energy system is to electrify where electrification is possible. Although electrification is a viable solution for a large part of the energy system, there are problems in the transport sector due to the low energy density of batteries. While batteries are sufficient for running lighter vehicles, they are as of today still not energy dense enough to run heavy transport such as trucks, aircrafts and ships. Especially for aviation, it is difficult to find a sustainable fuel due to its strict performance requirements (Mathiesen et al. 2014).

1.1 Potential Aviation Solutions

Several potential solutions to powering the aviation sector in a sustainable way have been suggested and researched in recent years. Some provide a completely new take on aircraft technology, introducing new designs of aircrafts and their way of being powered, whilst other solutions seek to emulate fossil fuels to directly replace them in the existing aircraft fleet. Among the first category of solutions are electrical aircrafts with batteries. Even though electrical aircrafts are not viable today, they have the potential to be a part of the overall solution in powering the aviation sector in a sustainable way in the future. For instance, in Norway there is a goal of using only electrical aircrafts for the domestic routes before 2040 (Avinor 2014).

However, sustainable aviation solutions that can be used for e.g. transatlantic flights are more likely to be found in the latter category of potential solutions, and these solutions are already technologically

available today. Here, sustainable fuels are being developed to have the same properties as fossil fuels and are able to directly replace them in existing aircraft. Such fuels are collectively known as synthetic fuels, or synfuels, and can be produced in numerous ways. The ways showing the most potential are synfuels derived from bio-organic sources, however, using carbon and hydrogen from alternative sources is also a way which shows great potential for the future, and which can reduce the dependency on bio-sources (Mathiesen et al. 2014).

At the time of writing, several synfuels have already been approved for use in commercial flights as a partial substitute for the regularly used Jet A1 fuel. The ASTM D7566 standard, Standard Specification for Aviation Turbine Fuel Containing Synthesized Hydrocarbons, lists five production methods which are approved for the production of synthetic jet fuels, as of may 2019 (ASTM 2019). These are:

1. Fischer-Tropsch Hydroprocessed Synthesized Paraffinic Kerosene (FT-SPK)
2. Synthesized Paraffinic Kerosene from Hydroprocessed Esters and Fatty Acids (SPK-HEFA)
3. Synthesized Iso-Paraffins from Hydroprocessed Fermented Sugars (SIP)
4. Synthesized Kerosene with Aromatics Derived by Alkylation of Light Aromatics from Non-Petroleum Sources (SPK/A)
5. Alcohol-to-Jet Synthetic Paraffinic Kerosene (ATJ-SPK)

1.2 Biogas for Synthetic Fuels in Denmark

Of the aforementioned methods, method 1, 4 and 5 can be used to produce jet fuel from biogas. Producing synthetic jet fuel from biogas might a good idea, as there are several benefits to the use of biogas. The main benefit is that the production and use of biogas provides and excellent link between the agricultural sector, and the heat, electricity and transport sectors.

Biogas is ideally produced through anaerobic digestion of animal manure and waste products, e.g. straw from corn production, wastewater sludge and organic food waste, utilizing an otherwise lost potential. Energy crops can also be included in the anaerobic digestion, however, the growth of energy crops requires a use of land, making the use of energy crops not as ideal as the use of the aforementioned waste products.

The use of the waste products from mainly the agricultural sector comes with additional benefits. These include the degassing of manure so that fewer greenhouse gases are released into the air, as well as making the nutrients in the manure more easily accessible for the crops, without reducing the amount of carbon which is returned to the soil notably (DEA 2014, 2013). Additionally, the use of biogas substitutes a use of fossil fuels, reducing greenhouse gas emissions even further both directly

and indirectly (DEA 2018*b*). Finally, biogas can be used for several purposes, e.g. it can be stored for use in gas turbines as a back-up for the electricity and heating sectors, or used to produce fuels for the transport sector (DEA 2016*b*).

1.3 The Goals of This Project

This project seeks to conduct a screening of a few potential pathways for the production of synthetic jet fuel based on biogas, which are not necessarily approved yet. The goal of the screening is to show the different technology options available for each of the unique segments of the pathways, describe how they work and discuss their advantages and disadvantages, as well as to discuss economic considerations for the pathways. Additionally, the study seeks to construct Sankey diagrams of the pathways to show the differences between the full pathways on primarily an energy basis.

Finally, the project seeks to conduct a case study of the production of synthetic jet fuel on Funen, Denmark. The case study seeks to include considerations regarding the technical solution, considerations regarding the incorporation of this production in the Funish energy system, and economic considerations for the business model of the production. This production of sustainable jet fuel should be ready to go on stream in 2025, and should be considered a pilot project for a larger effort to make Denmark self-suppliant in sustainable jet fuel some time before 2050. As such, the project mainly focuses on the pilot project for 2025, but it also presents some considerations regarding the larger effort towards 2050.

1.4 Reading Guide

The report began with an introduction to the problem which this project works on. This introduction was followed by a presentation of the goals of the project.

In the following chapter, Chapter 2, an introduction to each unique process segment of the considered pathways is given. The chapter begins with an introduction to the chapter, where the considered pathways are presented. Then each unique process segment is presented in Section 2.1 through Section 2.9, with references to expanded screenings in the appendix. It is presented how the technologies work and what their advantages and disadvantages are, as well as some overall economic considerations for the technologies. If the reader is already knowledgeable about some of the technologies, the respective sections of the report can be skipped.

In Chapter 3, Sankey diagrams of the potential pathways are constructed. The chapter begins with an estimation of the amount of biogas available in 2025 in Section 3.1, which is followed by an introduction to the methodology behind the creation of the Sankey diagrams, and a presentation of the efficiency values used for each technology option in Section 3.2. Afterwards, six potential pathways are presented

and discussed in Section 3.3. Finally, some additional considerations regarding the differences between central and decentral production of jet fuel are discussed in Section 3.4.

In Chapter 4, a case study of a production of jet fuel on Funen, Denmark in 2025 is presented. The case study begins with considerations regarding an ideal plant location in Section 4.1. These considerations are followed by considerations regarding the amount of recoverable heat that a plant would be able to sell to the district heating grid in Section 4.2. After these considerations have been completed, a Base Scenario for the case study is defined in Section 4.3. In this section, all costs and revenues of the plant in the case study are presented. An Net Present Value calculation of the Base Scenario is presented in Section 4.3.3. After the Base Scenario has been defined, sensitivity analysis is conducted on several parameters in Section 4.4 through Section 4.6. A final discussion of the results is had in Section 4.7.

In Chapter 5, a final conclusion of the report is reached. The report ends with some final considerations regarding a vision of Denmark being self suppliant in sustainable jet fuel by 2050 in Chapter 6.

Chapter 2

Introduction of Pathways

The focus of this project is the potential pathways from biogas to jet fuel. There are two main pathways which are analyzed, where the first is based on the Fischer-Tropsch (FT) technology, and the second is based on methanol as an intermediate product. A third pathway, which is related to the methanol pathway, is through the Oxidative Coupling of Methane (OCM) process. This pathway is also presented, but only lightly discussed in relation to the methanol pathway.

An overview of the analyzed pathways and their relevant process segments can be seen in Figure 2.1. Each box in the figure represents a process segment and is referred to as a segment throughout the project, e.g. the process box with syngas production is referred to as the syngas production segment. Throughout Chapter 2, Figure 2.1 is shown with a red ring highlighting which process segment that is introduced in that section of the chapter.

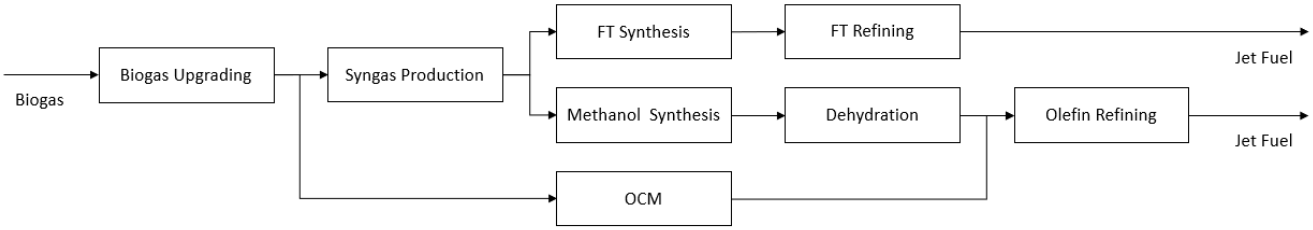

FIGURE 2.1: An overview of the unique process segments that are a part of the analyzed pathways. Each of the three pathways can be seen as the arrows moving through the segments from left to right, going through the FT synthesis, methanol synthesis and OCM segments, respectively.

The FT pathway consists of a biogas upgrading segment, a syngas production segment, a FT synthesis segment, and a FT refining segment. The methanol pathway also consists of a biogas upgrading segment and a syngas production segment, then a methanol synthesis segment, a methanol dehydration segment and an olefin refining segment. The OCM pathway consists of a biogas upgrading segment, an OCM process segment and an olefin refining segment. For the FT and methanol pathways, the biogas only has to be upgraded if the gas needs to be transported through the natural gas grid before utilization in a gas-to-liquids (GTL) plant. For the OCM pathway, the biogas always has to be upgraded.

Throughout this chapter, each unique process segment is introduced with references to more expanded descriptions of some of the technologies in the appendix. It is explained how the technologies work and what some key considerations for the different technologies are.

2.1 Biogas Upgrading

Biogas can be used directly in a GTL plant, however, when biogas is needed in processes that do not happen at the location of the biogas plant, it will often be necessary to send the gas through the natural gas grid. Biogas does not fulfill the requirements of a gas that is allowed to enter the natural gas grid though. It needs to be cleaned for impurities, commonly referred to as upgraded, before it can enter. The requirements for gas to enter the natural gas grid can be seen in Appendix A. The major impurity which has to be removed from the biogas if it should have sufficient quality for the natural gas grid is carbon dioxide (CO_2). As such, the focus in this section is put on CO_2 removal and not on the removal of any other impurities.

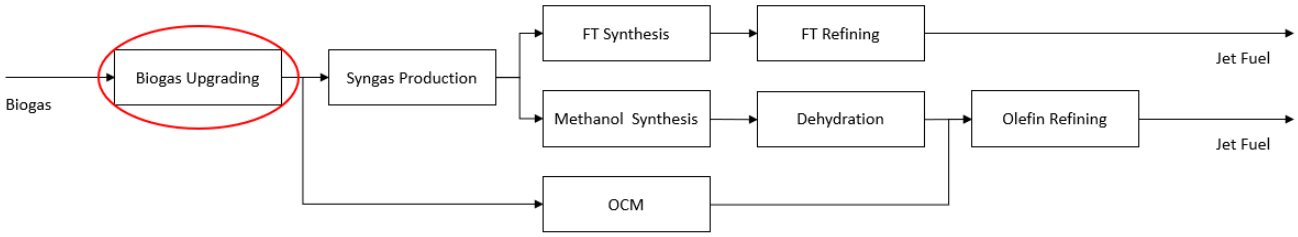

FIGURE 2.2: The overview of the pathways and the unique process segments. This section contains a short description of biogas upgrading.

The upgrading of biogas can be done through both separation and methanation. In this section both separation and methanation is introduced generally, with references to descriptions of specific technologies and their advantages and disadvantages in the appendix. Additionally, the economy of separation and methanation is discussed.

2.1.1 Separation

One way of removing the CO_2 from the biogas, is by separating the CO_2 from the methane. This can be done through multiple different technologies. The three technologies that are mainly used in Denmark are water scrubbing, chemical scrubbing and membrane separation, however both pressure swing adsorption and organic physical scrubbing have a noticeable share when looking at the global market (Danish Gas Technology Centre 2018, Hjuler & Aryal 2017). Choosing a separation technology today should mainly rely on the OPEX and CAPEX of the plant as the different technologies all have

proven to have a low methane loss as well as a high methane purity (Angelidaki et al. 2018). Six separation technologies are described in Appendix B with Tables B.1 to B.6 showing their pros and cons.

2.1.1.1 Economy of Separation

In Bauer et al. (2013) a comprehensive scrutiny of biogas upgrading through the use of different technologies have been made, including an analysis of the economy of investing in each technology. In Figure 2.3 the specific investment cost as a function of the plant size in Nm^3/h is shown. The specific investment cost of each technology follows the same pattern of being much cheaper per capacity as the size of the plant increases.

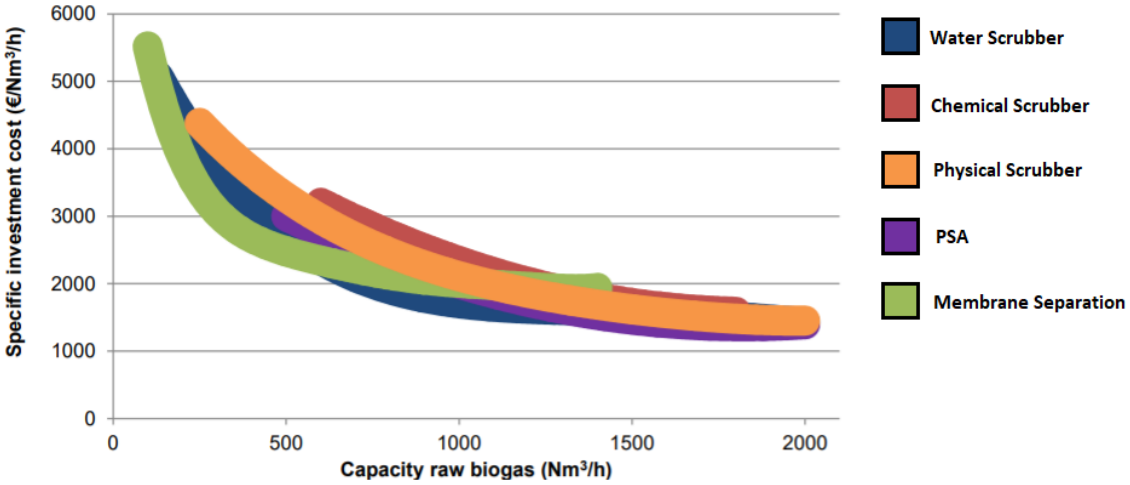

FIGURE 2.3: The specific investment cost for different types of upgrading units. Source: (Bauer et al. 2013).

A more recent estimation made by the Danish Gas Technology Centre covered both CAPEX and OPEX of the three mainly used technologies in Denmark. Their results are shown in Figure 2.4 as costs per upgraded Nm^3 methane.

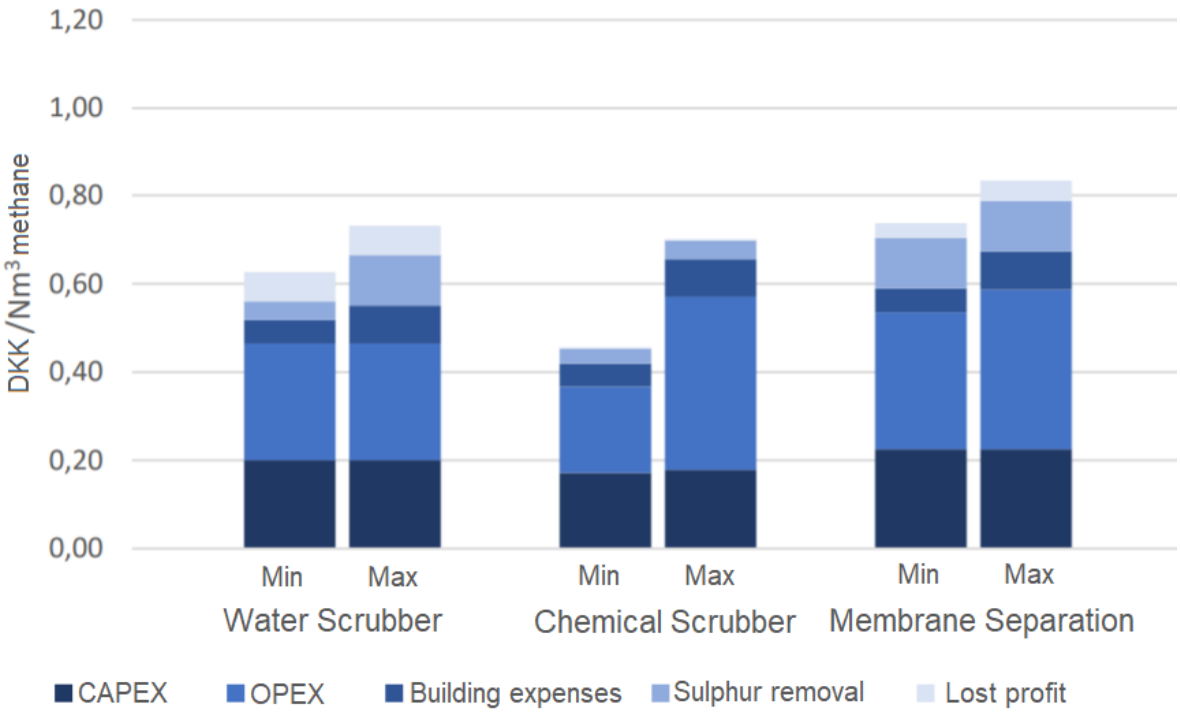

FIGURE 2.4: The cost of upgrading biogas to biomethane per 1 Nm^3 biomethane for plants that have a 1500 Nm^3/h capacity. Covering the three most employed technologies in Denmark: a water scrubber, a chemical scrubber and a membrane separation plant. Source: (Danish Gas Technology Centre 2018).

They estimated that a plant with 1500 Nm^3/h capacity will cost 0.35-0.60 DKK/Nm^3 with an extra cost of 0.10-0.20 DKK/Nm^3 for sulphur removal. The chemical scrubber has the potential of having a reduced overall cost, depending on how well the excess heat from the process is reused (Danish Gas Technology Centre 2018).

2.1.2 Methanation

Another way to upgrade biogas is through the use of hydrogen (H_2) in methanation. This can be done both in a biological way and a chemical way. Methanation happens through Equation (2.1) (Lecker et al. 2017):

$$CO_2 + 4\,H_2 \longrightarrow CH_4 + 2\,H_2O \tag{2.1}$$

Equation (2.1) is often referred to as a combination of Equation (2.2) and Equation (2.3).

$$CO_2 + H_2 \longrightarrow CO + H_2O \tag{2.2}$$

$$CO + 3\,H_2 \longrightarrow CH_4 + H_2O \tag{2.3}$$

While Equation (2.2) is the reverse water-gas shift reaction, both Equation (2.1) and Equation (2.3) are in the literature referred to as the Sabatier reaction (Sveinbjörnsson & Münster 2017, Lecker et al. 2017).

For biogas upgrading, methanation has the advantage of using CO_2 to produce an extra amount of methane, thus it achieves a higher amount of useful methane and it does not emit CO_2 as a biogas separation unit does. In a theoretical situation with 100% methanation efficiency, all the CO_2 would be converted to methane. The amount of CO_2 in the biogas depends on the type of biomass input to the digestor plant where the biogas is produced and the composition of biogas can therefore vary.

Methanation is also a relevant technology for energy storage. By using hydrogen produced in an electrolysis plant to do methanation, electric energy can be stored as methane and injected into the natural gas grid. As an electrolysis plant often has a flexible production, depending on electricity prices, there is often a need for hydrogen storage between the electrolyser and methanation plant, as methanation normally has a less flexible production. The different technologies for hydrogen storage and electrolysis are not analyzed in this project. However a small discussion on the economy of electrolysis is had in Section 2.1.2.1. Biological and chemical methanation is described and their differences elaborated upon in Appendix B.2.

2.1.2.1 Economy of Methanation

A very limited amount of large-scale methanation plants have been made, which makes the exact costs of a plant hard to estimate. For chemical methanation, Outotec GmbH reported investment costs of 400 €/kW synthetic natural gas (SNG) for a 5 MW plant and 130 €/kW SNG for a 110 MW plant back in 2014, while other sources reported investment costs of up to 1500 €/kW SNG (Götz et al. 2016). In the technology catalogue from the Danish Energy Agency and Energinet the investment cost for chemical methanation is in 2020 expected to be 910 €/kW SNG (DEA, Energinet 2019). Data about the economy of biological methanation is scarce, but in literature it has both been concluded that biological methanation is cheaper and more expensive than chemical methanation, depending on the source. Even though there are large uncertainties, smaller plants seem to be more in favor of biological methanation while larger plants seem to favor chemical methanation economically (GRTgaz 2014, Götz et al. 2016).

To do methanation the hydrogen needed would have to come from somewhere, which would probably be an electrolysis plant. However the cost of building an electrolysis plant is a larger expense than the methanation plant itself. The investment cost for an electrolysis plant is in Götz et al. (2016) reported to be in the range of 800-3000 €/kW electricity input. This equals an investment cost of the electrolysis

for a methanation plant of 1500-5500 €/kW SNG, when assuming an electrolysis efficiency of 70%, a methanation energy efficiency of 78% and immediate use of the hydrogen.

The largest cost for an electrolysis plant occurs during its operation and is the payment for electricity. This cost can vary a lot, depending on the exact hour, as the price of electricity has large fluctuations.

2.2 Synthesis Gas Production

The next unique process segment is the synthesis gas production segment. Synthesis gas, or syngas, is the input to both methanol and Fischer-Tropsch (FT) synthesis and the production of syngas is therefore an intermediate process in the conversion of biogas to jet fuel, as seen in Figure 2.5.

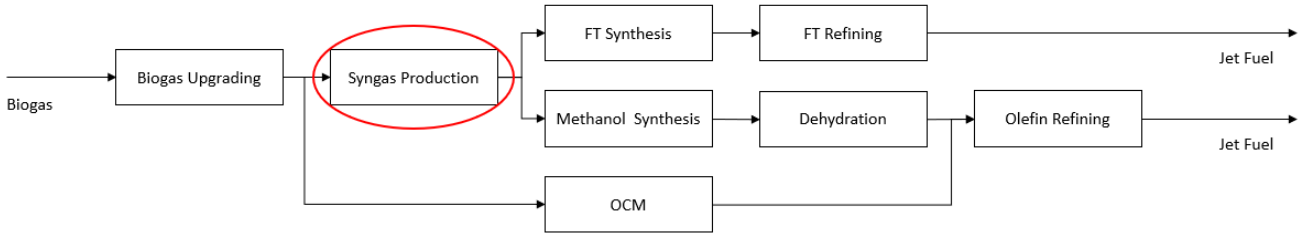

FIGURE 2.5: The overview of the pathways and the unique process segments. In this section, the technologies available for the syngas production segment are screened.

Syngas is a mixture of mainly H_2 and CO, with some impurities depending on the input to the syngas production. Syngas can be produced both from biogas and pure methane, and the technology selection depends both on the input, as well as the downstream syngas utilization. When syngas is produced from biogas, or in general when CO_2 is included with methane, it is important to select a technology that can convert both the CO_2 to CO and the CH_4 to CO and H_2 (Ashraf 2015).

Syngas production is the most expensive part of a gas-to-liquids (GTL) plant. There have therefore been created several technologies to produce syngas which are continuously improved, each with their own benefits. Three technologies have been screened, and an introduction to these and their characteristics can be seen in Appendix C. In this section, the main advantages and disadvantages are discussed.

2.2.1 Advantages and Disadvantages of Syngas Producing Technologies

Each of the screened syngas producing technologies have their advantages and disadvantages, and are most suitable for certain purposes in the industry. The focus here is on advantages and disadvantages relating to methanol and Fischer-Tropsch (FT) synthesis, with some focus on the current applications of the technologies in the industry today.

For steam reforming, the main advantage is that it has been used extensively in the industry compared to both autothermal reforming and partial oxidation, although mainly to produce hydrogen. Additionally, steam methane reforming does not require oxygen, which both autothermal reforming and partial oxidation do (Maitlis & de Klerk 2013). As previously mentioned, syngas production is typically the most expensive process in a GTL plant, and even more so, when air separation to produce pure oxygen is required (Bertau et al. 2014, de Klerk 2011*a*). The main downside of steam methane reforming is that it has the highest methane slip and CO_2 emissions (Maitlis & de Klerk 2013). Additionally, the technology cannot be used alone, unless the H_2:CO ratio of the syngas is heavily adjusted using water gas shifting, or unless some H_2 is removed. Having to remove some H_2 is not necessarily a disadvantage though, as some H_2 is typically needed for the refining process of a GTL plant.

Autothermal reforming and partial oxidation generally have the same advantages and disadvantages. Both have more favorable H_2:CO ratios and lower methane slip than steam methane reforming. On the other hand, both usually require higher temperatures (Maitlis & de Klerk 2013).

One of the main considerations when choosing a syngas production technology for a methanol or FT process, is the required H_2:CO input of the process. For the optimal running of a methanol producing plant, the Stoichiometric Number (SN) should ideally be between 2.0-2.1 (Bertau et al. 2014). The Stoichiometric Number is defined as:

$$SN = (mol\ H_2 - mol\ CO_2)/(mol\ CO + mol\ CO_2) \tag{2.4}$$

For a FT based GTL plant, the ideal H_2:CO varies depending on the type of FT process that is employed. The FT process, including the ideal H_2:CO ratio, is described in depth in Appendix D, but in general the H_2:CO ratio should be roughly 2 for the FT process (de Klerk 2011*a*).

In Table 2.1, typical H_2:CO ratios and stoichiometric number values of the syngas produced by the different technologies can be seen.

Process	H_2:CO	SN
Steam Reforming	4-7	2.7-3.0
Autothermal Reforming	2.5-3.5	1.5-1.6
Partial Oxidation	1.6-1.9	1.5-1.6

TABLE 2.1: Typical H_2:CO ratios and stoichimetric numbers of the syngas from the syngas producing technologies (Bertau et al. 2014, de Klerk 2011*a*).

As can be seen from the table, the H_2:CO ratios and stoichiometric numbers of the syngas produced by the different technologies do not match the required input to the FT and the methanol processes, respectively. In practice, for large-scale plants, a single syngas producing technology is rarely used. Instead, a combination is usually employed. This is done both to achieve the ideal H_2:CO ratio or stoichiometric number and to allow some flexibility, and to reap additional benefits from each technology.

The most commonly employed combination in the industry, is the combination of a steam reformer and an autothermal reformer (de Klerk 2011*a*, Bertau et al. 2014).

2.3 Fischer-Tropsch Synthesis

In the FT pathway, the next process segment after the syngas production segment is the FT synthesis segment, as shown in Figure 2.6. In this section, an introduction to the segment is given, and a more thorough screening can be found in Appendix D.1.

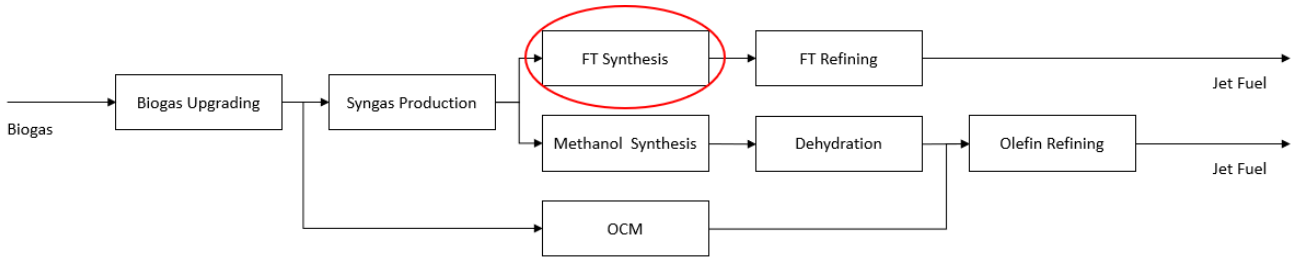

FIGURE 2.6: The overview of the pathways and the unique process segments. In this section, the FT synthesis segment is introduced.

FT synthesis is not a single process but refers to the overall process of catalytically converting syngas into a mixture of primary products, mainly linear hydrocarbons, and secondary products, including branched chain and cyclic aliphatic hydrocarbons as well as some aromatics and oxygenates. The mixture of products produced by FT synthesis is collectively known as Synthetic Crude Oil, or syncrude, due to its comparability to conventional crude oil. The FT process can to a satisfactory degree be described by the following reaction equations (Spivey et al. 2010).

- The formation of alkanes:

$$(2\,\mathrm{n}+1)\,\mathrm{H_2} + \mathrm{nCO} \longrightarrow \mathrm{C}_n\mathrm{H}_{2n+2} + \mathrm{nH_2O} \tag{2.5}$$

- The formation of alkenes:

$$2\,\mathrm{nH_2} + \mathrm{nCO} \longrightarrow \mathrm{C}_n\mathrm{H}_{2n} + \mathrm{nH_2O} \tag{2.6}$$

- The formation of oxygenates:

$$2\,\mathrm{nH_2} + \mathrm{nCO} \longrightarrow \mathrm{C}_n\mathrm{H}_{2n+2}\mathrm{O} + (n-1)\,\mathrm{H_2O} \tag{2.7}$$

- The formation of aldehydes and ketones:

$$(2\,n-1)\,\mathrm{H_2} + \mathrm{nCO} \longrightarrow \mathrm{C}_n\mathrm{H}_{2n}\mathrm{O} + (n-1)\,\mathrm{H_2O} \tag{2.8}$$

- The formation of carboxylic acids and esters:

$$(2\,n-2)\,\mathrm{H_2} + \mathrm{nCO} \longrightarrow \mathrm{C}_n\mathrm{H}_{2n}\mathrm{O_2} + (n-2)\,\mathrm{H_2O} \tag{2.9}$$

The value of n can be be from one to over 100 and denotes that the reactions occur to produce hydrocarbons of many different lengths. FT synthesis processes produce hydrocarbons with a distributed carbon length. The main factors that influence the product of the FT synthesis are the catalyst and operating conditions.

As mentioned, the FT process is catalytic. As of 2010, the only employed catalysts in the large-scale FT industry are iron-based (Fe) catalysts and cobalt-based (Co) catalysts (Spivey et al. 2010, de Klerk 2011*a*). One of the main differences between these two types of catalysts is that the Co-based catalysts are more hydrogenating than Fe-based catalysts, making the syncrude more paraffinic for the Co-based catalyst, and more olifinic for the Fe-based catalyst. Another difference is that Fe-based catalysts are water gas shift active, while the Co-based are not. A final point worth mentioning is that the Fe-based catalyst is generally cheaper and easier to handle, whereas the Co-based catalyst has a longer lifetime (Spivey et al. 2010, Maitlis & de Klerk 2013). For a screening of the catalysts, see Appendix D.1.1.

For the operating conditions, the most important is the temperature. FT processes are usually divided into low-temperature FT (LTFT) processes at 170-230 °C and high-temperature FT (HTFT) processes at 250-340 °C. The main difference between the two, is that the HTFT processes generally produce shorter hydrocarbons than the LTFT processes (de Klerk 2011*a*). For a screening of the effect of the temperature, as well as the pressure, space velocity and H_2:CO ratio of the syngas input on the process, see Appendix D.1.2.

2.4 Fischer-Tropsch Synthetic Crude Oil Refining

In the FT pathway, the final segment after the FT synthesis segment is the FT refining segment, as seen in Figure 2.7. In this section an introduction to the FT refining segment is given. A screening of the segment can be found Appendix D.2.

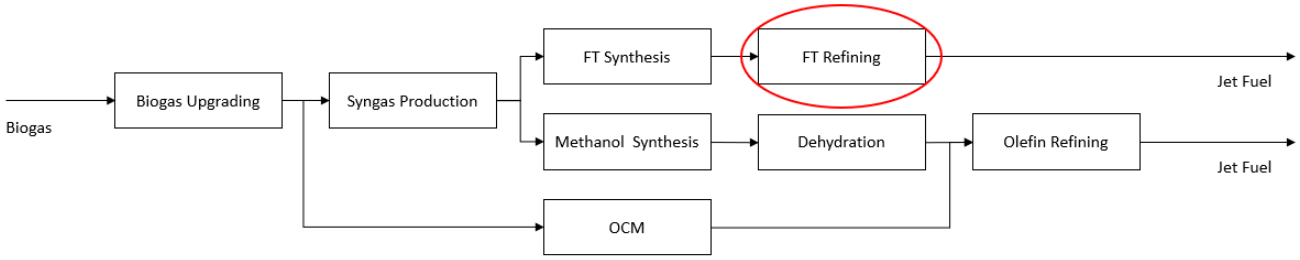

FIGURE 2.7: The overview of the pathways and the unique process segments. In this section, an introduction to the FT refining segment is given.

Jet fuel is mainly in the carbon range of n-C_{10} to n-C_{16}. This interval is set by the standard specifications that jet fuel must live up to (de Klerk 2011*a*, de Klerk 2011*b*). For an expanded description of these chemical specifications, see Appendix D.2.1. As the hydrocarbons generally have to be in the aforementioned range, most of the syncrude product from the FT process must be refined. There are mainly five technologies which are used in FT refining. These are aromatic alkylation, oligomerization, hydrotreating, aromatization and hydrocracking/hydroisomerization. Generally, hydrocarbons that are shorter than C_{10} are oligomerized to increase their length and hydrocarbons that are longer than C_{16} are hydrocracked to reduce their length. The remaining refining techniques are used to improve the properties of the hydrocarbons (de Klerk 2011*a*). A more thorough description of the refining techniques can be found in Appendix D.2.2.

2.5 Economy of Fischer-Tropsch GTL Plants

This section presents some considerations regarding the economics of FT based GTL plants. Traditionally, this type of plants have been of a world-scale size with gas inputs in the order of gigawatts. In the last decade, more and more technology developers have emerged that offer small-scale GTL technologies. However, as small-scale plants have not yet been commercially established for a long enough period of time to provide data on their economics, this section focuses on the economics of large-scale FT based GTL plants.

2.5.1 Investment Costs

World-scale GTL plants are huge and very expensive, often requiring investments in the billions of US dollars. The relative cost of the different parts of a such plant can be seen in Figure 2.8.

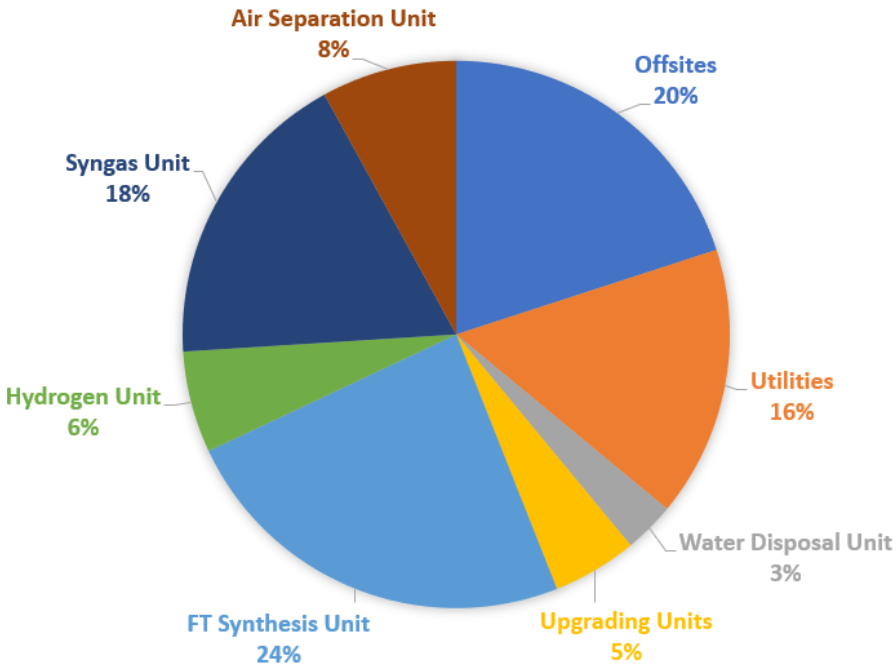

FIGURE 2.8: Relative investment costs of different parts of a FT based GTL plant (Maitlis & de Klerk 2013).

In this figure, the air separation unit and syngas unit can be seen as the cost of the segment of the plant for syngas production, the FT synthesis unit as the main segment of the plant where the syncrude is produced, and the upgrading units as the refining segment of the plant. The two main takeaways from the figure are that the syngas production segment is generally the most expensive part of a FT bases GTL plant, and that the refining segment is relatively cheap (Maitlis & de Klerk 2013).

As there are only a few commercial GTL plants in the world, the amount of economic data from the industry is small. Of the existing plants, it has been possible to find an investment cost in U.S. Dollars per barrel per day (USD/bpd) for five of them. The capacity of these plants and their investment costs can be seen in Table 2.2.

Plant	Capacity (bpd)	Investment Cost (USD)	Cost (USD/bpd)	Source
Mossel Bay GTL	33,000	2.4bn	72,727	(de Klerk 2011*a*)
Bintulu GTL	12,500	850m	68,000	(de Klerk 2011*a*, Rapier 2010)
Oryx GTL	34,000	1.2bn	35,294	(de Klerk 2011*a*, Maitlis & de Klerk 2013, Enerdata 2014)
Escravos GTL	34,000	9.5bn	279,411	(Maitlis & de Klerk 2013, Enerdata 2014)
Pearl GTL	260,000	19bn	73,076	(de Klerk 2011*a*, Maitlis & de Klerk 2013, Enerdata 2014)

TABLE 2.2: An overview of the size and cost of GTL plants where the data is available.

There are two points which are worth mentioning regarding these costs. The first is that both the Mossel Bay GTL and Pearl GTL plants do not process only FT based fuels, but also associated natural gas liquid (NGL) products. For the Mossel Bay GTL plant, the 33,000 bpd total is split into 10,500 bpd from the NGL segment, and 22,500 bpd from the FT segment (de Klerk 2011*a*). For the Pearl GTL plant,

the 260,000 bpd total is split into 120,000 bpd from the NGL segment and 140,000 bpd from the FT segment.

The second point worth mentioning is regarding the Oryx and Escravos GTL plants. The Oryx GTL plant was build first, and the Escravos GTL plant was designed to be a clone of this, raising questions about the huge price difference between the two. Oryx GTL began its operation during the planning of the Escravos GTL, and the Oryx GTL plant had several start-up problems which took years to solve. This may be a part of the explanation for the big difference in price (de Klerk 2011*a*).

Finally, a few remarks regarding small-scale GTL plants. The design of a small-scale GTL plant differs greatly from that of a world-scale plant. A small-scale GTL plant will not be able to benefit from economies of scale to the same degree as larger plants, if any at all, but the design requirements for a small-scale plant are different and present alternative solutions that can exploit other opportunities to be cost effective. The main advantage that small-scale GTL plants have over large-scale GTL plants, is the reduced risk of investment. Investing in a large-scale GTL project that ends up failing could set the investor back billions in US dollars, whereas the failure of a small-scale GTL plant would be much less severe (Maitlis & de Klerk 2013).

2.5.2 Operation and Maintenance Costs

Typical relative operation costs, excluding the cost of the feed, of a GTL plant can be seen in Figure 2.9.

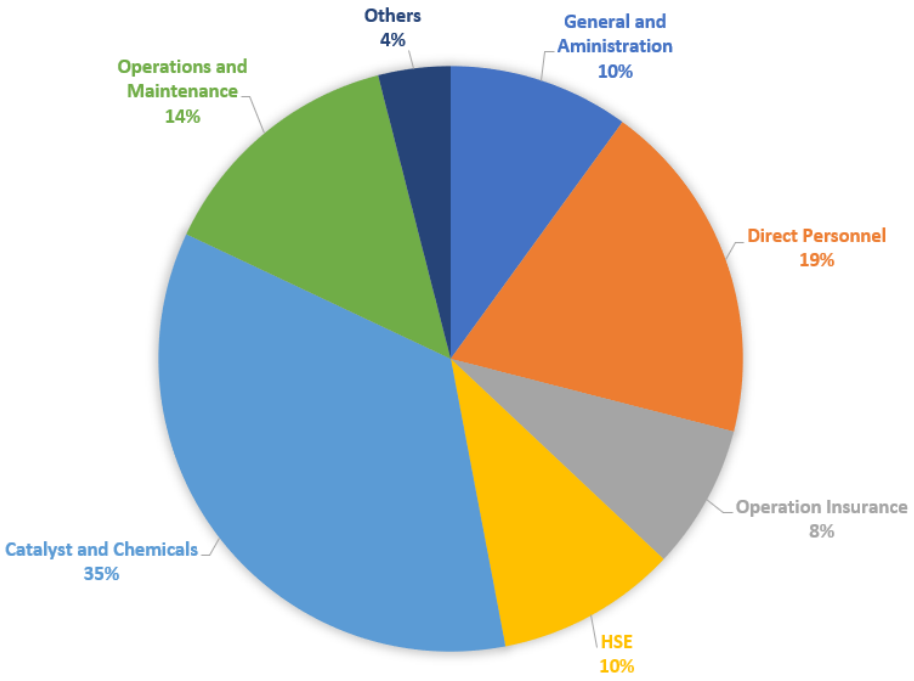

FIGURE 2.9: Relative operation and maintenance costs, excluding the feed, of a FT based GTL plant (Maitlis & de Klerk 2013).

As can be seen, the biggest operation expenses of a FT based GTL plant are for the chemicals and catalysts used in the process, as well as the handling of these, when excluding the feed expense.

The largest expense for a GTL plant is for the feed gas. The feed cost is especially important in relation to the cost of crude oil, and the products produced. When looking at a plant with a natural gas feed which produces synthetic crude oil, the plant must be able to synthesize the crude oil from natural gas at a cost lower than the price difference between natural gas and crude oil, otherwise the GTL plant will not be profitable. As such, increases in the price of the feed or reductions in the price of crude oil, and the relationship between these two is one of the main factors affecting the economics of a GTL plant (Maitlis & de Klerk 2013).

2.6 Methanol Synthesis

An alternative pathway to the FT pathway is the methanol pathway. In the methanol pathway, the next step after the syngas production segment is the methanol synthesis segment, as seen in Figure 2.10. In this section, an introduction to the methanol synthesis process is given.

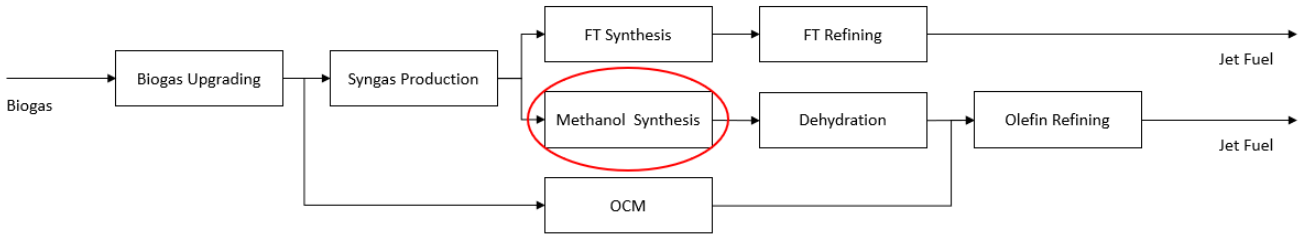

FIGURE 2.10: The overview of the pathways and the unique process segments. In this section, the methanol synthesis segment is introduced.

The production of methanol from syngas can be described by the following reaction equations (Bertau et al. 2014):

$$CO + H_2 \longrightarrow CH_3OH \tag{2.10}$$

$$CO_2 + 3\,H_2 \longrightarrow CH_3OH + H_2 \tag{2.11}$$

$$CO + H_2O \longrightarrow CO_2 + H_2 \tag{2.12}$$

The methanol synthesis process is a catalytic process, and the catalysts employed are generally based on copper (Cu) with some zinc (Zn) and aluminum (Al). The process is highly exothermic and usually

takes place at a temperature between 220-280 °C and 50-100 bars of pressure (Bertau et al. 2014). For a more thorough screening of the methanol synthesis segment, see Appendix E.1.

2.7 Dehydration of Methanol to Light Olefins

Methanol, and other alcohols such as ethanol and various isomers of butanol, can be used to produce jet fuel through a refining process where it is first dehydrated to light olefins, then oligomerized to heavier olefins, and finally hydrogenated to paraffins mainly in the jet fuel range.

As such, the next step in the methanol pathway after the methanol synthesis segment is the methanol dehydration segment, as seen in Figure 2.11. In this section, the methanol dehydration segment is introduced.

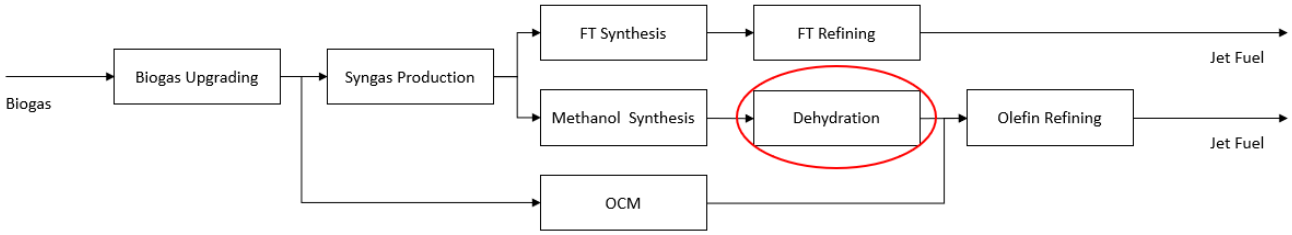

FIGURE 2.11: The overview of the pathways and the unique process segments. In this section, the methanol dehydration segment is introduced.

The process of dehydrating methanol is most commonly known as a Methanol-to-Olefins (MTO) process (Tabak & Yurchak 1990, Bertau et al. 2014). Overall, the process of converting methanol to olefins can be described by the following reactions:

$$2\,CH_3OH \longrightarrow CH_3OCH_3 + H_2O \longrightarrow (CH_2)_2 + 2\,H_2O \tag{2.13}$$

The process is catalytic and can take place over a wide variety of catalysts. Originally, the process was developed over the ZSM-5 catalyst. The process is exothermic and is usually operated at between 400-550 °C and 1-5 bar (Tabak & Yurchak 1990, Bertau et al. 2014). For an expanded introduction to the MTO-process, see Appendix E.3.

2.8 Oxidative Coupling of Methane to Light Olefins

Before presenting the next step in the methanol pathway, an alternative technology to reach light olefins, which could revolutionize the GTL industry, is here presented. The production of syngas from methane is a very costly process, and is considered to constitute up towards 60% of the investment cost of a methanol synthesis plant. Therefore, it is also most of the total cost of a methanol based GTL plant (Bertau et al. 2014). For this reason, much research has been conducted to find a way to avoid this costly step. One way that has received attention is the oxidative coupling of methane (OCM), which can seen in a pathway context in Figure 2.12.

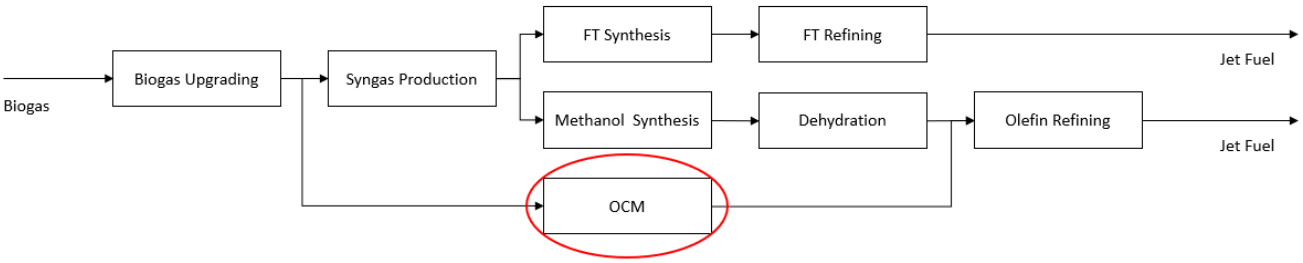

FIGURE 2.12: The overview of the pathways and the unique process segments. In this section, the OCM segment is briefly presented.

The chemical reaction was discovered in the 1980's but it has not been possible to commercialize it successfully. Atleast not until recently, where Siluria and Linde Engineering in 2014 partnered up to create the first commercial process converting methane directly into ethylene in a single step. Siluria has done the research into and provides the catalyst, whilst Linde Engineering provides the reactor technology around it (Linde Engineering 2019*a*, Siluria 2019).

The OCM reaction can be described by Equation (2.14), however, in reality several more reactions occur in the OCM process.

$$2\,CH_4 + O_2 \longrightarrow C_2H_4 + 2\,H_2O \tag{2.14}$$

This process produces ethylene directly from methane, and thus skips both the syngas production segment, the methanol synthesis segment and the methanol dehydration segment, but instead has the OCM segment, when compared to the methanol pathway. The technology has been proven with a 400 tonne ethylene per year demonstration plant, and the next step by the developers is to include customers for plants in the size of 30 to 1000 kilotonnes ethylene per year (Linde Engineering 2019*b*). With further development and upscaling of the technology, it may provide an efficient way to produce fuels from methane, both economically and technically, in the near future.

2.9 Refining and Upgrading of Light Olefins to Fuel Products

The final segment of both the methanol and the OCM pathway, is the olefin refining segment, as seen in Figure 2.13.

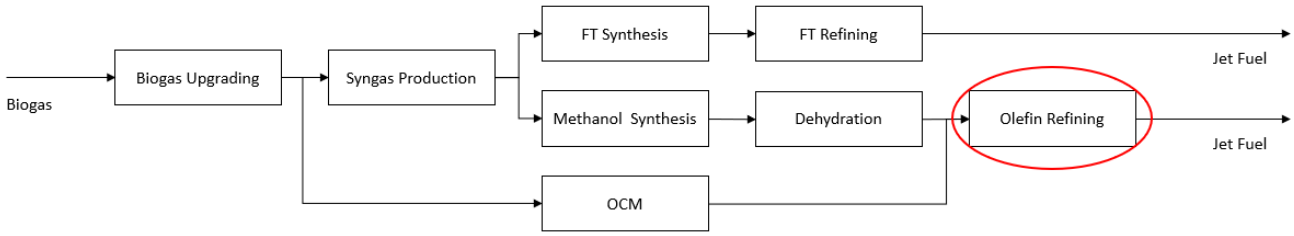

FIGURE 2.13: The overview of the pathways and the unique process segments. In this section, the olefin refining segment is introduced.

In the production of fuels from light olefins, the light olefins are first oligomerized to produce heavier olefins and then hydrotreated to create final products. The general methodology towards jet fuel refining was described in Section 2.4. A description of all the relevant refining techniques is given in Appendix D.2.2, while a more thorough description of the oligomerization process can be found in Appendix E.4.

2.10 Economy of Methanol GTL plants

For the methanol pathway, many points regarding the economy are the same as for the FT pathway. The cost of the syngas production segment of a FT based GTL plant is very high, and this is even more so the case of a methanol based GTL plant. For a methanol producing plant, the syngas production segment can cost up towards 60% of the investment cost (Bertau et al. 2014). Additionally, the economy of a methanol plant also largely depends on the price of the feed. In Bertau et al. (2014) an economic analysis of a 5000 metric tonnes per day methanol plant as if it was located in the U.S. Gulf Coast Region is presented. Here, a cost of 208 USD per tonne of methanol is estimated, with 46% of the cost being the cost of the natural gas feed to the plant. The correlation between the cost of producing methanol and the feed cost can be seen in Figure 2.14.

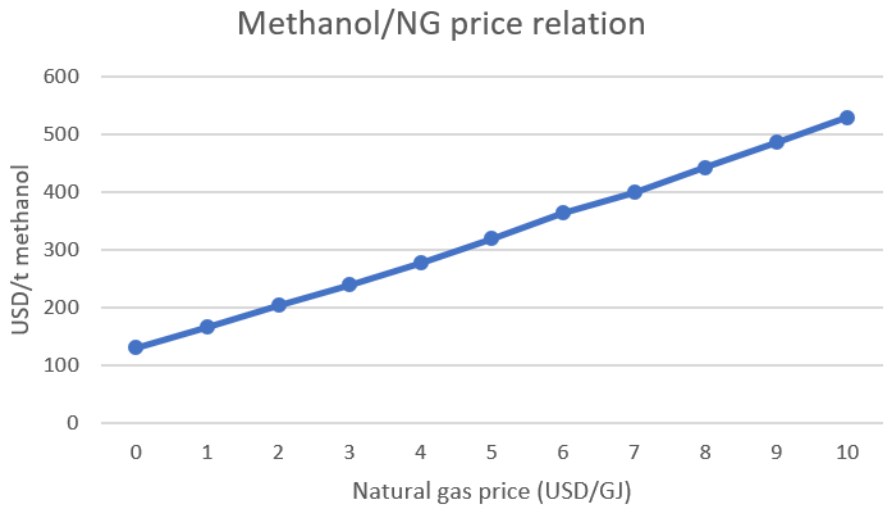

FIGURE 2.14: The cost of methanol production in a 5000 metric tonnes per day methanol plant, with varying natural gas input prices. USD in 2013 values (Bertau et al. 2014).

The overall costs of a large-scale methanol based GTL plant is harder to estimate though, as such plants do not exist. Even estimates on the costs of the final fuel production technologies alone, e.g. the MOGD process, are hard to come by. The first large-scale methanol based GTL is set to go on stream in 2019 though (Caspian News 2019). The plant is based on the Haldor Topsøe TIGAS technology, and will have a size of 15,500 barrels per day (bpd) at an investment cost of 1.7 billion USD, making the cost roughly 110,000 USD/bpd which is in the same magnitude as FT based GTL plants. However, as the plant has not yet opened, the cost may still increase due to start-up problems.

Chapter 3

Energy Flow Analysis of the Pathways

This chapter presents the considered potential pathways for producing jet fuel in the future, along with their energy efficiencies and flows based on both literature study of relevant scientific articles, industrial experience as presented in the literature and stoichiometric calculations.

3.1 Biomethane Projection 2025

As mentioned, one of the goals of this project is to provide a case study of GTL production of jet fuel which is to be operational by 2025 on Funen, Denmark. Therefore, the amount of biomethane available for a such production in 2025 has to be estimated.

Several studies in the last decade have attempted to estimate both the biogas and biomass potential in Denmark towards 2050. In DEA (2018*b*) it has been estimated that the Danish biogas production will be roughly 23 PJ/y in 2025. Of this, roughly 8 PJ/y are expected to be used for electricity, heating and process purposes, whilst the remaining 15 PJ/y are upgraded through either separation or methanation to methane, and sent to the gas grid. Assuming that all of the methane is to be utilised in GTL plants for fuel production, Sankey diagrams of the potential pathways can be designed with a biogas input of 15 PJ/y. The Sankey diagrams always show the energy flows for a year, and as such, the units are in PJ instead of PJ/y.

3.2 Energy Flows of the Process Segments

To depict the energy flows of the different pathways, an Excel-model has been developed. In the model, each technology that can be included in the pathways has been defined with general values for its inputs and outputs, normalized to 1 unit of the primary input. For instance, the syngas production step done by autothermal reforming is normalized to have a 1 unit input of methane, and the outputs correlated to this are 0.92 units of syngas, 0.04 units of usable heat and 0.04 units of heat loss. If the input to the autothermal reformer then was 5 PJ of biogas, the syngas output would be 5 PJ times 0.92 which

is 4.6 PJ. This amount of syngas could then be the input of another technology with normalized values. As such, with the values normalized, the technologies can be combined in various combinations, irrespectively of the input size. When doing this for all the technologies, then the model can be used as a tool to make several different Sankey diagrams. Only the values of the technologies which are used for the Sankey diagrams will be presented here. The full overview of all screened technologies and their normalized inputs and outputs as they look in Excel can be seen in Table K.1 to Table K.5 in Appendix K.

Overall, GTL plants are very integrated facilities, where each segment of the plant is heavily interconnected with the others and there are countless loops for steam, heat, tail gas and other initial, intermediate and final components. This was however not deemed feasible to show in such detail in a Sankey diagram. Instead, the Sankey diagrams have been designed as one-way flow diagrams, where the efficiency achieved for each technology by the heavy integration of a GTL plant is used. This for instance means, that heat leaving a process and is used to preheat its input, is subtracted out and not shown in the Sankey diagram. These considerations are explained in more detail when each technology is described.

In total, six potential pathways are presented, four of which are related to the Fischer-Tropsch pathways, one which is related to the methanol pathway and one which is related to the oxidative coupling of methane pathway. An additional pathway for both the methanol and OCM pathway can be seen in Appendix F. The values used for the technologies in the pathways are presented in this section. The presented pathways are shown as if the technologies were used in a central GTL plant. There are many considerations to be had regarding a central plant vs many decentral GTL plants. These considerations are discussed in Section 3.4 after the pathway presentation. A single Sankey diagram of a decentral pathway can be found in Appendix F.3.

3.2.1 Biogas Upgrading Segment

The first technologies are in the category of biogas upgrading. As the GTL plant and not the upgrading of biogas is the main focus in Chapter 4, only one of each is used for the pathway presentations. For the presentation of the potential pathways, the water scrubber is used for the separation and chemical methanation is used for the methanation.

An overview of the energy flows in water scrubbing and chemical methanation can be seen in Table 3.1.

	Water Scrubber		Chemical Methanation	
Flow Direction	In	Out	In	Out
Biogas	1.00	0	1.00	0
Methane	0	0.97	0	1.68
Syngas	0	0	0	0
Methanol	0	0	0	0
Hydrogen	0	0	0.82	0
Syncrude	0	0	0	0
Olefins	0	0	0	0
Jet Fuel	0	0	0	0
Gasoline	0	0	0	0
Unrecovered Organics	0	0.03	0	0
Recoverable Heat	0	0	0	0.15
Lost Heat	0	0.05	0	0.01
Electricity	0.05	0	0.01	0
Other Products	0	0	0	0

TABLE 3.1: The normalized energy flows of the biogas upgrading segment.

As mentioned, the values of the inputs and outputs of each technology have been normalized to the main input of each process. For water scrubbing, the values have been normalized relative to an input of 1 unit of biogas. The remaining values are a 0.05 unit input of electricity, a 0.97 unit output of methane, a 0.03 unit output of lost organics and a 0.05 output of heat losses. The heat loss is set to equal the electricity input, while values for the lost organics output, the electricity input and the overall methane output is found in Angelidaki et al. (2018).

For the chemical methanation, the values have again been normalized relative to an input of 1 unit of biogas. With 1 unit of biogas input, the methanation plant has a hydrogen input of 0.82 units and an electricity input of 0.01 units. The hydrogen input is set to stoichiometrically match the amount of CO_2 in the biogas, when the CO_2 content is 40.5 vol% (Lemvig Biogas 2019). The electricity amount is found in DEA, Energinet (2019). The output of methane of 1.68 units is calculated stoichiometrically and the total heat output is calculated from the difference in the lower heating values of the outputs and inputs. The heat lost is assumed to be 5% of the total heat output, and thus the amount of recoverable heat is 0.15 units and the heat loss is 0.01 unit. The heat loss is assumed this low due to the heat produced being at quite high temperatures and therefore easier to recover and use. The amount of methane leaving the chemical methanation process is 1.73 times larger than the methane amount leaving the water scrubber process. Equally all other flows for the downstream technologies after the chemical methanation are 1.73 times larger than for the water scrubber. The effect of this difference can be seen

in the difference between the pathways in Section 3.3.3 and Section 3.3.4.

3.2.2 Syngas Production Segment

The next segment is the syngas production segment. Three technologies for the syngas production segment have been reviewed. These are steam reforming, autothermal reforming and partial oxidation. The syngas production segment of GTL plants rarely consist of a single production technology, but rather of a combination of at least two of the three. Additionally, the differences between the technologies are not found in their energy flows, but in other properties of the technologies. For the simplicity of the Sankey diagrams, the syngas production segment of the pathways are based on the values for the autothermal reformer. An overview of the energy flows in the syngas production segment can be seen in Table 3.2 below.

	Autothermal Reforming	
Flow Direction	In	Out
Biogas	0	0
Methane	1.00	0
Syngas	0	0.92
Methanol	0	0
Hydrogen	0	0
Syncrude	0	0
Olefins	0	0
Jet Fuel	0	0
Gasoline	0	0
Unrecovered Organics	0	0
Recoverable Heat	0	0.04
Lost Heat	0	0.04
Electricity	0	0
Other Products	0	0

TABLE 3.2: The normalized energy flows of the syngas production segment.

The values of the inputs and outputs of the syngas production segment have been normalized to 1 unit input of methane. The corresponding values for the other flows of the segment are 0.92 units output of syngas, 0.04 units output of usable heat and 0.04 units output of heat losses. The selected values are primarily based on Maitlis & de Klerk (2013), Rostrup-Nielsen (1993, 1994).

The 0.92 units of syngas produced from the 1 unit input of methane in the syngas production segment is the overall conversion efficiency of the syngas production segment. In reality the syngas production segment has a lower conversion rate to syngas than what is shown, but with a recycling of the unreacted gases that slip through, as well as an input of light gases which is recycled back from the FT-reactor the high overall efficiency is achieved.

The 0.04 units of usable heat is a surplus of heat which can be used for other processes or as district heating, and the 0.04 units of heat losses is a surplus of heat which cannot be recovered. The reforming of methane is an endothermic process, and some of the methane is combusted to provide the heat of reaction. Not all of the heat is absorbed in the syngas product and this remaining heat is that which is shown in the outputs.

Finally, in reality there is an electricity requirement for pumps etc. for the syngas production segment, however this is covered by the internal production of electricity for the GTL plant. More on this in the description of the FT synthesis segment in Section 3.2.3.

3.2.3 Fischer-Tropsch Synthesis Segment

The next segment is either the FT synthesis segment or the methanol synthesis segment, depending on which pathway that is analyzed. First, the technologies for the FT pathway are presented.

Three FT process have been screened. These are the Iron-based Catalyst High Temperature Fischer-Tropsch (Fe-HTFT) process, the Cobalt-based Catalyst Low Temperature Fischer-Tropsch (Co-LTFT) process, and the Iron-based Catalyst Low Temperature Fischer-Tropsch (Fe-LTFT) process. There is however no difference in the energy flows of the different FT processes. The difference between them is found in their refining segments, and in properties which cannot be seen in the energy flows. Therefore, the following explanation is valid for all three of the FT processes. An overview of the energy flows in the FT synthesis segment can be seen in Table 3.3.

	Fischer-Tropsch Synthesis	
Flow Direction	In	Out
Biogas	0	0
Methane	0	0
Syngas	1.00	0
Methanol	0	0
Hydrogen	0	0
Syncrude	0	0.75
Olefins	0	0
Jet Fuel	0	0
Gasoline	0	0
Unrecovered Organics	0	0
Recoverable Heat	0	0.23
Lost Heat	0	0.01
Electricity	0	0.01
Other Products	0	0

TABLE 3.3: The normalized energy flows of the FT synthesis segment.

For all of the processes, the values have been normalized to 1 unit input of syngas. The output values corresponding to the 1 unit input of syngas are 0.23 units of usable heat, 0.01 units of usable electricity, 0.75 units of syncrude and 0.01 units of heat losses. The selected values are primarily based on de Klerk (2011*a*), Maitlis & de Klerk (2013), Rostrup-Nielsen (1994). The 0.23 units output of usable heat and the 0.01 units output of heat losses are heat surpluses due to the fact the FT process is highly exothermic. 5% of the heat has been assumed to be unrecoverable as it was also the case for the biogas upgrading segment, which was presented in Section 3.2.1. Additionally, heat inputs and outputs have been subtracted in the same way as they were for the syngas production segment which was presented in Section 3.2.2, and thus only the surpluses are shown.

As previously mentioned, FT based GTL plants are self suppliant in electricity through power generation via steam turbines. Therefore, none of the segments of the GTL plant have an electricity input. In Maitlis & de Klerk (2013) it is estimated, that a 17,000 bpd FT based GTL plant exports 20 MW of electricity. It is based on this, that the electricity output has been estimated. The total output has been attributed to the FT synthesis segment for the simplicity of the Sankey diagram, as it has the largest excess of heat and thus the best circumstances for producing electricity via steam turbines. In reality there is also an electricity input to the segment, however, this has again been subtracted out and only the surplus production of electricity is shown.

3.2.4 Fischer-Tropsch Refining Segment

As previously mentioned, the three FT processes have unique refining segments, each with unique inputs and outputs. An overview of the energy flows in the FT refining segments can been seen in Table 3.4.

	Fe-HTFT		Co-LTFT		Fe-LTFT	
Flow Direction	In	Out	In	Out	In	Out
Biogas	0	0	0	0	0	0
Methane	0	0	0	0	0	0
Syngas	0	0	0	0	0	0
Methanol	0	0	0	0	0	0
Hydrogen	<0.01	0	0.02	0	0.02	0
Syncrude	1.00	0	1.00	0	1.00	0
Olefins	0	0	0	0	0	0
Jet Fuel	0	0.53	0	0.65	0	0.60
Gasoline	0	0.31	0	0.33	0	0.36
Unrecovered Organics	0	0.02	0	<0.01	0	0.01
Recoverable Heat	0	0	0	0	0	0
Lost Heat	0	0	0	0	0	0
Electricity	0	0	0	0	0	0
Other Products	0	0.14	0	0.04	0	0.04

TABLE 3.4: The normalized energy flows of the FT refining segment.

First off, the values for the Fe-HTFT process are presented. The input and output values are normalized to 1 unit input of syncrude. Apart from the syncrude, there is also a very small input of hydrogen which is smaller than <0.01 units. For the outputs, there is 0.02 units of unrecovered organics, which are alcohols leaving with the waste water, 0.53 units of jet fuel, 0.31 units of gasoline and 0.14 units of other products, which are mainly liquefied petroleum gas (LPG) followed by fuel gas and small amounts of petrochemicals. This amount of inputs and outputs is based on a fuel refinery design designed to maximize the production of jet fuel that lives up to the properties of the ASTM-standards, whilst the byproducts also live up to their relative standards. The values are based on de Klerk (2011*a*), de Klerk (2011*b*). It should be mentioned, that the light hydrocarbons in both LPG and fuel gas ideally should be recycled in the GTL plant to increase the overall yield of desirable products. However, it has not been possible to find a source with a final product distribution where this is done, and therefore these amounts of byproducts have been included as final products. Additionally, the alcohols that are a lost in this design, can potentially be refined to usable products in a more complex refinery design.

The next FT process is the Co-LTFT process. As for the Fe-HTFT process, the input and output values for the Co-LTFT process are normalized to 1 unit input of syncrude. The input of hydrogen is 0.02 units, whilst the outputs are <0.01 units of unrecovered organics, 0.65 units of jet fuel, 0.33 units of gasoline and 0.04 units of other products which is mainly fuel gas. The design methodology of the refinery design behind these outputs is the same as for the Fe-HTFT process refining, from de Klerk (2011*a*), de Klerk (2011*b*). As was the case of refining of the Fe-HTFT process, the fuel gas should ideally be recycled.

The final FT process is the Fe-LTFT process. The input and output values are normalized to 1 unit input of syncrude. The input of hydrogen is 0.02 units, whilst the outputs are 0.60 units of jet fuel, 0.36 units of gasoline and 0.04 units of other products, which are mainly fuel gas. The design methodology of the refinery design behind these outputs is the same as for the other FT processes, from de Klerk (2011*a*), de Klerk (2011*b*). As was the case of refining of the previous processes, the fuel gas should ideally be recycled.

Additional differences between the different FT pathways are discussed in their respective pathway presentations in Section 3.3.

Finally, it is worth mentioning, that for all of the FT refining segments there is a net heat output. As data on this was not possible to find though, it has not been included. Most likely, it would be in the same order of magnitude the refining in the methanol pathway.

3.2.5 Methanol Synthesis Segment

The second pathway is the methanol pathway, and in this pathway the next segment after the syngas production segment is the methanol synthesis segment. There are several other pathways within the alcohol-to-jet family of technologies that could be analysed, e.g. ethanol or isobutanol to jet fuel, however the focus here is only on methanol. An overview of the energy flows in the methanol synthesis segment can be seen in Table 3.5.

	Methanol Synthesis	
Flow Direction	In	Out
Biogas	0	0
Methane	0	0
Syngas	0	0
Methanol	1.00	0.72
Hydrogen	0	0
Syncrude	0	0
Olefins	0	0
Jet Fuel	0	0
Gasoline	0	0
Unrecovered Organics	0	0.06
Recoverable Heat	0	0.21
Lost Heat	0	0.01
Electricity	0	0
Other Products	0	0

TABLE 3.5: The normalized energy flows of the methanol synthesis segment.

With the input and output values normalized to 1 unit input of syngas, there is a 0.21 unit output of usable heat, 0.06 unit output of unrecovered organics, 0.72 unit output of methanol and 0.01 unit output of heat losses, with the data based mainly on Bertau et al. (2014), Rostrup-Nielsen (1993). The outputs of 0.21 units of usable heat and 0.01 unit of heat losses are due to the methanol synthesis being highly exothermic. The assumption which was previously employed regarding 5% of the heat not being recoverable has also been employed for the methanol synthesis segment. Additionally, the subtraction of inputs and outputs of heat in a segment also applies here, meaning that only the heat surplus of the segment is shown.

The 0.06 units output of unrecoverable organics comes the from purge gas. The bypass conversion of syngas to methanol in the methanol reactor is typically very low, down between 10-25%. Therefore there is a large make-up gas loop, which makes it possible to recycle gases in the plant. In this loop, there is a build-up of both inert and excess gases which must be purged. Additionally, there is byproduct formation in the methanol process, which must be cleaned out (Bertau et al. 2014). However, it is not all of the purge gas that is necessarily completely lost. Some is recovered, and can be reused in processes throughout the GTL plant, or used as fuel gas. Sufficient data on this has not been found though, and this use of purge gases has therefore not been included in the figure.

The 0.72 units output of methanol is the overall conversion efficiency of syngas to methanol in the gas loop, in the same way as it was presented for the gas loop of the syngas production segment in

Section 3.2.2.

Finally, data on the typical electricity production of a methanol GTL plant was not possible to find, except that the plant is self suppliant in electricity. Therefore, no export of electricity is shown in the output values of the segment.

3.2.6 Methanol-to-Olefins Segment

The refining of methanol to jet fuel starts with the dehydration of methanol to light olefins in the MTO process. An overview of the energy flows in the methanol dehydration segment can be seen in Table 3.6.

	Methanol-to-Olefins	
Flow Direction	In	Out
Biogas	0	0
Methane	0	0
Syngas	0	0
Methanol	1.00	0
Hydrogen	0	0
Syncrude	0	0
Olefins	0	0.86
Jet Fuel	0	0
Gasoline	0	0
Unrecovered Organics	0	0
Recoverable Heat	0	0.05
Lost Heat	0	<0.01
Electricity	0	0
Other Products	0	0.08

TABLE 3.6: The normalized energy flows of the methanol-to-olefins segment.

The inputs and outputs are normalized to 1 unit input of methanol, and the outputs are 0.05 units of usable heat, less than 0.01 units of lost heat, 0.09 units other products and 0.86 units of olefins. A lot of research has been conducted in recent years to improve this process. The values used here are mainly based on the DMTO (Dimethyl ether or Methanol-to-Olefin) process as presented in Tian et al. (2015).

The 0.86 units of light olefins are C_2-C_4 olefins, whilst the 0.09 units of other products are higher olefins up to C_6 as well as some aromatics and paraffins, which could potentially be used elsewhere in a GTL plant, but here has been assumed to be final products. The total heat output has been calculated from

the heat of reaction as presented in Tian et al. (2015), and split between recoverable heat and heat losses as previously described.

3.2.7 Oxidative Coupling of Methane Segment

As mentioned in Section 2.8 there is an alternative route to light olefins, namely the Oxidative Coupling of Methane (OCM) process which is the third pathway. An overview of the energy flows in the OCM segment can be seen in Table 3.7.

	Oxidative Coupling of Methane	
Flow Direction	In	Out
Biogas	0	0
Methane	1.00	0
Syngas	0	0
Methanol	0	0
Hydrogen	0	0
Syncrude	0	0
Olefins	0	0.83
Jet Fuel	0	0
Gasoline	0	0
Unrecovered Organics	0	0
Recoverable Heat	0	0.16
Lost Heat	0	0.01
Electricity	0	0
Other Products	0	0

TABLE 3.7: The normalized energy flows of the OCM segment.

The values for the OCM segment are normalized to 1 unit input of methane. The outputs of the process are 0.16 units of usable heat, 0.83 units of light olefins which are primarily ethylene and 0.01 units of heat losses.

These values are strictly theoretical and are calculated based on the heating values of the inputs and outputs of Equation (2.14). They do not have an influence from data in the literature unlike the values previously presented for the other pathways. As such, this is the best case scenario, and the production of light olefins is likely to be slightly lower in reality. For the other technologies, practical efficiencies are typically roughly 80% of their theoretical efficiencies, however this has not been included in the values used for the OCM Sankey diagram (Rostrup-Nielsen 1994).

3.2.8 Light Olefin Refining Segment

The final segment of both the methanol and OCM pathways is the light olefin refining segment, which includes both oligomerization and hydrotreating. An overview of the energy flows in the light olefins refining segment can be seen in Table 3.8.

	Olefin Refining (MOGD)	
Flow Direction	In	Out
Biogas	0	0
Methane	0	0
Syngas	0	0
Methanol	0	0
Hydrogen	0.04	0
Syncrude	0	0
Olefins	1.00	0
Jet Fuel	0	0.49
Gasoline	0	0.16
Unrecovered Organics	0	0
Recoverable Heat	0	0.03
Lost Heat	0	<0.01
Electricity	0	0
Other Products	0	0.36

TABLE 3.8: The normalized energy flows of the olefin refining segment.

The inputs and outputs are normalized to 1 unit input of light olefins. A 0.04 units input of hydrogen is required for the hydrotreating, and the overall outputs of the processes are 0.03 units of recoverable heat, less than 0.01 units of heat losses, 0.49 units of jet fuel, 0.16 units of gasoline and 0.36 units of other products, which is mainly diesel with small amounts of fuel gas and LPG. The values are mainly based on the Mobil Olefins to Gasoline and Distillate (MOGD) process as presented in Tabak & Yurchak (1990), Tabak et al. (1986), Bertau et al. (2014).

The main concern with basing the values on the MOGD process, is that the products in the distillate range can be between carbon number C_{10}-C_{20} whilst jet fuel is mainly in the range C_{10}-C_{16}. The carbon number distribution of the products has not been able to be found for either the MOGD process or a similar one. Therefore, the values are based on the MOGD process where the distribution is assumed to be equal across all carbon numbers, with equal amounts being produced of each length even though this is generally not the case for oligomerization processes. Therefore, it has been assumed that 60% of the distillate range hydrocarbons are used for jet fuel whilst the remaining 40% have been assumed to

be used for diesel. In theory it should be possible to both recycle the lower olefins in the fuel gas, LPG and gasoline range to oligomerization processes and the higher olefins to hydrocracking processes. However, no studies or data on processes optimizing such a scheme geared towards maximizing the production of jet fuel have been found and this has therefore not been included in this project. Generally, alcohol based GTL plants seem to be geared towards gasoline or diesel production instead of jet fuel production for reasons unknown to the authors, however some companies do provide the technology to produce some jet fuel though the alcohol-to-jet pathway, e.g. LanzaTech (LanzaTech 2019).

3.3 Pathway Sankey Diagrams

In this section, the Sankey diagrams of six of the potential pathways are presented, along with additional discussion regarding differences both relating to their energy flows and other considerations. All of these Sankey diagrams are based on the values presented in the previous section, Section 3.2.

3.3.1 The Fe-HTFT Pathway with Methane from Biogas Separation

The first pathway is the Fe-HTFT pathway, and the energy flows of this pathway can be seen in Figure 3.1.

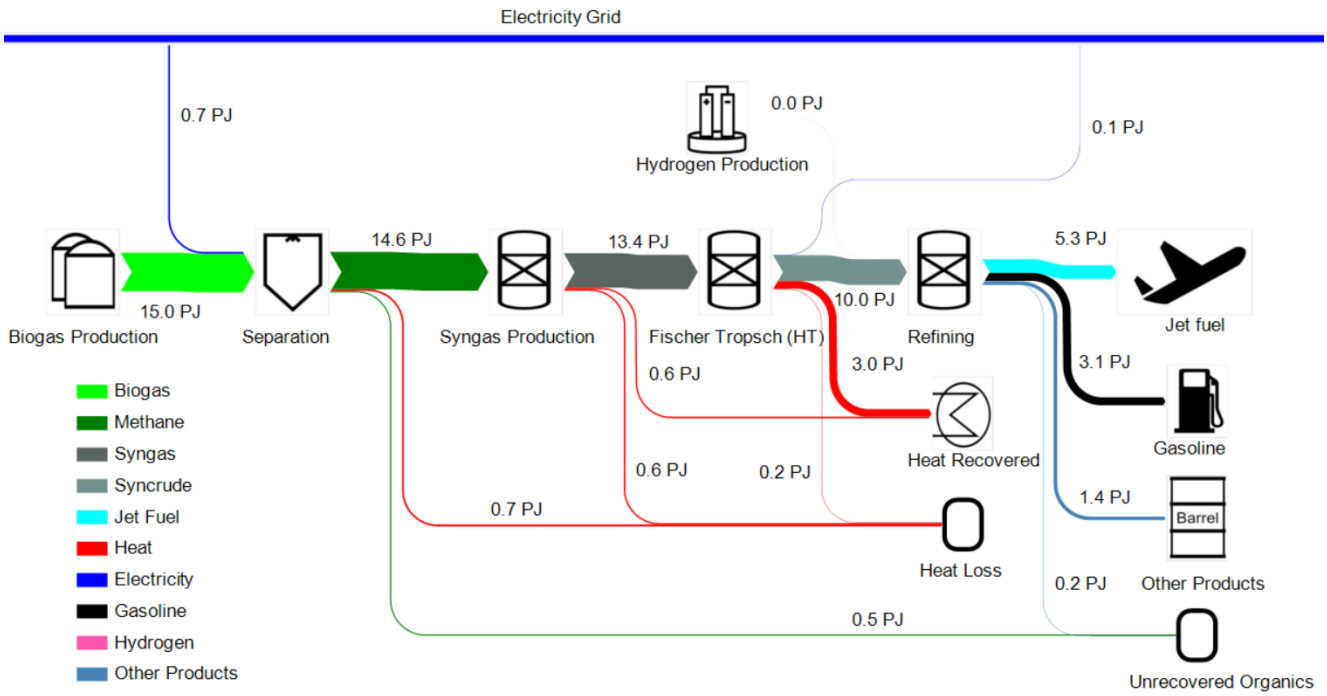

FIGURE 3.1: The Sankey diagram of a Fe-HTFT GTL plant with methane from biogas upgraded by separation.

For this pathway, the biogas is upgraded by separation. The methane is led through the natural gas grid to the GTL plant, where it is reformed to syngas, the syngas is converted to syncrude in the Fe-HTFT process and the syncrude is refined in the corresponding refining segment.

With a 15 PJ input to the Fe-HTFT pathway with biogas separation, there is a yield of 5.33 PJ of jet fuel which is roughly 35.5% of the input, as well as 3.14 PJ of gasoline which is roughly 20.9% of the input. This makes the overall yield of the conversion of biogas to transportation fuels roughly 56.4% on an energy basis.

There are differences in the suitability of the syncrude from each FT-technology in the refining to jet fuel. HTFT processes produce a syncrude with products of a lighter carbon number distribution, making the amount of final byproducts larger than that of LTFT processes. Generally, it is easier to reduce the carbon number of the hydrocarbons in LTFT-syncrude, than increasing the carbon number of HTFT-syncrude. For these reasons, the yield of refining LTFT-syncrude is also higher for transportation fuels (de Klerk 2011*a*, de Klerk 2011*b*). Therefore, the LTFT pathways are likely to be more suitable for jet fuel product, than the HTFT pathway.

3.3.2 The Co-LTFT Pathway with Methane from Biogas Separation

The second pathway is the Co-LTFT pathway, and the energy flows of this pathway can be seen in Figure 3.2.

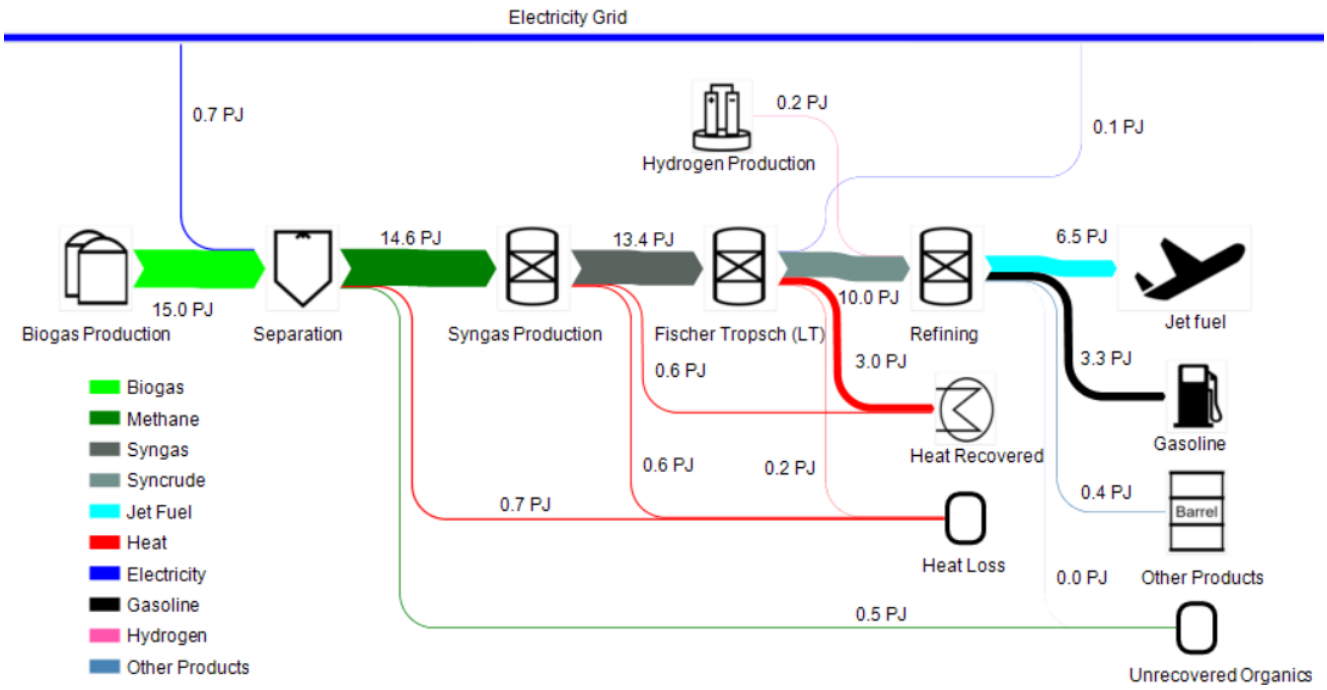

FIGURE 3.2: The Sankey diagram of a Co-LTFT GTL plant with methane from biogas upgraded by separation.

For this pathway, the biogas is upgraded by separation. The methane is led through the natural gas grid to the GTL plant, where it is reformed to syngas, the syngas is converted to syncrude in the Co-LTFT process and the syncrude is refined in the corresponding refining segment.

With a 15 PJ input to the Co-LTFT pathway with biogas separation, there is a yield of 6.52 PJ of jet fuel which is roughly 43.5% of the input, as well as 3.29 PJ of gasoline which is roughly 21.9% of the input. This makes the overall yield of the conversion of biogas to transportation fuels roughly 65.4% on an energy basis.

There are both advantageous and disadvantages of using Co-LTFT compared to Fe-HTFT. The most obvious advantage is that the yield of jet fuel is quite a bit higher for Co-LTFT. Additionally, it is easier to refine the syncrude from Co-LTFT than that of Fe-HTFT. But Co-LTFT has a large downside in that, when the refining of Co-LTFT is designed to maximize the production of jet fuel, it is not possible to produce gasoline which lives up to the requirements of the European standard for gasoline, EN228 (de Klerk 2011*a*, de Klerk 2011*b*). In this standard, the gasoline has to have a research octane number of 95, and the gasoline produced through the proposed design here only has a research octane number of 93.5 (de Klerk 2011*a*). This complication stems from the property, that syncrude from a FT-process based on a cobalt catalyst is less olifinic than syncrude from a FT-process based on an iron catalyst. Due to this, the gasoline produced from this Co-LTFT refinery design cannot be sold as a final product, but has to be blended with components that can increase the research octane number of the gasoline, or the refinery has to be designed differently, with a lower jet fuel yield as a consequence. Fe-LTFT has many of the advantageous of both of the other two FT processes.

3.3.3 The Fe-LTFT Pathway with Methane from Biogas Separation

The third pathway is the Fe-LTFT pathway, and the energy flows of this pathway can be seen in Figure 3.3.

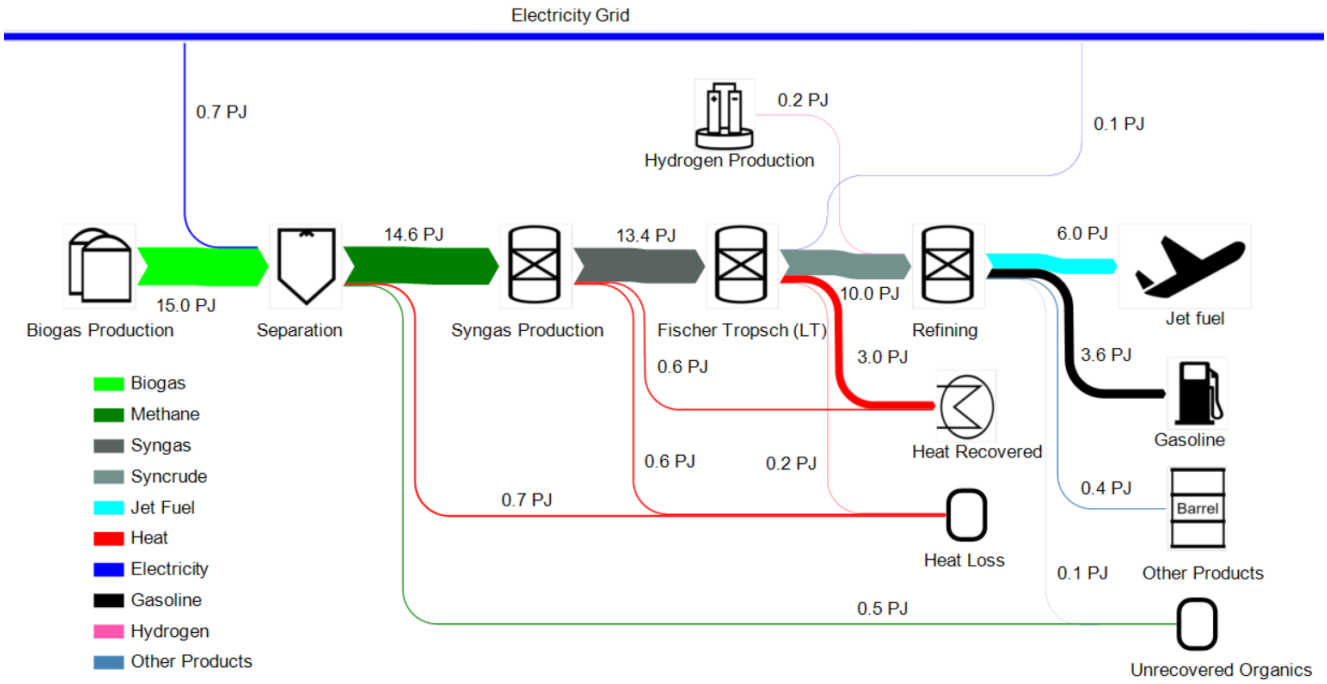

FIGURE 3.3: The Sankey diagram of a Fe-LTFT GTL plant with methane from biogas upgraded by separation.

For this pathway, the biogas is upgraded by separation. The methane is led through the natural gas grid to the GTL plant, where it is reformed to syngas, the syngas is converted to syncrude in the Fe-LTFT process and the syncrude is refined in the corresponding refining segment.

With a 15 PJ input to the Fe-LTFT pathway with biogas separation, there is a yield of 6.04 PJ of jet fuel which is roughly 40.2% of the input, as well as 3.63 PJ of gasoline which is roughly 24.2% of the input. This makes the overall yield of the conversion of biogas to transportation fuels roughly 64.4% on an energy basis. So compared to the Co-LTFT technology the overall, as well as the jet fuel yield, is slightly lower. However, in this pathway the gasoline does live up to the requirements as the research octane number is 95.3.

3.3.4 The Fe-LTFT Pathway with Methane from Biogas Methanation

The fourth and final FT pathway which is presented, is the Fe-LTFT pathway with methane from biogas methanation. This ultimately leads to larger energy flows throughout the whole pathway from biogas to jet fuel, as large amounts of hydrogen are included in the biogas upgrading segment for the methanation of the CO_2 in the biogas. The Sankey diagram for this pathway can be seen in Figure 3.4.

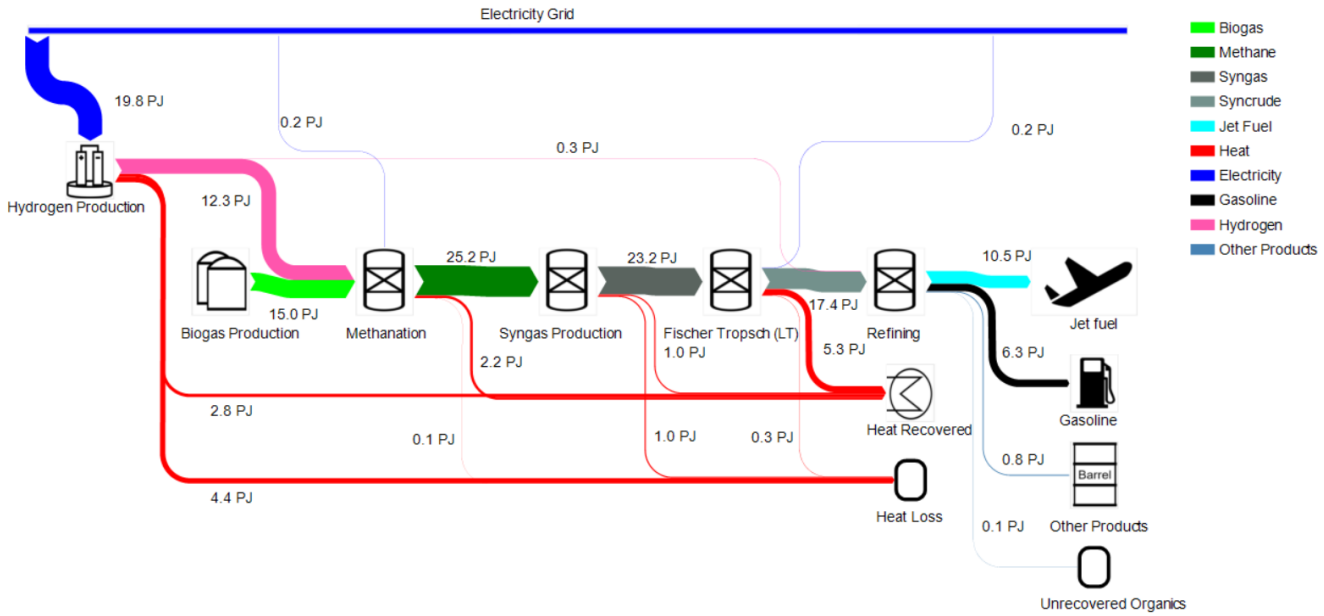

FIGURE 3.4: The Sankey diagram of a Fe-LTFT GTL plant with methane from biogas upgraded by methanation.

For this pathway, the biogas is upgraded by methanation. The methane is led through the natural gas grid to the GTL plant, where it is reformed to syngas, the syngas is converted to syncrude in the Fe-LTFT process and the syncrude is refined in the corresponding refining segment.

With a 15 PJ input to the Fe-LTFT pathway with biogas methanation, there is a yield of 10.47 PJ of jet fuel and 6.30 PJ of gasoline.

At first glance it would appear that biogas methanation is far superior to biogas separation, as much larger fuel yields are achieved from the same source of carbon. However, as presented in Section 2.1.2, methanation is still quite expensive and will probably need more years, before it becomes market competitive.

3.3.5 The Methanol Pathway with Methane from Separation

The fifth pathway is the methanol pathway, with biogas from separation. The Sankey diagram of this pathway can be seen in Figure 3.5.

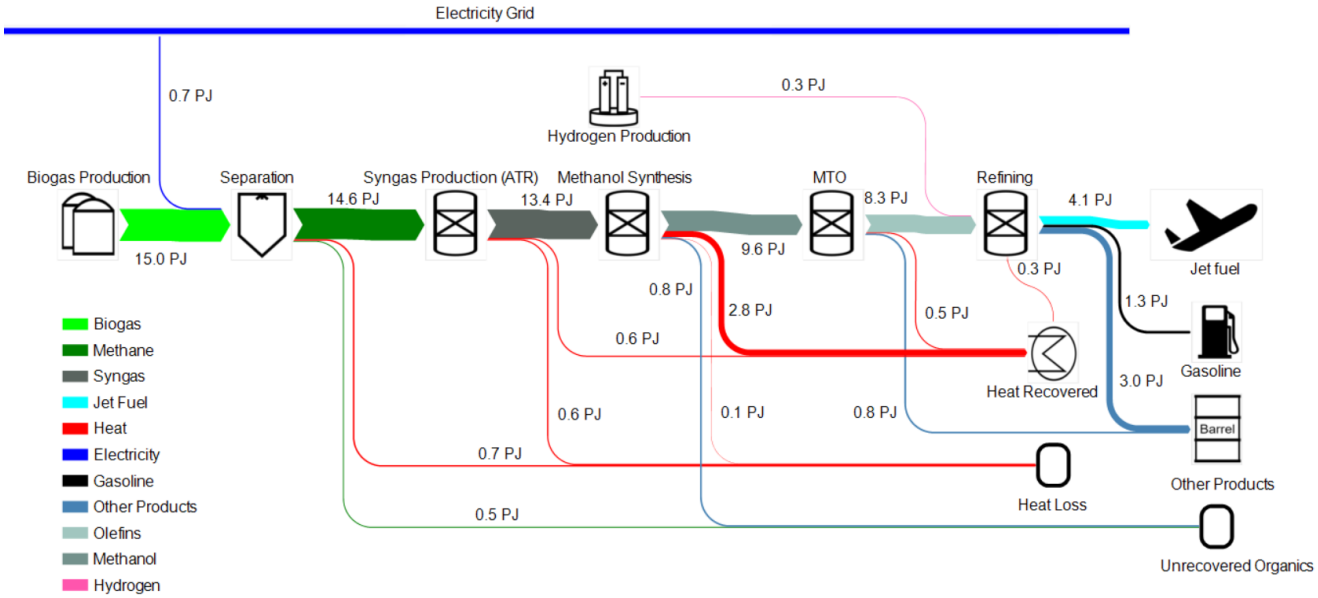

FIGURE 3.5: The Sankey diagram of a methanol based GTL plant with methane from biogas upgraded by separation.

For this pathway, the biogas is upgraded by separation. The methane is led through the natural gas grid to the GTL plant, where it is reformed to syngas, the syngas is converted to methanol in the methanol synthesis process, the methanol is dehydrated to light olefins, and the light olefins are refined to final fuel products.

With a 15 PJ input to the methanol pathway with biogas separation there is a yield of 4.08 PJ of jet fuel which is roughly 27.2% of the input, 1.30 PJ of gasoline which is roughly 8.6% of the input and roughly 2.7 PJ of diesel which is roughly 18% of the input. This makes the overall yield of the conversion of biogas to transportation fuels through the methanol pathway roughly 53.8% on an energy basis. Compared to the FT based GTL pathways the overall yield of transport fuels is slightly lower. However it may be possible to increase the selectivity towards jet fuel and have a higher production of jet fuel than through the FT pathways, if the refining segment is designed to maximize jet fuel production. As it has not been possible to find literature on a technology in the methanol pathway with focus on jet fuel production though, it has not been possible to analyze this. The methanol pathway with methane from biogas methanation can be seen in Appendix F.1 in Appendix F.

3.3.6 The OCM Pathway with Methane from Biogas Separation

The sixth pathway is the OCM pathway based on methane from biogas separation. The Sankey diagram of this pathway can be seen in Figure 3.6.

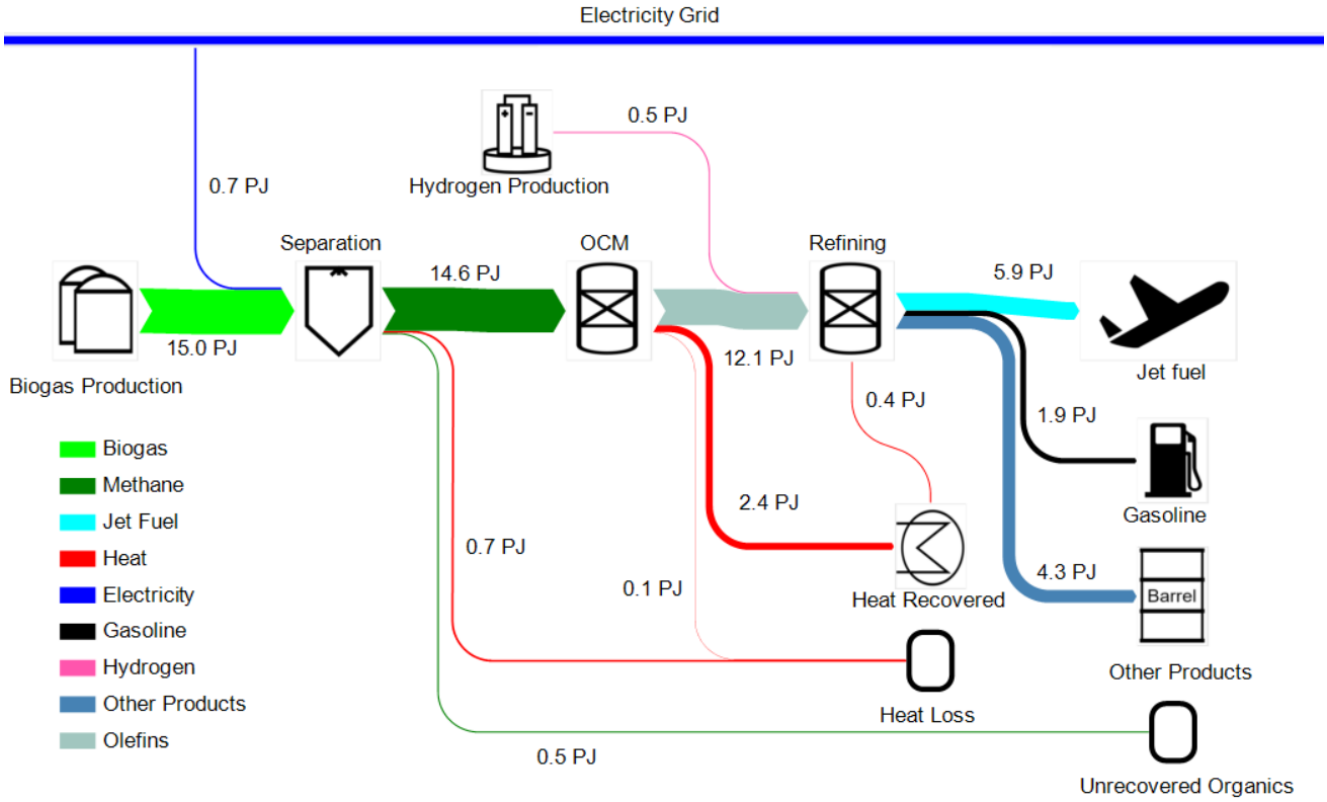

FIGURE 3.6: The Sankey diagram of a OCM based GTL plant with methane from biogas upgraded by separation.

For this pathway, the biogas is upgraded by separation. The methane is led through the natural gas grid to the GTL plant, where it is used to produce light olefins which are refined to final fuel products.

With a 15 PJ input to the OCM pathway with methane from biogas separation, there is a yield of 5.94 PJ of jet fuel which is roughly 39.6% of the input, 1.90 PJ of gasoline which is roughly 12.6% of the input and 4.29 PJ of other products where 3.9 PJ is diesel which is roughly 26% of the input. This makes the overall yield of the conversion of biogas to transportation fuels roughly 78.2% on an energy basis. Looking at the Fe-LTFT pathway with a transportation fuel yield of 64.2% and the methanol pathway with a yield of roughly 53.8%, the yield of desirable products is quite a bit higher for the FT pathway than the methanol pathway, but the yield of the OCM pathway is even higher than that. A part of the explanation can be found in the fact that the pathway has fewer process segments than the other two pathways. Additionally, the the yields of the OCM process have been calculated strictly theoretically. The yields in a commercial plant are likely to be lower. The pathway has the potential to be very

efficient, but is not yet realistic as the OCM technology is not ready yet. The OCM pathways with methane from biogas methanation can be seen in Appendix F.2 in Appendix F.

3.4 Considerations for Central versus Decentral GTL

The energy flows of the different technology pathways are one of the main important things to consider when choosing a pathway for further study, as the technology with the largest input to desirable output conversion rate has a clear advantage compared to the other technologies. There are however also other parameters in the establishment of a GTL plant to consider. These primarily come from the advantages and disadvantages of establishing decentral GTL plants at the same site as the biogas production, compared to establishing a central plant which was previously considered. The differences between central and decentral GTL are discussed in a few different categories, consisting of considerations regarding technology, CO_2 utilization, waste heat utilization and the economy of the plant.

3.4.1 Technology Differences

The main technology difference between central and decentral GTL plants, is that since the decentral plant is located at the same place as the production of biogas, the biogas does not have to be upgraded to be transported in the natural gas grid. The biogas would still need to be upgraded to be used in an OCM pathway, but could be used directly in the syngas production segments of FT and methanol based GTL plants. A single Sankey diagram of the combined energy flows of many decentral Fe-LTFT diagrams can be found in Appendix F.3. The plants would have to be designed differently than a central plant as discussed in this section, but the energy flows of the processes are assumed to be the same. Thus, the only difference in the Sankey diagram is that the biogas upgrading segment is not included.

For the simplicity of the technology discussion, only the case of the FT and methanol technologies is discussed. Introducing CO_2 as an input to the syngas production segment would require it to be designed differently than if there was no CO_2 input. Co-feeding with CO_2 generally lowers the H_2:CO ratio of the produced syngas. This effect is illustrated in Figure 3.7.

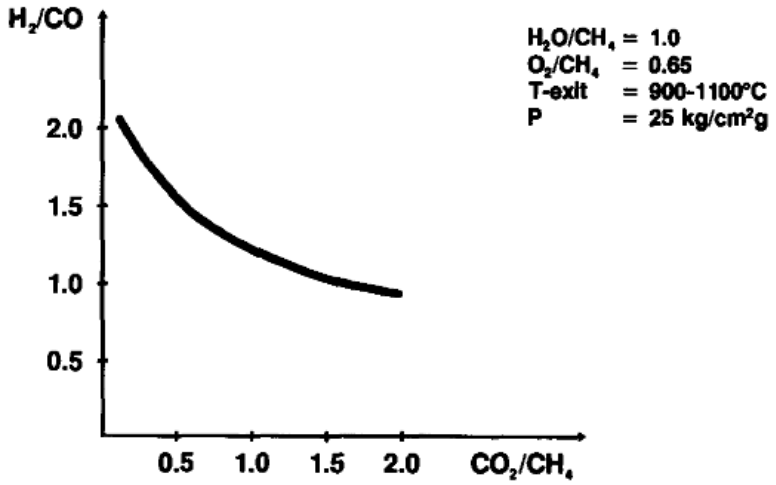

FIGURE 3.7: The effect of adding CO_2 as a co-feed to an autothermal reforming process. The figure shows the varying CO_2:CH_4 feed ratio on the x-axis, the varying H_2:CO ratio of the product syngas on the y-axis, and the other constant operating conditions in the top right corner. Source: (Rostrup-Nielsen 1993).

This effect can be useful when designing a syngas production segment based mainly on steam reforming, as the syngas from steam reforming alone has a H_2:CO ratio too high to be used for GTL plants. The extreme case of this is called dry reforming, where CO_2 completely replaces steam as the co-feed with methane in the reforming process (de Klerk 2011*a*). Often, the natural gas sources that current GTL plants use as feed contain some CO_2, where balancing of the reforming process is done by the addition of additional CO_2, addition or removal of steam, additional water gas shift balancing, and in the overall design of the syngas production segment (Bertau et al. 2014). Although the CO_2 content of biogas is larger than that of the natural gas which is typically used, it should be possible to apply the same balancing methodology to achieve a desirable H_2:CO ratio in the syngas product. Several technology providers for small-scale GTL plants offer solutions which can take CO_2-rich gases as input, including but not limited to Greyrock, Primus Green Energy and GasTechno (Greyrock 2019, Primus GE 2019, GasTechno 2019).

3.4.2 Carbon Dioxide Utilization Differences

In addition to the differences in the design of the syngas production segment, as explained in the previous section, there is another difference regarding the utilization of CO_2 for central GTL compared to decentral. A decentral GTL plant can utilize the CO_2 from the biogas, however, this is not necesarily the case for a central GTL plant. The gas input for the central plant is methane which has been transported through the natural gas grid. If the biogas is upgraded to methane through methanation, the CO_2 in the biogas is upgraded to be a part of the methane gas which is used as the input at the

GTL plant. However, if the biogas is upgraded by separation, this CO_2 is most likely lost, and the carbon efficiency of the overall pathway reduced. The options for the central GTL plant with methane from biogas separation to be able to include the CO_2 from the biogas are transport of the CO_2 to the GTL plant, either by establishing a pipeline or transport in pressurized containers, or carbon capture of an amount of CO_2 equal to the amount lost at the separation plant. Alternatively, the CO_2 at the separation could be captured and sold off as a chemical.

As such, one of the trade-offs for a central GTL plant is that in order for the central plant to have the same carbon utilization as the decentral plant, there has to be invested in either the more expensive upgrading technology, methanation, transport of the CO_2 through e.g piping, or carbon capture at the GTL plant. These extra costs have to be weighted against the economic benefits of having a central plant, as discussed in Section 3.4.4.

3.4.3 Waste Heat Utilization Differences

A concern for decentral GTL plants is the utilization of waste heat. The production of biogas in Denmark is mostly a byproduct of the agriculture, where farmers collect the manure of their livestock and deposit it in anaerobic digesters. Therefore, the biogas production is often situated out in the countryside where there is no connection to a district heating grid. Without a connection to a district heating grid, it is hard for a GTL plant to offset the large amounts of surplus heating which is produced in the exothermic reactions of the plant. For a central GTL plant, the utilization of waste heat is a smaller concern, however not completely unproblematic. The plant can most likely be placed within reasonable distance of both the natural gas grid for its gas input as well as a district heating grid to be able to offset the surplus heat. However, a central GTL plant produces very large amounts of heat, which is more than what most Danish district heating grids need. Even for the large district heating grids, there may be problems regarding off-setting the heat at some times. GTL plants have a constant heat production when producing their primary product, however the heat demand in district heating grids changes throughout the year. So even though the overall production of heat from a GTL plant throughout a year may not be able to cover the yearly heat demand of a district heating grid, it may produce more heat than needed at specific times. This is likely to be the case in the summer, where the heating demand is usually very low compared to the winter. As such, it may not be possible to offset all of the heat from a central GTL plant even though it has access to a district heating grid, but it will most likely be better than for a decentral GTL plant which may not be able to offset any heat at all.

3.4.4 Economy Differences

The economy of GTL plants was discussed in Section 2.5 and Section 2.10, however, a few additional points are made here. The main difference in the economy of GTL plants due to being central or

decentral is mainly the size of the plants. Decentral plants are much smaller than central plants, as a decentral plant only has a single biogas plant as its feed, whilst a central plant can draw from all biogas plants connected to the national gas grid. The overall economy of a large GTL plant may not be better compared to a small GTL plant, as economies of scale do not necessarily apply as discussed in Section 2.5. The technology choices are however affected by the economy of small versus large plants, as some technologies are not viable in small-scale GTL plants, the most important being the air separation unit. If the GTL plant is to use a syngas production technology that requires oxygen, most commonly autothermal reforming, it is recommended to design the single train capacity of the plant to utilize one world-scale air separation unit. In a GTL plant a train is a complete production module, from feed to product, and world-scale plants usually have more than one train. For a FT based GTL plant this size is a single train capacity of 17,000 bpd (Maitlis & de Klerk 2013). For a methanol plant, autothermal reforming is generally used if the capacity of the plant exceeds 2500 tonnes of methanol per day, otherwise single or two-step reforming with steam reforming is used (Dahl et al. 2014).

3.5 Pathway Selection for Case Study

As mentioned, the final goal of this project is to provide a case study of GTL plants based on a pathway with a biogas input of 15 PJ/y on Funen, Denmark by 2025. For several reasons, it has been chosen that the case study should be of a central FT based GTL plant, based on the Fe-LTFT technology and with methane from biogas separation. The OCM pathway has not been considered for the case study, as it is not yet commercially established, making data for a case study unavailable.

The first reason is regarding the technology. From the discussion of the Fe-LTFT pathway as presented in Section 3.3, it appears that the Fe-LTFT pathway is best suited for jet fuel production. Compared to the other FT processes, the Fe-LTFT process produces the syncrude which is the most suitable for refining to jet fuel, when also considering the co-products. Even though the yield of jet fuel is lower than for the Co-LTFT process, the fact that the gasoline byproduct from the Fe-LTFT process lives up to the EN 228 specification for gasoline in the EU, whilst the gasoline from the Co-LTFT process does not, makes the Fe-LTFT process preferable. In general, the larger alkene content of the Fe-LTFT process compared to the Co-LTFT process makes the refining process to jet fuel easier (de Klerk 2011*a*). This is the main advantage of the Fe-LTFT process over the Co-LTFT process.

Compared to the methanol pathway, the Fe-LTFT pathway also has a higher jet fuel and overall fuel yield, as the Fe-LTFT pathway has a transport fuel yield of 64.2% whilst the methanol pathway has a transport fuel yield of 53.8%. This difference is mainly a result of the lack of data regarding the refining processes though. For the FT pathways, it was not possible to find data on the heat losses of the processes, and for the methanol pathway, it was not possible to find data on a refining process optimized for jet fuel production.

As such, in reality the two pathways are likely to have fuel outputs that are closer to being the same than shown in these Sankey diagrams. There are however other reasons that the Fe-LTFT pathway is the preferred pathway for a case study.

The second reason that the Fe-LTFT pathway is chosen, is the industrial experience behind the FT technology for large-scale plants. Several commercial GTL and CTL plants based on the FT technology are in operation, whereas the very first large-scale plant through the methanol pathway is set to go on stream in late 2019 (Caspian News 2019). The fact that several FT based GTL plants have been in operation for several years makes it easier to estimate the general costs of such plants, compared to methanol based GTL plants, as there are no operating plants to draw experience from. As such, there was found little sense in e.g. conducting net present value analysis of a plant in the methanol pathway.

The third reason is regarding the focus of the case study being on a central plant versus many decentral plants. The economic question is also part of the reason why central GTL has been chosen over decentral GTL. Small-scale GTL plants are still very new, and have only been established to a small degree in recent years. Even though economy of scale may not hold for GTL plants, it is hard to tell whether small-scale plants are economically viable as economic data for small-scale plants is not yet readily available. Additionally, there are other advantages for central GTL over decentral GTL, as discussed in Section 3.4. The main advantage is that central GTL has a large heat output, which most likely can be utilized to a larger degree than heat from decentral plants as the decentral plants would be placed at the biogas plants, most likely far from district heating.

The fourth and final reason is regarding the focus on methane from biogas separation and not biogas methanation. As discussed in Section 3.1, as the case study is for a plant which is to go on stream in 2025, the biogas upgrading is assumed to happen almost entirely through separation. This is because it is expected that methanation will have a very small market share of the upgrading technologies in 2025.

Chapter 4

Funen as a Case Study

This chapter presents a case study of a central Fe-LTFT based GTL plant with biomethane from biogas separation, which is to go on stream in 2025 on Funen. The study is based upon the energy flows found in Figure 3.3 in Section 3.3.3. As it is a case study of a GTL plant, the flows from the syngas production segment and forward are used. These are summarized in Table 4.1. The assumption that all of the biomethane that is in the natural gas grid in 2025 can be used in the GTL plant of this case study is obviously unrealisitc. However it is used as a base value and lowering the amount of biomethane input flow would also lower all other flows as well. The only cost that might change due a smaller input is the investment cost per production capacity due to economies of scale, but as discussed in Section 2.5.1 there is uncertainty whether this has any influence at all. Therefore, it is here assumed that a smaller as well as a larger GTL plant than what is presented in this case study would have the same feasibility, if it could obtain the biomethane input for its capacity.

Energy Type	**Inputs**	**Outputs**
Methane	14.55	0
Hydrogen	0.17	0
Jet Fuel	0	6.04
Gasoline	0	3.63
Unrecovered Organics	0	0.09
Heat Recoverable	0	3.62
Heat Lost	0	0.74
Electricity	0	0.14
Other Products	0	0.45

TABLE 4.1: Summarization of the energy flows in and out of a Fe-LTFT based GTL plant with 14.55 PJ biomethane input. All values are in PJ.

The case study contains considerations regarding the costs and revenues of building a GTL plant in Odense and elaborates on what the requirements are for jet fuel prices, the production cost of biomethane and the biogas subsidies, to make such a plant feasible.

4.1 Plant Location

The first thing to consider for the case study is the location of the plant. There are mainly three things to consider for the plant location. These are the access to the natural gas grid, the access to a district heating grid and the distance to buyers of the fuel products.

As the plant is to be located on Funen, the amount of potential plant locations is quite limited. The plant needs access to a large district heating grid to be able to sell as much of its waste heat as possible. A table of the heat demand of the Funish district heating grids can be seen in Table H.1 in Appendix H.

As the recoverable heat output of the GTL plant is 3.62 PJ each year, it can be seen in Table H.1 that only the district heating grid in Odense is large enough to take it in. But not only does the overall heat demand of the grid have to be large enough to take in the heat, there also has to be a point of the grid, where the capacity is large enough to take in the large amounts of heat. This means that the GTL plant most likely has to be placed either at the coal CHP plant, or at least at a transmission line in the grid. A map of the transmission lines of the district heating grid in Odense can be seen in Figure I.1 in Appendix I .

In addition to access to the district heating grid, the GTL plant needs access to the natural gas grid. Due to the very large amount of gas that is required for the GTL plant, it will most likely have to be connected to the grid at the transmission level, or at the largest level of the distribution grid. A map of the transmission grid and the largest level of the distribution grid for natural gas can be seen in Figure J.1 in Appendix J.

Finally, the GTL plant has to be placed with local buyers of fuels in mind. The further away from the buyers the GTL plant is placed, the larger the cost of transporting the fuel will be. If there are large transport costs, the buyer may not be willing to pay the full price for the fuel.

Most likely, the jet fuel would be sold for use at either Kastrup Airport in Sealand, Eastern Denmark, or Billund Airport in Jutland, Western Denmark. The automobile fuels could be sold for use at any service station in Denmark. As the case study is for a plant on Funen, the placement of the GTL plant should be decided mainly based on the access to district heating and the natural gas grid, as the options are heavily limited due to these two requirements.

4.2 Heals Sales Potential

The second thing to consider, is the possibility of selling heat. The heat demand in Odense, similarly to the heat demand of the rest of Denmark, has large variations throughout the year. The winter period has a large demand compared to the summer, as shown in Figure 4.1 as the blue curve, where the heat demand of Odense in 2016 is depicted. Because of such a large demand in some periods, while not

in others, some heat producing sources will only be able to deliver heat to the district heating grid during the winter period, while others, the cheaper sources, produce all year round. As Odense has enough supply for its heating demand, the heat from the GTL plant will replace an existing source that is prioritized lower than the heat from the GTL plant.

One source that produces heat all year around is the waste combustion. The waste has to be combusted continously as there is a limit to how long the waste is allowed to be stored. Therefore, the excess heat from the GTL plant will not substitute any of that. However the excess heat from the GTL plant is high value heat due to its high temperature and will not need a heat pump to reach sufficient temperatures for the district heating grid. Therefore it is rated second, right after the heat from waste combustion. Third, fourth and fifth are heat produced from biomass, heat pumps and coal respectively (Fjernvarme Fyn 2018).

As the heat from the GTL plant is rated second, the production from it can be found as the area between the red curve and the green curve in Figure 4.1. The green curve is the heat produced from waste combustion, where the annual heat production from waste combustion has been equally distributed out over the whole year. The red curve is the heat production from the waste combustion and the excess heat from the GTL plant put together. Note how the red curve follows the blue curve in periods of low heat demand. Every hour where the heat demand is below 167.5 MW some of the heat that can be recovered at the GTL plant will not be used.

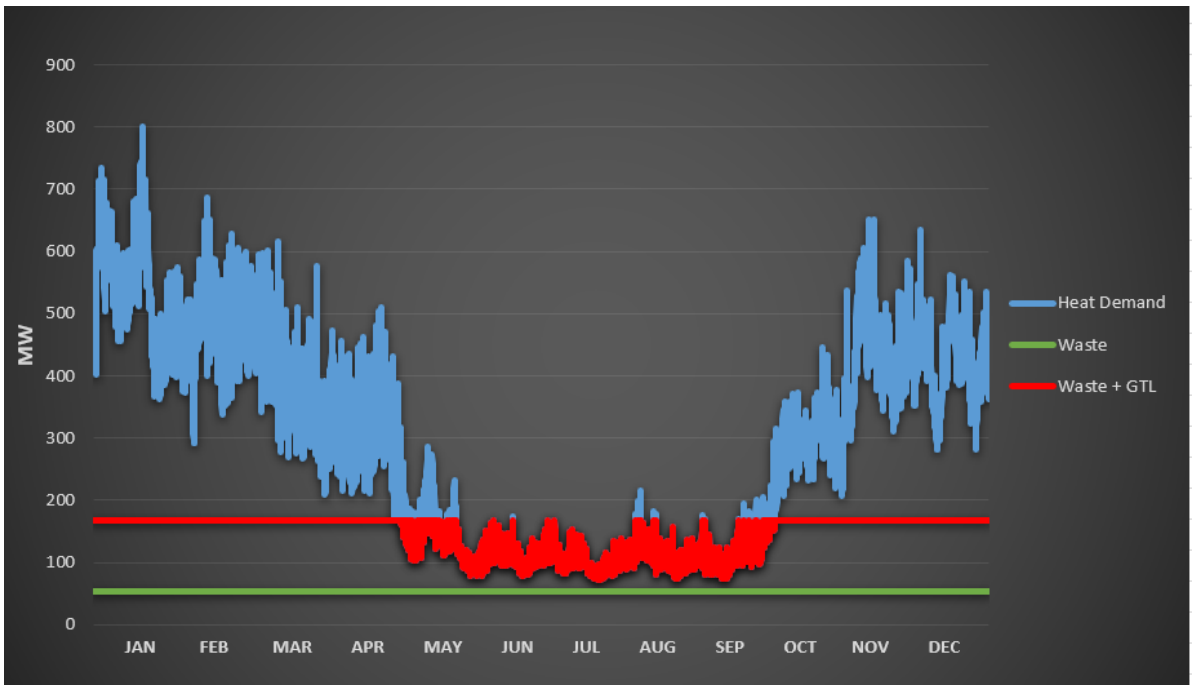

FIGURE 4.1: The blue line is the heat consumption in Odense, the green line is heat delivered to the district heating grid from waste combustion and the red line is heat delivered to the district heating grid from waste combustion and the GTL plant added together (Fjernvarme Fyn 2016, 2017).

As shown in Table 4.1, the heat which it is possible to recover from the GTL plant is expected to be 3.62 PJ during one year. However as the heat demand in some periods is too low to absorb all of the production, the actual amount of heat that can be sold to the district heating grid is only 2.91 PJ. This amount is, as mentioned, equal to the area between the red and green curve in Figure 4.1, assuming that the heat demand in Odense from 2025 and forward is equal to that of 2016. For further utilization of the recoverable heat, a seasonal storage would have to be implemented.

4.3 Base Scenario

With the amount of potential heat sales identified, a Base Scenario has been established. The main goal of the Base Scenario is to provide initial numbers for a feasibility calculation of a GTL plant in Odense. Afterwards the scenario is used to conduct sensitivity analysis on various parameters as well as creating other scenarios. To create the Base Scenario all used monetary values that are found in literature have been changed into a 2019 value by using the inflation rates of all years between the year of the source and 2019. The inflation rates have been found in DEA (2018*c*).

4.3.1 Costs

In this section the costs presented. The costs are split into investment cost, operation and maintenance cost and the feed cost.

4.3.1.1 Investment Cost

General considerations regarding the capital cost of FT based GTL plants were presented in Section 2.5.1. In this section, the estimation of a specific investment cost for the case study is discussed.

The plants which were previously presented in Table 2.2 are world-scale plants, and the economics of a plant with a fuel output of 9.67 PJ, which corresponds to an output of 4900 bpd, may not be relateable to these plants. Some producers of small-scale GTL plants do report cost from being competetive to being 1.5 times larger than for world-scale plants though (Brancaccio 2019).

Several studies have been conducted, trying to estimate the cost of mainly FT based coal-to-liquids and biomass-to-liquids plants. Many of these studies have been reviewed in Haarlemmer et al. (2014) and their costs normalized and compared. The main conclusion of the literature review is, that looking at a single price estimate of a X-to-liquids plant can lead to false expectations. It is found that the estimates in the literature vary greatly.

As such, the cost of a FT based GTL plant is hard to estimate, but a price is needed for this Base Scenario nonetheless. In Maitlis & de Klerk (2013) an economic analysis of a 17,000 bpd FT based GTL plant is

presented. Here, and investment cost of roughly 2 billion USD is estimated, making the cost roughly 118,000 USD/bpd. This cost is used in the Base Scenario, as it appears to be an acceptable compromise to make based on the previous discussion, and the more general discussion in Section 2.5.1.

Using this price per capacity and converting it to DKK in present value, the investment cost used in the Base Scenario becomes 4.17 billion DKK. A sensitivity analysis on the investment cost has been conducted in Section 4.6.

4.3.1.2 Operation and Maintenance Costs

General considerations regarding the operation and maintenance cost of FT based GTL plants were presented in Section 2.5.2. In this section, an estimation of specific operation and maintenance costs will be discussed.

The operation and maintenance costs can be split into two main categories: the cost of the feed to the plant and all of the other operation and maintenance costs. The cost of the feed is a topic of discussion and a focus of sensitivity analysis throughout this chapter. In this section, the focus is on the operation and maintenance costs. Just as the investment cost was estimated in Maitlis & de Klerk (2013), the operating and maintenance costs have also been estimated. For a 17,000 bpd plant, the cost is estimated to be 8.7 USD/barrel. Likewise, in Haarlemmer et al. (2014), the production costs were analysed. Here, the same conclusion as for the investment cost was reached, although the variance in the production costs was not found to be as large as the variance in the investment cost.

As the investment cost in the economic analysis from Maitlis & de Klerk (2013) was used, so is the operation and maintenance cost. This cost was estimated to be 8.7 USD/bpd, and when converted to DKK in present value, the annual operation and maintenance cost becomes 111 million DKK for the Base Scenario.

4.3.1.3 Feed Cost

The far most important cost, not just for the operation but in general, is the cost of the feed to the plant. The cost of the feed is the main expenditure in the lifetime of the plant. The feed inputs are as shown in Table 4.1 hydrogen and methane. It is in all scenarios assumed that the 0.17 PJ hydrogen input, which is an input to the refining of syncrude, is coming from the syngas production inside the plant itself and there is therefore no hydrogen cost.

When screening different studies, the found prices of biomethane are not necessarily the same, however they generally lie within a small range. A biomethane price from DEA (2018*b*) has been used for the Base Scenario as the analysis within this report covers multiple studies. The used biomethane price is a price for upgraded biogas produced from manure and straw and as it is from 2018, it has been adjusted into a 2019 value. This makes the biomethane price for the Base Scenario 141.1 DKK/GJ. In addition

to the price of the feed gas itself, the distribution, energy saving and emergency supply tariffs for gas also have to be paid. The highest paid tariff is the distribution tariff, but both the distribution tariff and the energy saving tariff both depend on the amount of gas bought. When buying an amount of gas as large as what is expected in this case study, these two tariffs are significantly lowered. The tariffs per cubic meter of gas can be found in Dansk Gas Distribution (2019). The energy tariff does not have to be paid, when the gas is used for a process where another product is produced, so the extra cost due to the tariffs is 5.8 DKK/GJ giving a total gas price of 146.9 DKK/GJ (PwC 2019). In the Base Scenario any subsidies on biogas have been neglected.

With an annual biomethane input to the GTL plant of 14.55 PJ, the cost of biomethane becomes 2.15 billion DKK annually. Sensitivity analysis on the biomethane price has been conducted in Section 4.4.

4.3.2 Revenues

All revenues are due to sales of the main product, jet fuel, and co-products such as gasoline and heat. While some products are not sellable, others have a decent value on the market. The products that are valued in this subsection are the products that are referred to as outputs in Table 4.1. Obviously both unrecovered organics and heat lost will not be given any sales value, as they are losses.

4.3.2.1 Jet Fuel Sales

With jet fuel being the main product of the GTL plant, receiving a decent payment for it is crucial for the plant to be feasible.

Due to the recent increase in awareness on the amount of CO_2 emissions from aviation, the willingness to pay for renewable jet fuel is significantly larger than the price of conventional jet fuel. In the Base Scenario, the willingness to pay found in Skøtt (2019) of 250 DKK/GJ is used. By selling the 6.04 PJ jet fuel, the annual revenue becomes 1.50 billion DKK.

As there is a large uncertainty on the exact willingness to pay for renewable jet fuel, a sensitivity analysis has been made on the parameter in Section 4.5.

4.3.2.2 Gasoline Sales

Gasoline is the main co-product of the GTL plant meaning it also has a large influence on the feasibility of the plant. However as there is no considerable demand for renewable gasoline, it has been assumed to be sold at a price equal to the existing market price of regular gasoline plus the CO_2 tariff. The CO_2 tariff is added as an increase to the selling price of the gasoline, because when the tax does not have to be paid by the buyer it means the selling price can be increased by an equal amount. The used gasoline price is the import price of gasoline, which in 2025 is expected to be 100.7 DKK/GJ in present value and

the CO_2 tax is 12.5 DKK/GJ, meaning the selling price of gasoline becomes 113.2 DKK/GJ (DEA 2018*c*, 2019*a*). The annual revenue by selling the 3.63 PJ gasoline is 407 million DKK.

With respect to creating an NPV calculation in Section 4.3.3, the gasoline price has an escalation rate of 1.66% each year, according to the average of the annual fuel price increase found in DEA (2018*c*).

4.3.2.3 Heat Sales

Another major co-product is the heat coming from the multiple processes of the GTL plant. The amount that can be sold was found in Section 4.2 and is 2.91 PJ annually.

The exact price of excess heat will in the future largely depend on how the legislation on the subject will be. As such, the amount of money that can be earned from sales of excess heat in the future can both increase and decrease relatively to today.

In the Base Scenario a price of 40.3 DKK/GJ in present value has been used, which is based upon a sales value of excess heat from 2015 (Tang 2016). This leads to an annual earning of 119 million DKK.

4.3.2.4 Electricity Sales

As mentioned in Section 3.2.3, due to the highly exothermal processes at the GTL plant it is possible to produce electricity through steam turbines. The majority of this is used internally, however some can be sold on the electricity market. The amount that can be sold annually is 0.14 PJ.

An electricity price for 2025 has been found in Dansk Energi (2017). In this source three scenarios were examined, all showing an increase in the electricity price towards 2025. In this project's Base Scenario the electricity price of the moderate scenario in the source has been used. In present value the price is 99.9 DKK/GJ, leading to an annual earning of 14 million DKK.

4.3.2.5 Other Sales

The 0.45 PJ of other products consist of roughly two-thirds fuel gas and one-third petrochemicals. Fuel gas is in the Base Scenario assumed to have no sales value.

Petrochemicals on the other hand are in literature described to have a value that is higher than the value of the produced conventional fuels (de Klerk 2011*a*). However as no exact price has been found on petrochemicals, it has been assumed to be equal to the gasoline import price of 100.7 DKK/GJ in the Base Scenario, see Section 4.3.2.1. The annual earning from petrochemicals is 14.3 million DKK.

4.3.3 Net Present Value

For the Base Scenario an NPV calculation has been made based upon the already mentioned annual cash flows. Furthermore a discount rate of 10% has been used. The discount rate is this high to cover the uncertainties and risk for investors, when engaging in this project. The lifetime of the plant has been assumed to be 25 years based upon a case study example in Maitlis & de Klerk (2013) and depreciation of the plant is assumed to happen linearly throughout the whole lifetime. Furthermore, for each year with profit a 22% corporate tax has to be paid (SkatteInform 2019).

In the Base Scenario none of the years have any profit giving an NPV result of -5.68 billion DKK. This is a very negative result which means that the project is far from feasible. However as many of the inserted costs and revenues used to calculate the NPV of the Base Scenario contain uncertainty, sensitivity analysis on the major parameters have been conducted in the following sections.

4.4 Sensitivity Analysis on the Biomethane Price

In this section, sensitivity analysis on the price of biomethane has been conducted. The main reason for doing sensitivity on this parameter is that the biomethane price of the future is very difficult to estimate. It depends a lot on the market demand for renewable methane, its production and upgrading method and whether the biogas production is subsidized or not.

4.4.1 Additional Scenarios

To have some reference points, two other scenarios have been established, in which the only difference compared to the Base Scenario is that they have a lowered price of biomethane.

4.4.1.1 Natural Gas Price Scenario

One scenario will be referred to as the NG Scenario, referring to the fact that the price of biomethane in the scenario is equal to that of natural gas. This scenario represents a highly subsidized situation. The reasoning for including this scenario is that when subtracting the biogas subsidies on biogas that is upgraded, which is on 107.6 DKK/GJ in 2019, from the biomethane price used in the Base Scenario, the price becomes lower than the price of natural gas (DEA 2019*b*). As it does not make sense to sell renewable gas cheaper than natural gas, the price has been made equal to the natural gas price.

The biomethane price used for this scenario is equal to a 10 years average of the natural gas price, when buying gas amounts larger than one million GJ. This price is in present value 54.4 DKK/GJ (DEA 2016*a*).

For the NG Scenario the NPV becomes 6.36 billion and it has a discounted payback period of only 6 years. For this scenario the GTL plant is very feasible.

4.4.1.2 Natural Gas Price Plus Certificate Scenario

Another scenario which will be referred to as the Certificate Scenario, also includes the natural gas price, but in addition to this an assumed biomethane certificate price of 1 DKK/Nm^3, equalling 27.8 DKK/GJ calculated from methane's lower heating value, has to be paid. This scenario is included because multiple gas consumers request renewable gas, which gives biomethane an additional value compared to natural gas. So the overall biomethane price in the Certificate Scenario is 82.3 DKK/GJ.

The NPV becomes 2.95 billion DKK with a discounted payback period of 10 years. As such, in this scenario the GTL plant is also feasible.

4.4.2 Net Present Value as a Function of the Biomethane Price

In Figure 4.2 a sensitivity analysis on the price of biomethane is shown. The x-axis is the price of biomethane in DKK/GJ and the y-axis is the NPV in million DKK. The blue curve shows how the NPV changes when changing the biomethane price.

The green, red and orange markers show the situation for the Base Scenario, the NG Scenario and the Certificate Scenario respectively. While the black marker shows where the NPV is equal to zero. This is the case with a biomethane price equal to 106.4 DKK/GJ.

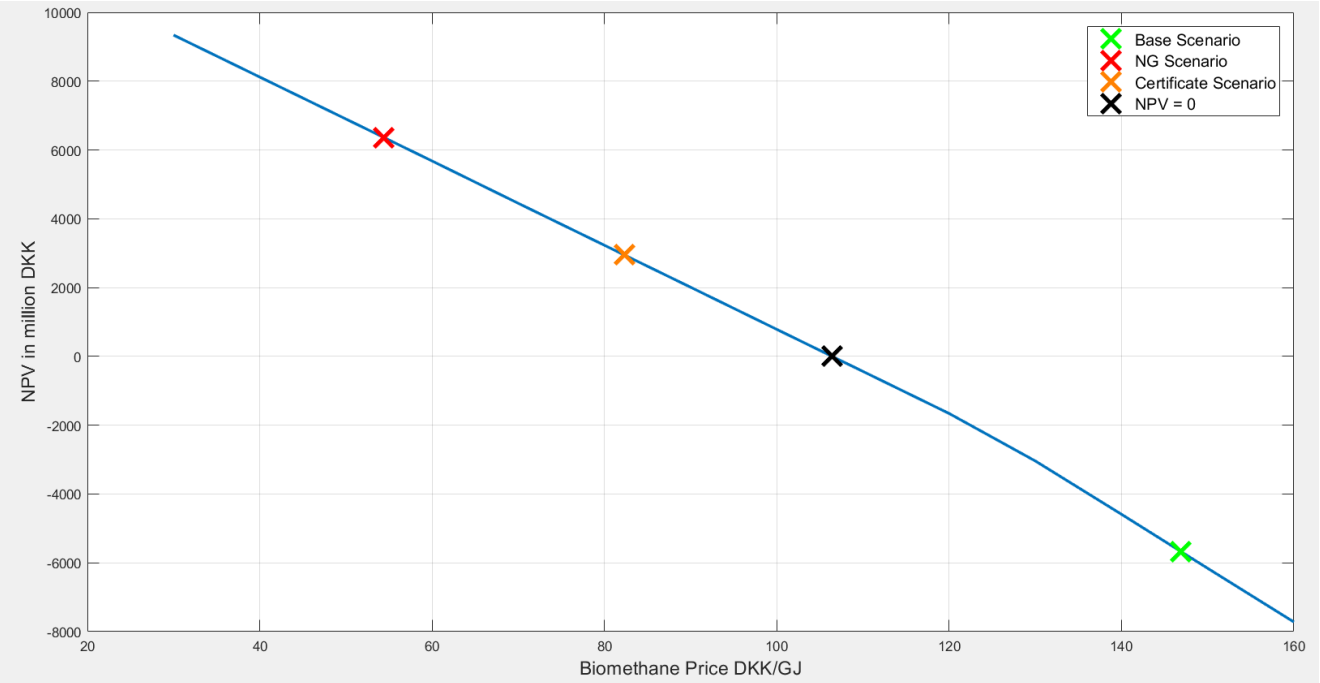

FIGURE 4.2: The blue curve shows how the NPV changes as a function of the biomethane price. The green, red and orange markers show where the Base Scenario, the NG Scenario and the Certificate Scenario are on the curve respectively. The black marker shows where the NPV is equal to zero.

Note how far away the Base Scenario is from being feasible, while the two other scenarios are feasible with a decent margin.

The difference between the biomethane price of the Base Scenario and the biomethane price necessary to make the NPV equal to zero is 40.5 DKK/GJ, meaning that this is the necessary subsidy on biogas to make the GTL plant feasible.

4.5 Sensitivity Analysis on the Jet Fuel Sales Price

The jet fuel price which has been used in the three scenarios so far is, as already stated, equal to the willingness to pay found in Skøtt (2019) which is 250 DKK/GJ. Due to this price being largely uncertain a sensitivity analysis on the jet fuel price has been conducted. It has been conducted on each of the three previously presented scenarios and can be found in Figure 4.3. The vertical dotted line and the vertical connected line are the expected conventional jet fuel price and the willingness to pay, respectively. The expected conventional jet fuel price is inserted as the import price expected in 2025 which is 97.8 DKK/GJ in present value (DEA 2018*c*).

The green curve shows the sensitivity analysis on the jet fuel price for the Base Scenario. The jet fuel price necessary for the NPV to become equal to zero and thus meaning the scenario is feasible is

348.7 DKK/GJ. This is 98.7 DKK/GJ above the mentioned willingness to pay and 250.9 DKK/GJ above the price of conventional jet fuel. As such, the willingness to pay has to increase quite a bit for this scenario to be feasible.

The red curve shows the sensitivity analysis for the NG Scenario. Here, the jet fuel price needed to get a feasible scenario is 123.4 DKK/GJ, this is 126.6 DKK/GJ below the willingness to pay and only 25.7 DKK/GJ above the price of conventional jet fuel. This means that the NG Scenario would be almost feasible by only receiving the price of conventional jet fuel and it needs less than half of the willingness to pay for renewable jet fuel to become feasible.

The orange curve shows the sensitivity analysis for the Certificate Scenario. The jet fuel price has to be 191.2 DKK/GJ for a feasible scenario. This is 58.8 DKK/GJ below the willingness to pay and 93.5 DKK/GJ above the conventional jet fuel price. This is once more suggesting that the scenario definitely is feasible and the willingness to pay can even be lowered by quite a bit, without changing the feasibility of it.

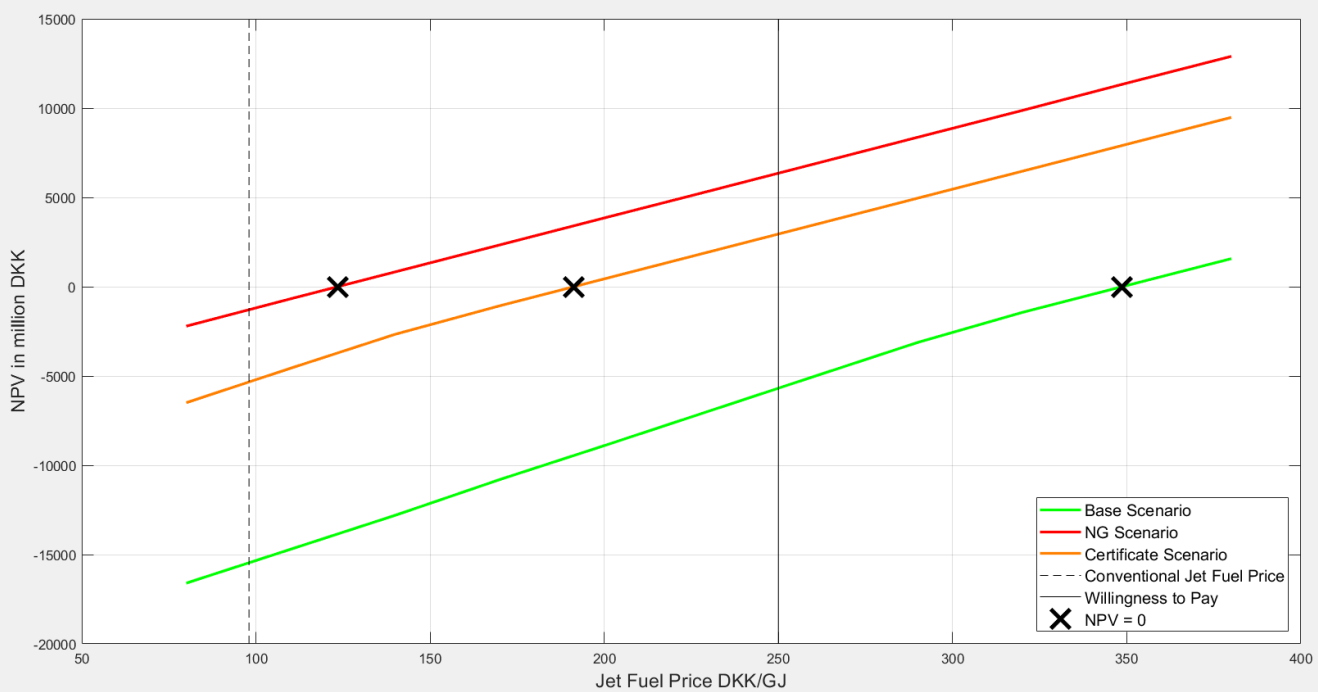

FIGURE 4.3: Sensitivity analysis on the jet fuel price is shown for both the Base Scenario as the green curve the NG Scenario as the red curve and the Certificate Scenario as the orange curve.

4.5.1 Aviation Price Increase

In addition to calculating what the prices for jet fuel should be in the different scenarios for them to have an NPV equal to zero, it has been calculated how much extra a passenger has to pay in each of the respective scenarios to fly on the produced renewable jet fuel.

To do so, the specific energy consumption for aviation is needed. It has been found in MJ per passenger kilometer (pkm) and is in 2025 expected to be approximately 1.35 MJ/pkm (Mathiesen et al. 2014).

The specific energy consumption is used to calculate the price increase per passenger kilometer for each of the three scenarios, compared to flying on conventional jet fuel.

The results of this are shown in the third column of Table 4.2.

Scenario	Jet Fuel Price Increase (DKK/GJ)	Passenger Kilometer Price Increase (DKK/pkm)	Copenhagen → London Price Increase (DKK)
NG Scenario	25.7	0.035	33.9
Certificate Scenario	93.5	0.126	123.5
Base Scenario	250.9	0.339	331.3

TABLE 4.2: The jet fuel price increase, the passenger kilometer price increase and price increase for going from Copenhagen to London, when looking at each of the three scenarios.

The first column shows which scenario it is, while the second column shows the already mentioned jet fuel price increase in each of the respective scenarios compared to the price on 97.8 DKK/GJ for conventional jet fuel.

The last column shows the price increase for a travel distance example. In this case from Copenhagen to London, which is a length of 978 km measured on Google Maps Distance Calculator.

Notice how the NG Scenario only has a price increase on a passenger kilometer of 0.035 DKK and a small increase in the travel price from Copenhagen to London of33.9 DKK. The Base Scenario on the other hand has a much larger price increase on a passenger kilometer of 0.339 DKK, which gives a price increase from Copenhagen to London of 331.3 DKK. The Certificate Scenario is in between with a price increase on a passenger kilometer of 0.126 DKK and a travel price increase from Copenhagen to London of 123.5 DKK.

4.6 Sensitivity Analysis on the Investment Cost

In Section 4.3.1.1 the investment cost of a GTL plant was estimated and due to the uncertainty of this estimation, sensitivity has been made on the parameter in this section. The NPV as a function of the investment cost is shown in Figure 4.4, with the investment cost being varied from half the initially used investment cost, 2.09 billion DKK, to the double of the initially used investment cost, 8.34 billion DKK.

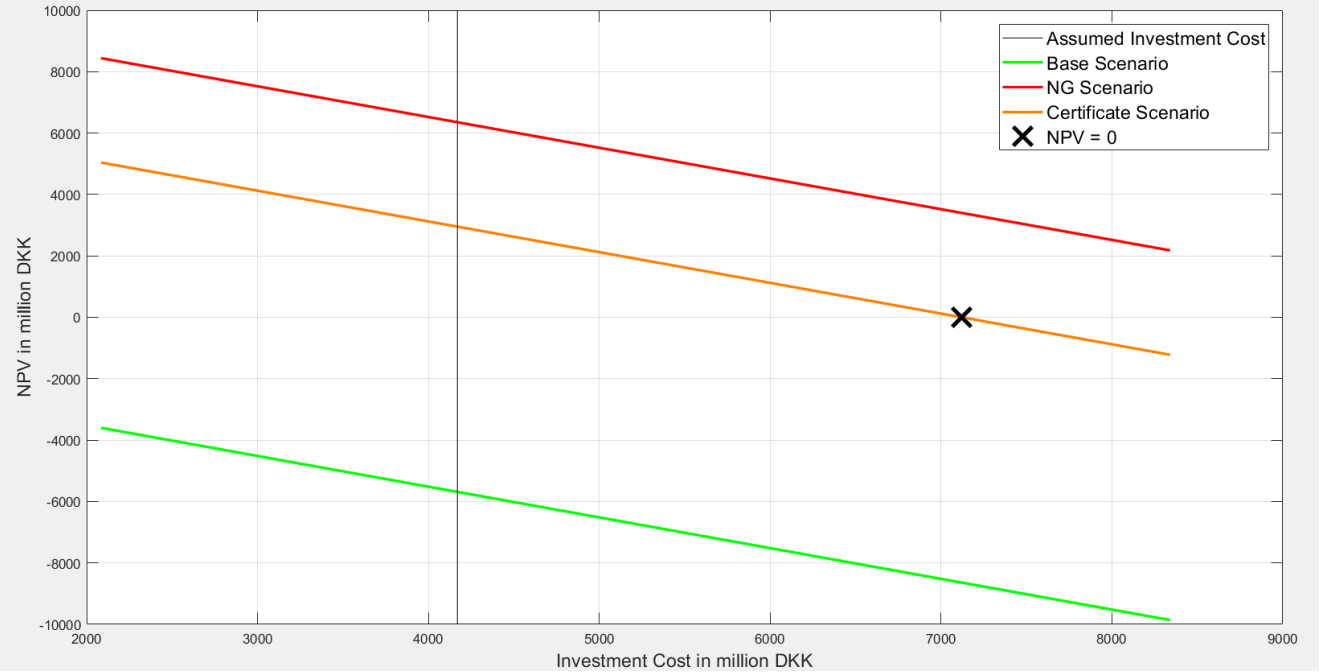

FIGURE 4.4: The NPV as a function of the investment cost is shown for the different scenarios. The green, red and orange lines show the sensitivity analysis for the Base, NG and Certificate Scenarios respectively.

Notice how only the Certificate Scenario changes between being feasible and unfeasible during this investment cost interval. This is expected as the investment cost is directly subtracted from the NPV. With an NPV equal to 2.95 billion DKK for the Certificate Scenario, and an investment cost of 4.17 billion DKK, doubling the investment cost gives a negative NPV of a little over a billion. The Certificate Scenario has an NPV equal to zero when the investment cost is 7.12 billion DKK meaning that the investment cost can increase by a fairly large amount without the scenario becoming unfeasible. The fact that the curves for none of the other scenarios cross the line where the NPV is equal to zero, shows that they are feasible and unfeasible by quite a large margin.

4.7 Discussion of the GTL Plant Feasibility

From the results outlined in this case study it is possible to deduct multiple things. First of all, the initial Base Scenario became very unfeasible, with an NPV of -5.68 billion DKK. However, changing the price of biomethane slightly has a massive influence on the feasibility, meaning the results of the two scenarios with a much lower biomethane prices, the NG Scenario and the Certificate Scenario, became feasible with their respective NPVs of 6.36 billion DKK and 2.95 billion DKK. It is difficult to say, which scenario is closest to being accurate and what the price of biomethane will be in the future, but it has been calculated that the necessary subsidy on biogas to make a plant feasible is 40.5 DKK/GJ. This does not seem like an unreasonably large subsidy compared to the mentioned overall

subsidy of today on upgraded biogas at 107.6 DKK/GJ, and it might be a reasonable subsidy for the future. In the energy agreement of 2018 an amount of 240 million DKK annually has been set aside to biogas production, with a focus on establishing more biogas production plants. So some sort of subsidy on biogas will continue to be given, but the exact size of it will depend on what the politicians decide. Furthermore, whether there will be subsidies on biogas throughout the whole lifetime of the GTL plant or only in the first period of its lifetime, will also have a large effect on the feasibility of the plant.

Secondly, the jet fuel price has a large influence on the feasibility of the GTL plant. The necessary price of jet fuel when biogas is unsubsidized was 348.7 DKK/GJ for the plant to become feasible, which means that the willingness to pay for sustainable jet fuel needs to increase to make a plant feasible, if biogas is unsubsidized. The feasibility relationship between the biomethane price and the jet fuel price is a factor of 2.41, meaning that if you have a scenario with a NPV of zero and then lower the biomethane price and the jet fuel price by 1 DKK and 2.41 DKK respectively, the NPV would still be zero. The linear relationship between the two parameters is shown in Figure 4.5 with the biomethane price on the x-axis and the jet fuel price on the y-axis. The black curve shows what the two parameters have to be, in order to get an NPV which is equal to zero. That is, every point on the curve can be seen as a scenario where the NPV is equal to zero, and the jet fuel price and the biomethane price in that scenario can be read as the y and x coordinate, respectively.

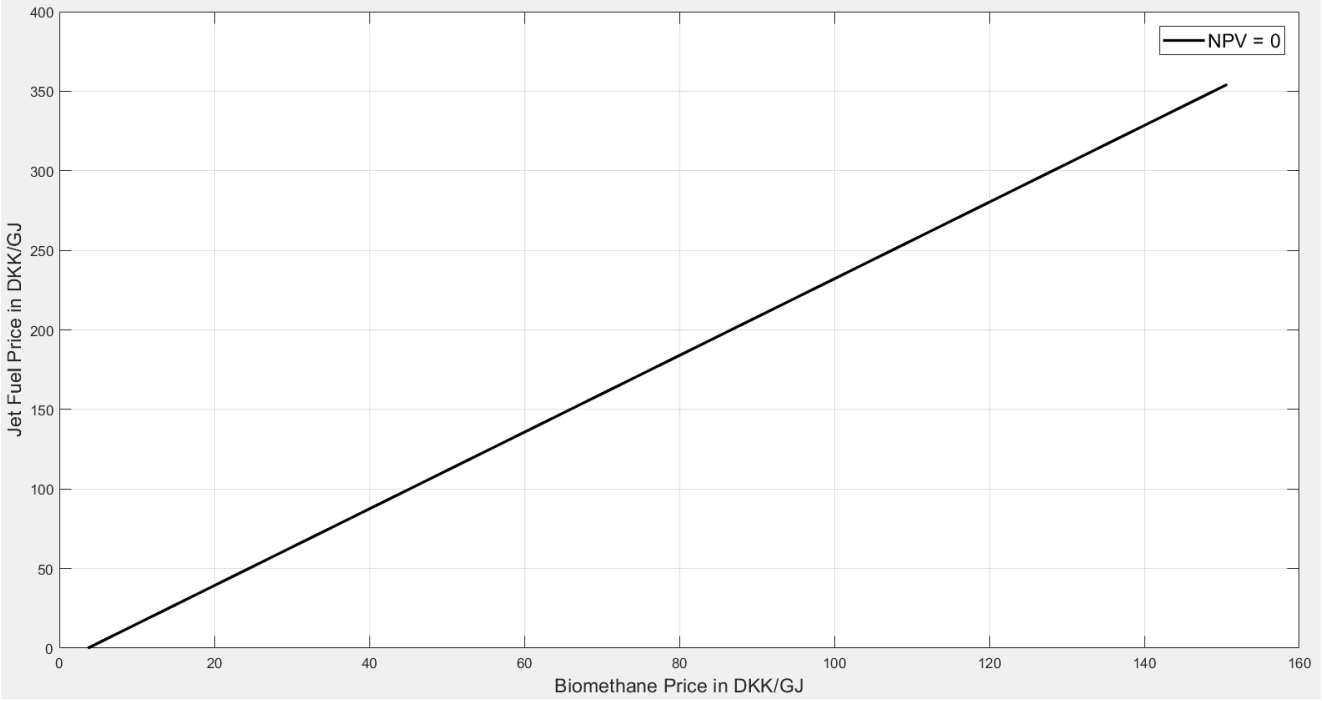

FIGURE 4.5: The black curve shows what the jet fuel price has to be at different biomethane prices to have an NPV equal to zero and thus a feasible GTL plant.

Notice how the curve crosses the x-axis in 3.69 DKK/GJ biomethane. This means that with a jet fuel price of 0 DKK/GJ and a biomethane price of 3.69 DKK/GJ, the GTL plant would be feasible due to the

sales of the co-products.

Speaking of the co-products, no sensitivity analysis have been made on these, however there is still an uncertainty on multiple of these parameters. The price of excess heat might become higher due to the larger importance of such heat in the district heating grid when coal is being phased out, leading to an additional revenue from these sales. Furthermore the gasoline has been assumed to not have any extra value compared to conventional gasoline, except for the extra value of no CO_2 tax, due to low demand on renewable gasoline. However, if ships and trucks are build in the future with the purpose of consuming this renewable, co-produced gasoline, the demand for it mmay rise.

Chapter 5

Conclusion

In this project, the pathways from biogas to jet fuel through the Fischer-Tropsch process, through methanol synthesis and through a Oxidative Coupling of Methane process have been analyzed. Furthermore, a case study of a gas-to-liquids plant on Funen, Denmark which is to go on stream in 2025 has been conducted.

In the analysis of the pathways, technologies available for the unique process segments of the pathways have been presented. For each unique process segment, the energy flows of the available technologies have been determined. For the technologies where looping of the various flows is used, the overall efficiencies of the processes have been determined. These efficiencies have been used in a developed excel tool to construct Sankey diagrams of the analyzed pathways. Sankey diagrams of six main pathways have been presented, and the key considerations for each pathway discussed. Additional considerations regarding central and decentral gas-to-liquids plants have been discussed separately.

For the Fischer-Tropsch pathways, the low-temperature Fischer-Tropsch process based on a iron catalyst was found to be the best for jet fuel production. When the pathway is based on biogas separation, an input of 15 PJ of biogas was found to give a jet fuel yield of 6.04 PJ, or 40.2% of the input, and a gasoline yield of 3.63 PJ, or 24.2% of the input, making the total transport fuel yield 9.67 PJ, or 64.4% of the input. For the methanol pathway when based on biogas separation, an input of 15 PJ of biogas was found to give a jet fuel yield of 4.08 PJ or 27.2% of the input, a gasoline yield of 1.30 PJ or 8.6% of the input and a diesel yield of 2.7 PJ or 18.0% of the input, making the total transport fuel yield 8.08 PJ or 53.8% of the input. As such, the Fischer-Tropsch pathway is found to be superior to the methanol pathway. However, these results are discussed, and the lack of data for both pathways and in especially the energy losses in the Fischer-Tropsch refining segment gives some uncertainty and the optimization of the methanol pathway. Therefore, the methanol pathway is likely to be closer to the Fischer-Tropsch pathway in reality.

Due to the higher fuel yield of the Fischer-Tropsch pathway amongst other reasons, the case study was choosen to be based on a central plant with the low-temperature Fischer-Tropsch process based on a iron catalyst. As the case study was only a case study of the gas-to-liquids plant, the energy flows in the biogas upgrading segment were not included. The energy flows of the case study were 14.55 PJ

of biomethane and 0.17 PJ of hydrogen as inputs, while the outputs were 6.04 PJ of jet fuel, 3.63 PJ of gasoline, 0.09 PJ of lost organics, 3.62 PJ of recoverable heat, 0.74 PJ of lost heat, 0.14 PJ of electricity and 0.45 PJ of other products.

In the case study three scenarios were established. One scenario known as the Base Scenario, which was an unsubsidized scenario where the biomethane price of 146.9 DKK/GJ was equal to the price of producing, upgrading and transporting the biogas/biomethane, resulted in an NPV calculation of -5.68 billion DKK. This means that the GTL plant would be unfeasible with no subsidies. Two other scenarios where large subsidies were assumed both resulted in a feasible GTL plant. They were introduced as the NG Scenario, with a biomethane price of 54.4 DKK/GJ, and the Certificate Scenario, with a biomethane price of 82.3 DKK/GJ, and resulted in NPV calculations of 6.36 billion DKK and 2.95 billion DKK respectively. Furthermore, the necessary subsidy for the GTL plant to be feasible at an NPV of zero was found. This was found to be 40.5 DKK/GJ, giving a biomethane input price of 106.4 DKK/GJ.

Sensitivity analysis was also conducted on the willingness to pay for renewable jet fuel and it was found that the necessary jet fuel price for the GTL plant to be feasible in the Base Scenario is 348.7 DKK/GJ. When relating this directly to the cost of flying, a price increase compared to flying on conventional fuel of 0.339 DKK per passenger kilometer was found, or when relating it to the 978 km flight from Copenhagen to London, it would be a price increase of 331.3 DKK. For the NG Scenario and Certificate Scenario the price increase were 0.035 and 0.126 DKK per passenger kilometer, respectively and the price increase from Copenhagen to London would be 33.9 and 123.5 DKK respectively.

Furthermore it was found that the relationship between the biomethane buying price and the jet fuel selling price was a factor of 2.41. This means that when having a feasible scenario with an NPV calculation equal to zero and then increasing the price of biomethane by 1 DKK/GJ, the price of jet fuel would also have to be increased by 2.41 DKK/GJ, for the NPV to still equal zero.

To sum it all up, the production of sustainable jet fuel from biogas can be viable, but there must be a willingness to pay for the sustainable jet fuel which is significantly larger than the price of conventional jet fuels or the production of sustainable jet fuel must be subsidized by a sufficient amount somewhere in its production chain.

Chapter 6

Perspectives Towards 2050

This project ends with a few considerations regarding a vision of powering the entire Danish aviation sector with FT based sustainable jet fuel in 2050.

6.1 The Aviation Fuel Demand

In 2017 the demand for energy in the aviation sector was 43.6 PJ (DEA 2018*a*). Several energy system studies have made estimations of the demand of the Danish aviation sector in 2050. In the Danish Energy Agency's study from 2014, (*da:Energiscenarier frem mod 2020, 2035 og 2050*), the demand for fuel in the aviation sector is estimated to be 37.7 PJ in 2050, whilst it is 31.3 PJ in the IDA's Energy Vision (Mathiesen et al. 2015).

Several estimations have also been made in the Coherent Energy and Environmental System Analysis (CEESA). In the background report, CEESA 100% Renewable Energy Transport Scenarios Towards 2050, extensive sensitivity analysis has been conducted on parameters affecting the fuel demand, here amongst technology improvements and transport demand growth. Depending on the scenario, the fuel demand of the aviation sector is estimated to be between roughly 20 and 40 PJ, but the demand that is comparable to the others is the 40 PJ (Mathiesen et al. 2014). For all of the studies, an increase in the transport demand but also an increase in the aviation efficiency is expected, which keeps the fuel demand of the aviation sector at a slightly lower level than it is today (Mathiesen et al. 2014, 2015). For the simplicity of this discussion, the demand for jet fuel in 2050 has been assumed to be 35.0 PJ.

6.2 The Danish Biogas Potential

In order to produce such a large amount of jet fuel through the FT pathway from biogas, a large amount of biogas is needed. However, there is a limit to the amount of biogas that can be produced. Several Danish studies have tried to estimate the amount of biogas that could potentially be produced from

various waste sources, but also the amount that could be produced when including e.g. energy crops, and the overall bioenergy potential of Denmark.

Published studies generally seem to agree, that the amount of biomass available for energy purposes in Denmark is roughly 250 PJ/y (Mathiesen et al. 2014, Gylling et al. 2012, DEA 2014). However, the amount of this which can efficiently be used for biogas production is lower. In 2017, a study by Henrik B. Møller analyzed a few scenarios for the Danish biogas potential. The most ambitious of these, whilst still only using waste products, estimated that the Danish biogas potential is 70 PJ/y, and 105 PJ/y if methanation is included. Based on this and additional calculations made by Aarhus University, the community of the Danish gas distributors, 'Grøn Gas Danmark', estimated that a maximum production of 80 PJ/y biomethane is realistic and achievable by 2035, under the right circumstances (DEA 2018*b*, Møller 2017, GrønGasDanmark 2019). As such, biogas is a fairly large resource for the future Danish energy system, and it can be further increased if e.g. energy crops and other biomass is also used for biogas production, even though it is not as ideal.

6.3 A FT based GTL Plant for the 2050 Fuel Demand

To cover the Danish demand for jet fuel in 2050, a world-scale GTL plant is needed. In Section 3.3.3 it was shown, that a Fe-LTFT based GTL plant with an input of 14.55 PJ of biomethane could produce 6.04 PJ of jet fuel and 3.63 PJ of gasoline. This is a input to jet fuel yield of 41.5% and an input to gasoline yield of 24.9%. Using the input to jet fuel yield and the demand of 35.0 PJ of jet fuel in 2050, the required input to a GTL plant in 2050 is calculated to be 84.3 PJ of biomethane. Along with the 35.0 PJ of jet fuel, 21.0 PJ of gasoline is produced. In the barrels per day unit (bpd) this makes the size of the GTL plant roughly 28,400 bpd.

6.3.1 Biogas Limitations and Alternative Sources

There are several complications to consider with a plant of this size in the Danish energy system. One of the most notable complications is the large use of biomethane. As mentioned in Section 6.2, the biomethane potential from waste sources has been estimated to be 105 PJ/y, of which the danish gas distributors consider 80 PJ/y to be realistic to use. As such, a production of sustainable jet fuel in Denmark to cover the demand from the Danish aviation sector would require a very large amount of the Danish biogas, if not all of it and a bit more. For the GTL plant to be able to acquire this amount of biogas in a free market would most likely be impossible. Legislation would be needed to secure the feed for the GTL plant.

This would however leave other sectors which draw benefit from using biogas in an undesirable situation. The most notable one here is the electricity sector. In a future energy system which has largely

been electrified, the dependency on fluctuating electricity sources is expected to be big. There are two main concerns with this. The first is that there needs to be some other way to provide electricity when the production from wind turbines and solar panels is low. For the future, both international connections and combined heat and power plants with biomass are expected to be important in providing the base load. However, the second concern is a more rapid response to fluctuations and here biomass-fired plants are too slow in their response. A more ideal solution for this problem is gas turbines due to their low investment costs (DEA 2016*b*) and faster response times. Gas turbines can only be used if there is a feed gas available though.

Due to both GTL plants and the back-up electricity sector needing gas inputs, it is likely that there will be a shortage of biogas in the future. There are mainly three ways to provide additional gas resources. The first way is increasing the production of biogas through the inclusion of energy crops in the biogas plant, however this is not ideal as the growth of energy crops will use land space. The second way is through gasification of other biomass, e.g. wood, to obtain gasified carbon that can either be used directly with additional hydrogen in e.g. a FT process, or be further hydrotreated to produce methane for other purposes. However, the direct combustion of wood is generally more energy efficient than gasifying it (DEA, Energinet 2019). The third and final way is to use carbon capture from the air or a point source as a source of carbon, and use it in the same way the carbon from biomass gasification could be used. Although the technology is very expensive today, it comes with several advantages for a future energy system (Ishimoto et al. 2017). The main advantage is that the technology is completely independent of biomass, and as such does not tear on the very limited resource. Another main advantage is an excellent synergy with the electricity sector where both carbon capture, and electrolysis for hydrogen, can be used to balance the electricity grid. When there is plenty of electricity from the renewable sources, hydrogen and carbon can be produced and used for e.g. methane production, and when there is a low amount of electricity from e.g. wind turbines, the produced and stored methane can be used in gas turbines to provide back-up electricity.

6.3.2 GTL Plant Gasoline Utilization

Another big consideration for a large production of sustainable jet fuel in the future, is how the by-products of the process should be utilized. As mentioned previously, a FT based GTL plant which produces 35.0 PJ of jet fuel will also produce 21.0 PJ of gasoline, and this gasoline has to be utilized.

Today, the only part of the transport sector which is powered by gasoline is cars and small vans (Mathiesen et al. 2015). This makes these modes of transport the most straight forward market for gasoline in the future. However, in the various research projects regarding the design of the Danish energy system in the future, cars and small vans are largely expected to be electrified (Mathiesen et al. 2015, 2014). As such, if a world-scale FT based GTL plant for jet fuel production is to be implemented in 2050, the powering of the rest of the transport sector may have to be rethought. In the aforementioned

study by the Danish Energy Agency, the fuel demand for trucks is expected to be 39.6 PJ in 2050, with 22.6 PJ being supplied by biogas, 15.9 PJ by synthetic diesel and 1.1 PJ being electrified. And in the IDA study, the demand is expected to be 28.6 PJ, with 14.3 PJ being supplied by bio-electrofuels such as methanol or DME, and 14.3 PJ being supplied by CO_2-electrofuels (Mathiesen et al. 2015). As trucks are already expected to be powered by synthetic fuels to a large degree, the trucking sector may be the most obvious mode of transportation to power with the gasoline byproduct of a jet fuel GTL plant.

6.3.3 GTL Plant Heat Utilization

The final big consideration which is commented upon, is the utilization of recoverable heat from a future GTL plant. In addition to the transport fuels, there will also be a 21.0 PJ output of recoverable heat which can used in district heating. As there was complications for Odense in taking in the recoverable heat from a much smaller GTL plant, as shown in Section 4.2, only Copenhagen is considered to have a chance in utilizing the surplus heat of a larger GTL plant in the future.

The district heating company HOFOR reports that it delivers 99% of the district heating demand in Copenhagen, and 40% of the district heating demand of Copenhagen and its suburbs (HOFOR 2019*a*). Additionally, in their annual report for 2018, HOFOR reported a district heating delivery of 15.26 PJ (HOFOR 2019*b*). Using these figures, the district heating demand of Copenhagen and its suburbs is estimated to be 38.15 PJ.

With a recoverable heat production of 21.0 PJ from the GTL plant, and a heat demand of 38.15 PJ in Copenhagen and its suburbs, a future plant in Copenhagen would meet larger complications than the plant in the case study of 2025. In the case study, the GTL plant had a recoverable heat production of 3.62 PJ and the demand of Odense was in 2016 9.17 PJ (Fjernvarme Fyn 2016). As the amount of heat which can be delivered by the GTL plant compared to the demand is larger for Copenhagen than in the case study of Odense in 2025, there are likely to be larger complications in regards to the seasonal variations of the district heating demand. Ideally, there would be a solution to this complication in 2050 in the form of a viable heat storage technology. Alternatively, it may be worthwhile to build two or several smaller plants instead of one large plant to utilize the heat better, even though the benefit of economies of scale would be reduced.

Bibliography

Andriani, D., Wresta, A., Atmaja, T. D. & Saepudin, A. (2013), 'A review on optimization production and upgrading biogas through CO_2 removal using various techniques'.

Angelidaki, I., Treu, L., Tsapekos, P., Luo, G., Campanaro, S., Wenzel, H. & Kougias, P. (2018), 'Biogas upgrading and utilization: Current status and perspectives', *Biotechnology advances* **36**.
URL: *https://www-sciencedirect-com.proxy1-bib.sdu.dk/science/article/pii/S0734975018300119*

Ashraf, Muhammad Tahir & Bastidas-Oyanedel, J.-R. . S. J. (2015), 'Conversion efficiency of biogas to liquids fuels through fischer-tropsch process'.
URL: *https://www.researchgate.net/publication/280444540_Conversion_Efficiency_of_Biogas_to_Liquids_Fuels_through_Fischer-Tropsch_Process*

ASTM (2019), *ASTM D7566: Standard Specification for Aviation Turbine Fuel Containing Synthesized Hydrocarbons*, 19 edn, ASTM.
URL: *https://www.astm.org/Standards/D7566.htm*

Avinor (2014), 'Electric aviation'.
URL: *https://avinor.no/en/corporate/community-and-environment/electric-aviation/electric-aviation*

Bauer, F., Hulteberg, C., Persson, T. & Tamm, D. (2013), Biogas upgrading - review of commercial technologies, Technical report, Lund University.
URL: *http://www.sgc.se/ckfinder/userfiles/files/SGC270.pdf*

Bertau, M., Offermanns, H., Plass, L., Schmidt, F. & Wernicke, H.-J. (2014), *Methanol: The Basic Chemical and Energy Feedstock of the Future*, Springer Verlag Berlin Heidelberg.
URL: *https://link-springer-com.proxy1-bib.sdu.dk/book/10.1007%2F978-3-642-39709-7*

Brancaccio, E. (2019), 'Gtl: Small scale and modular technologies for gas to liquid industry'.
URL: *http://www.oil-gasportal.com/gtl-small-scale-and-modular-technologies-for-gas-to-liquid-industry/*

Caspian News (2019), 'Giant gas plant ready to open in turkmenistan'.
URL: *https://caspiannews.com/news-detail/giant-gas-plant-ready-to-open-in-turkmenistan-2019-4-8-42/*

Center, D. G. (2018), 'Gasselskabernes oversigtskort'.
URL: *https://www.dgc.dk/sites/default/files/filer/dokumenter/Gasledninger_Danmark_nov2016.pdf*

Cryo Pur (2019), 'Technology'.
URL: *http://www.cryopur.com/en/technology/*

Dahl, P. J., Christensen, T. S., Winther-Madsen, S. & King, S. M. (2014), 'Proven autothermal reforming technology for modern large-scale methanol plants'.
URL: *https://www.topsoe.com/sites/default/files/proven_atr_technology_for_modern_large_scale_methanol_plants_nitrogen_syngas_conference_feb_2014.ashx__0.pdf*

Danish Gas Technology Centre (2018), 'Estimering af omkostninger til opgradering af biogas'.
URL: *https://www.dgc.dk/sites/default/files/filer/publikationer/N1804_biogas_opgradering_priser.pdf*

Dansk Energi (2017), Elprisscenarier 2020-2035, Technical report, Dansk Energi.
URL: *https://www.danskenergi.dk/udgivelser/analyse-nr-27-elprisscenarier-2020-2035-2017-udgave*

Dansk Gas Distribution (2019), 'Distributionstariffer'.
URL: *http://www.danskgasdistribution.dk/media/1269/fyn-distributionstariffer-01-19-ny-version.pdf*

de Klerk, A. (2011*a*), *Fischer-Tropsch refining*, 1 edn, Germany Wiley-VCH.

de Klerk, A. (2011*b*), 'Fischer–tropsch fuels refinery design', *Energy Environ. Sci.* **4**, 1177–1205.
URL: *http://dx.doi.org/10.1039/C0EE00692K*

DEA (2013), Biogas i danmark - status, barrier og perspektiver, Technical report, Danish Energy Agency.
URL: *https://ens.dk/sites/ens.dk/files/Bioenergi/biogas_i_danmark_-_analyse_2014-final.pdf*

DEA (2014), Analyse af bioenergi i danmark, Technical report, Danish Energy Agency.
URL: *https://ens.dk/ansvarsomraader/bioenergi/bioenergi-i-danmark/analyse-af-bioenergi-i-danmark*

DEA (2016*a*), 'Eu - gaspriser - industri (2007-2017)'.
URL: *https://ens.dk/sites/ens.dk/files/Statistik/eu28-gas-industri2007-2017.xlsm*

DEA (2016*b*), Technology data for energy plants for electricity and district heating generation, Technical report, Danish Energy Agency, Energinet.
URL: *https://ens.dk/service/fremskrivninger-analyser-modeller/teknologikataloger/teknologikatalog-produktion-af-el-og*

DEA (2018*a*), Energistatistik 2017, Technical report, Danish Energy Agency.
URL: *https://ens.dk/sites/ens.dk/files/Statistik/pub2017dk.pdf*

DEA (2018*b*), Perspektiver for produktion og anvendelse af biogas i danmark, Technical report, Danish Energy Agency.
URL: *https://ens.dk/sites/ens.dk/files/Bioenergi/perspektiver_for_produktion_og_anvendelse_af_biogas_i_danmark_november_2018.pdf*

DEA (2018*c*), Samfundsøkonomiske beregningsforudsætninger for energipriser og emissioner, oktober 2018, Technical report, Danish Energy Agency.
URL: *https://ens.dk/sites/ens.dk/files/Analyser/samfundsoekonomiske_beregningsforudsaetninger_for_energipriser_og_emissioner_endelig2_justeret_gastabel_og_tekst.pdf*

DEA (2019*a*), 'Energistyrelsens prisdatabase'.
URL: *https://ens.dk/service/statistik-data-noegletal-og-kort/energipriser-og-afgifter*

DEA (2019*b*), 'Oversigt støttesatser 2019'.
URL: *https://ens.dk/ansvarsomraader/stoette-til-vedvarende-energi/biogas/stoette-til-opgradering-og-rensning-af-biogas*

DEA, Energinet (2019), 'Technology data for renewable fuels'.
URL: *https://ens.dk/sites/ens.dk/files/Analyser/technology_data_for_renewable_fuels_-_0001.pdf*

DMT Environmental Technology (2019), 'Product description carborex ms, biogas upgrading to biomethane'.
URL: *https://www.dmt-et.com/products/carborex-product-description/*

Dutcher, B., Fan, M. & Russell, A. G. (2013), 'Amine-based co_2 capture technology development from the beginning of 2013—a review'.
URL: *https://pubs-acs-org.proxy1-bib.sdu.dk/doi/10.1021/am507465f*

EMD International A/S (2014), Strategisk energiplan fyn – den indledende kortlægning af fjernvarmenet og gasnet på fyn, Technical report, Energiplan Fyn.
URL: *http://www.energiplanfyn.dk/wp-content/uploads/2016/11/Indledende_kortl%C3%A6gning _infrastruktur.pdf*

Enerdata (2014), 'The future of gas-to-liquids (gtl) industry'.
URL: *https://www.enerdata.net/publications/executive-briefing/future-gas-liquid-gtl-industry.html*

Engineering New Zealand (n.d.), 'Motunui synthetic fuels plant'.
URL: *https://www.engineeringnz.org/our-work/heritage/heritage-records/motunui-synthetic-fuels-plant/*

Fjernvarme Fyn (2016), 'Fvf varmebehov 2016'. Excel dokument.

Fjernvarme Fyn (2017), 'Årsberetning 2017'.
URL: *https://www.fjernvarmefyn.dk/media/2660/c-users-gl-desktop-aarsberetning2017-aarsberetning_2017.pdf*

Fjernvarme Fyn (2018), 'Heat recovery at fjernvarme fyn'.
URL: *https://datacenterindustrien.dk/wp-content/uploads/2_Fjernvarme-Fyn-Heat-Recovery.pdf*

GasTechno (2019), 'Gastechno homepage'.
URL: *https://gastechno.com/*

Ghaib, K., Nitz, K. & Ben-Fares, F.-Z. (2016), 'Chemical methanation of co2: A review', *ChemBioEng Reviews* **3**(6), 266–275.
URL: *https://onlinelibrary.wiley.com/doi/abs/10.1002/cben.201600022*

Greyrock (2019), 'Greyrock homepage'.
URL: *http://www.greyrock.com/*

GRTgaz (2014), 'Etude portant sur l'hydrogène et la méthanation comme procédé de valorisation de l'électricité excédentaire'.
URL: *http://www.grtgaz.com/fileadmin/engagements/documents/fr/Power-to-Gas-etude-ADEME-GRTgaz-GrDF-complete.pdf*

GrønGasDanmark (2019), 'Baggrundsnotat: Grøn gas er fremtidens gas'.
URL: *https://grongasdanmark.dk/sites/grongasdanmark.dk/files/media/dokumenter/Baggrund%20til%20faktaark%20-%20Gr%C3%B8n%20gas%20er%20fremtidens%20gas_0.pdf*

Gylling, M., Jørgensen, U. & Bentsen, N. S. (2012), +10 mio. tons planen - muligheder for en øget dansk produktion af bæredygtig biomasse til bioraffinaderier, Technical report, Aarhus Universitet, Københavns Universitet.
URL: *http://dca.au.dk/fileadmin/DJF/Bioraf/ti-mio-plan.pdf*

Götz, M., Lefebvre, J., Mörs, F., Koch, A. M., Graf, F., Bajohr, S., Reimert, R. & Kolb, T. (2016), 'Renewable power-to-gas: A technological and economic review', *Renewable Energy* **85**, 1371 – 1390.
URL: *http://www.sciencedirect.com/science/article/pii/S0960148115301610*

Haarlemmer, G., Boissonnet, G., Peduzzi, E. & Setier, P.-A. (2014), 'Investment and production costs of synthetic fuels - a literature survey', **66**, 667–676.
URL: *https://www-sciencedirect-com.proxy1-bib.sdu.dk/science/article/pii/S0360544214001157*

Hjuler, K. & Aryal, N. (2017), Review of biogas upgrading, Technical report, Danish Gas Technology Centre.
URL: *https://www.dgc.dk/sites/default/files/filer/publikationer/R1704_FutureGas_Biogas_Upgrading.pdf*

HOFOR (2019*a*), 'Bæredygtig omstilling på amagerværket'.
URL: *https://www.hofor.dk/baeredygtige-byer/amagervaerket/baeredygtig-omstilling-paa-amagervaerket/*

HOFOR (2019*b*), 'Årsrapport 2018'.
URL: *https://www.hofor.dk/wp-content/uploads/2019/05/HOFOR-Aarsrapport-2018_Samlet_lav-endelig-12.-april-2019_rettet-030519.pdf*

Hoyer, K., Hulteberg, C., Jernberg, J. & Nørregård, O. (2016), Biogas upgrading - technical review, Technical report, Energiforsk.
URL: *http://vav.griffel.net/filer/C_Energiforsk2016-275.pdf*

InvestmentMine (2019), '3 month ruthenium prices and price charts'.
URL: *http://www.infomine.com/investment/metal-prices/ruthenium/3-month/*

InvestmentMine (2019a), '1 week nickel prices and price charts'.
URL: *http://www.infomine.com/investment/metal-prices/nickel/1-week/*

InvestmentMine (2019b), '1 week cobalt prices and price charts'.
URL: *http://www.infomine.com/investment/metal-prices/cobalt/all/*

Ishimoto, Y., Sugiyama, M., Kato, E., Moriyama, R., Tsuzuki, K. & Kurosawa, A. (2017), 'Putting costs of direct air capture in context'.
URL: *https://www.american.edu/sis/centers/carbon-removal/upload/FCEA_WPS002_Ishimoto.pdf*

LanzaTech (2019), 'Lanzatech'.
URL: *http://www.lanzatech.com/*

Lecker, B., Illi, L., Lemmer, A. & Oechsner, H. (2017), 'Biological hydrogen methanation – a review', *Bioresource Technology* **245**.
URL: *https://www-sciencedirect-com.proxy1-bib.sdu.dk/science/article/pii/S0960852417314906*

Lemvig Biogas (2019), 'Grundlæggende viden om biogas'.
URL: *https://lemvigbiogas.com/viden-om-biogas/*

Linde Engineering (2019*a*), 'Gemini - oxidative coupling of methane (ocm)'.
URL: *https://www.linde-engineering.com/en/process_plants/petrochemical-plants/oxidative-coupling-methane/index.html*

Linde Engineering (2019*b*), 'Ethylene from natural gas'.
URL: *https://www.linde-engineering.com/en/about_linde_engineering/collaborate_innovate_deliver/innovate/ethylene-from-natural-gas/*

Maitlis, P. M. & de Klerk, A. (2013), *Greener Fischer-Tropsch Processes for Fuels and Feedstocks*, John Wiley & Sons, Incorporated.
URL: *https://ebookcentral.proquest.com/lib/sdub/detail.action?docID=1120964*

Mathiesen, B. V., Connolly, D., Lund, H., Nielsen, M. P., Schaltz, E., Wenzel, H., Bentsen, N. S., Felby, C., Kaspersen, P. S., Ridjan, I. & Hansen, K. (2014), Ceesa 100% renewable energy transport scenarios towards 2050, Technical report, The Danish Council for Strategic Research Programme Commissioned on Sustainable Energy and Environment.

URL: *https://www.researchgate.net/publication/286325394_CEESA_100_Renewable_Energy_Transport_Scenarios_towards_2050*

Mathiesen, B. V., Lund, H., Hansen, K., Ridjan, I., Djørup, S. R., Nielsen, S. & Østergaard, P. A. (2015), Ida's energy vision 2050, Technical report, Department of Development and Planning, Aalborg University.
URL: *https://vbn.aau.dk/ws/portalfiles/portal/222230514/Main_Report_IDAs_Energy_Vision_2050.pdf*

Møller, H. B. (2017), 'Biogas fra landbrugsråvarer: Så meget mere kan vi producere'.
URL: *https://www.danskgasforening.dk/sites/default/files/inline-files/GTD2017_Henrik_Moller.pdf*

Primus GE (2019), 'Primus ge homepage'.
URL: *https://www.primusge.com/*

PwC (2019), 'Godtgørelse af energiafgift på olie, gas og kul'.
URL: *https://www.pwc.dk/da/services/skat/afgifter/energiafgift-oli-gas-kul.html*

Rapier, R. (2010), 'Inside shell's bintulu gtl plant'.
URL: *http://www.energytrendsinsider.com/2010/11/14/inside-shells-bintulu-gtl-plant/*

Retsinformation (2018), 'Bekendtgørelse om gaskvalitet'.
URL: *https://www.retsinformation.dk/Forms/r0710.aspx?id=200169#idf480e540-f411-4c62-985c-836293f23d9c*

Rostrup-Nielsen, J. (1993), 'Production of synthesis gas', *Catalysis Today* **18**, 305–324.
URL: *https://www.sciencedirect.com/science/article/pii/092058619380059A*

Rostrup-Nielsen, J. (1994), 'Catalysis and large-scale conversion of natural gas', *Catalysis Today* **21**, 257–267.
URL: *https://www.sciencedirect.com/science/article/pii/0920586194801479*

Rönsch, S., Schneider, J., Matthischke, S., Schlüter, M., Götz, M., Lefebvre, J., Prabhakaran, P. & Bajohr, S. (2016), 'Review on methanation – from fundamentals to current projects', *Fuel* **166**, 276 – 296.
URL: *http://www.sciencedirect.com/science/article/pii/S0016236115011254*

Siluria (2019), 'Oxidative coupling of methane'.
URL: *http://siluria.com/Technology/Oxidative_Coupling_of_Methane*

SkatteInform (2019), 'Satser for selskaber'.
URL: *https://www.skatteinform.dk/dk/graenser-og-satser/graenser-og-satser/satser-for-selskaber/*

Skøtt, T. (2019), 'Biogas kan få energisystemet til at hænge sammen'.
URL: *http://www.biopress.dk/PDF/biogas-kan-fa-energisystemet-til-at-haenge-sammen*

Spivey, J. J., de Klerk, A. & Furimsky, E. (2010), *Catalysis in the Refining of Fischer-Tropsch Syncrude*, Catalysis Series, The Royal Society of Chemistry.
URL: *http://dx.doi.org/10.1039/9781849732017*

Sveinbjörnsson, D. & Münster, E. (2017), Upgrading of biogas to biomethane with the addition of hydrogen from electrolysis, Technical report, PlanEnergi.
URL: *https://futuregas.dk/wp-content/uploads/2018/06/FutureGas-WP1-Deliverable-1.1.1.-Technologies-and-status-of-methanation-of-biogas-2017_Final.pdf*

Tabak, S. A., Krambeck, F. J. & Garwood, W. E. (1986), 'Conversion of propylene and butylene over zsm-5 catalyst', *AIChE Journal* **32**(9).
URL: *https://doi.org/10.1002/aic.690320913*

Tabak, S. A. & Yurchak, S. (1990), 'Conversion of methanol over zsm-5 to fuels and chemicals', *Catalysis Today* **6**(3).
URL: *https://www.sciencedirect.com/science/article/pii/092058619085007B*

Tang, J. (2016), 'Kortlægning af udnyttet overskudsvarme i fjernvarmen'.
URL: *https://www.danskfjernvarme.dk/groen-energi/analyser/162909-kortlaegning-af-overskudsvarme*

The Ministry of Energy, Utilities and Climate (2019), 'Klimaindsatsen i danmark'.
URL: *https://efkm.dk/klima-og-vejr/klimaindsatsen-i-danmark/*

Tian, P., Wei, Y., Ye, M. & Liu, Z. (2015), 'Methanol to olefins (mto): From fundamentals to commercialization', *ACS Catalysis* **5**(3).
URL: *https://pubs-acs-org.proxy1-bib.sdu.dk/doi/10.1021/acscatal.5b00007*

Voelklein, M., Rusmanis, D. & Murphy, J. (2019), 'Biological methanation: Strategies for in-situ and ex-situ upgrading in anaerobic digestion', *Applied Energy* **235**, 1061 – 1071.
URL: *http://www.sciencedirect.com/science/article/pii/S0306261918317124*

Wang, W.-C. & Tao, L. (2016), 'Bio-jet fuel conversion technologies', *Renewable and Sustainable Energy Reviews* **53**, 801–822.
URL: *https://doi.org/10.1016/j.rser.2015.09.016*

Wu-Hsun, C. (1994), *Methanol Production and Use*, Dekker.

Zabava, B. S., Voicu, G., Paraschiv, G., Dinca, M., Ungureanu, N., Ionescu, M., Ferdes, M., Dutu, I. & Vladut, V. (2017), 'Advanced methods of biogas purification-a review'.
URL: *https://www.researchgate.net/publication/321155658_advanced_methods_of_biogas_purification-a_review*

Appendix A

Natural Gas Grid Requirements

In this appendix the requirements for gas in the Danish natural gas grid as well as extra requirements for upgraded biogas are presented.

For natural gas the water dew point may not surpass -8 °C at a pressure of 70 bar and the hydrocarbon dew point may not surpass -2 °C at a pressure of 70 bar. The gas is required to have an upper Wobbe Index between 50.76 and 55.8 MJ/Nm^3 and a relative density between 0.555 and 0.7. Under normal operating conditions the hydrogen sulfide (H_2S) and carbonyl sulfide (COS) levels of the natural gas have to be below 5 mg/Nm^3. Natural gas has to contain an odor to make gas leaks smellable and odor is normally added as either tetrahydrothiophene or mercaptan. The gas has to have either 10 mg/Nm^3 tetrahydrothiophene or 4 mg/Nm^3 mercaptan at the locations where it is utilized (Retsinformation 2018).

For biogas that enters the natural gas grid at distributional level, there are the following additional requirements (Retsinformation 2018):

1. A maximum of 3 mg/Nm^3 ammonia (NH_3)
2. A maximum of 0.5 mole percent of oxygen (O_2)
3. A maximum of 3.0 mole percent carbon dioxide (CO_2)
4. A maximum of 1.0 mg/Nm^3 siloxanes

Upgraded gas that enters the natural gas grid at the transmission level, has to satisfy requirement 1 and 4 as well.

At an upgrading plant it is required to have a continuous measurement of the following parameters (Retsinformation 2018):

- Upper Wobbe Index
- Water dew point

- Hydrogen sulfides (H_2S)

While also having periodical measurements of the following parameters (Retsinformation 2018):

- The relative density
- Oxygen content (O_2)
- Carbon dioxide content (CO_2)
- Ammonia content (NH_3)
- Siloxane content
- Odor concentration

Appendix B

Biogas Upgrading

B.1 Separation

B.1.1 Water Scrubber

The upgrading technology with the largest global market share is the water scrubber. In 2017, 41 % of all biogas upgrading plants were of this type (Hjuler & Aryal 2017).

In a water scrubber the difference in the solubility of CO_2 and methane in water is used to strip the biogas of CO_2. The plant normally consists of four main parts; a compressor, an absorption column, a flash column and a desorption column. This is illustrated in Figure B.1.

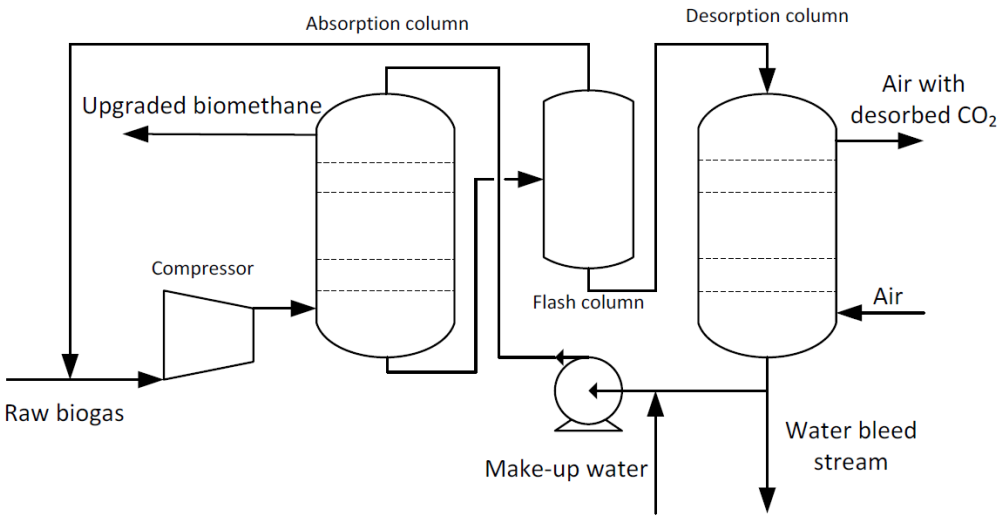

FIGURE B.1: Illustration of a water scrubbing plant. Source: (Bauer et al. 2013).

The biogas enters the absorption column from the bottom while water enters from the top. The pressure in the column is usually kept at 6-8 bar. At this pressure the solubility is approximately 26 times higher for CO_2 than methane in water. The upgraded biomethane is ejected out of the system in the top of the column while the water, which now contains CO_2 and a bit of methane, is ejected in the bottom

going into the flash column. In the flash column the pressure is lowered to recover as much methane from the water as possible. The gas from the flash column is then recirculated back into the absorption column. The same counts for the water after it has been through a desorption column working at atmospheric pressure and temperature, where the CO_2 is desorbed from the water and ejected (Hoyer et al. 2016). The advantages and disadvantages of a water scrubber are shown in Table B.1.

Technology	Pros	Cons
Water Scrubbing	- Simple process that can remove both CO_2 and moderate amounts of H_2S using water - High CH_4 purity (96-98%) and low CH_4 loss (<2%) from the system - No special chemicals required - Low operation and maintenance costs - Can co-remove moderate concentrations of VOCs and NH_3	- Energy and water intensive - Slow process due to lower CO_2 solubility ability in water - Possible corrosion problem when H_2S is not pre-removed - Clogging problem due to bacterial growth - No co-removal of O_2, N_2 and H_2 - Large column volume is necessary

TABLE B.1: Pros and cons of water scrubbing (Andriani et al. 2013, Hoyer et al. 2016, Hjuler & Aryal 2017, Angelidaki et al. 2018).

B.1.2 Chemical Scrubber

A chemical scrubber consists of two main columns, an absorber column and a stripper column, as shown in Figure B.2.

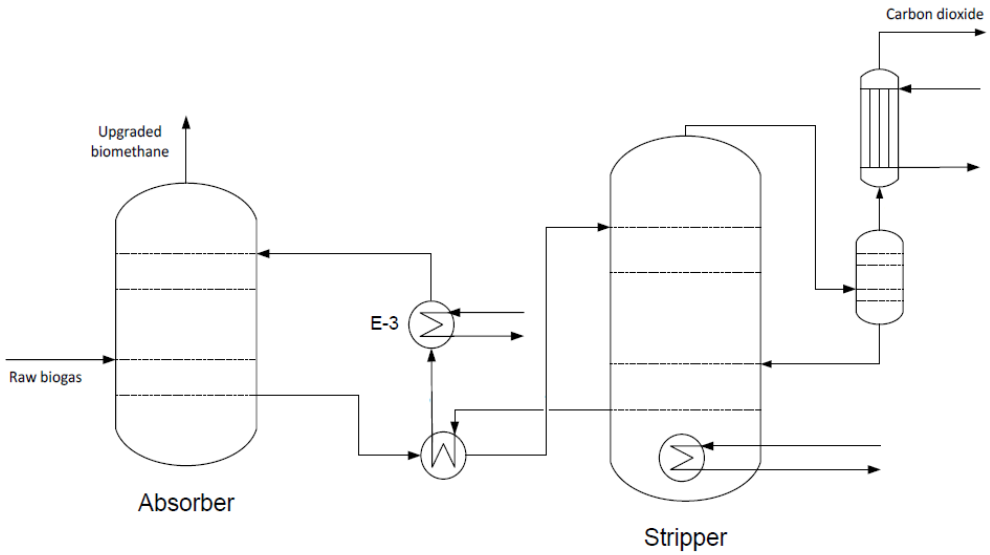

FIGURE B.2: Illustration of an amine scrubbing plant. Source: (Bauer et al. 2013).

The main difference from the water scrubber is that in the chemical scrubber the CO_2 molecules are chemically bound to the solvent to purify the biogas. The most common way to do chemical scrubbing is by using a water solution of amines (Dutcher et al. 2013). This is why chemical scrubbing often is referred to as amine scrubbing as well.

In the same way as in the water scrubber, the biogas enters the absorption column in the bottom, while the chemical solvent enters in the top. The column works at pressures of around 1-2 bar and with the reaction being exothermic, the solution has an increase in temperature in the column. The upgraded biomethane is led out of the system in the top of the column, while the liquid containing the chemically bound CO_2 is ejected in the bottom. The liquid is preheated in a heat exchanger before entering the stripper column, where the CO_2 is released from the liquid through further heating at a pressure between 1.5-3 bar. The amine solution without CO_2 leaves the column in the bottom, returning to the absorption column. CO_2, water vapor and some vaporized amine leaves the stripper column in the top going into a condenser, where the amine and water is condensed and sent back into the stripper column (Bauer et al. 2013). The advantages and disadvantages of a chemical scrubber are shown in Table B.2.

Technology	Pros	Cons
Chemical Scrubbing	- High CH_4 purity (96-99%) and very low CH_4 loss (<0.1%) - Dissolving more CO_2 per volume than water - Faster than water scrubbing - Smaller column volume necessary than in water scrubbing - Moderate amounts of H_2S can be co-removed - Can co-remove moderate concentrations of VOCs and NH_3	- Highly energy intensive - Solvent is difficult to handle - Possible corrosion problems when H_2S is not pre-removed - Waste chemicals may require treatment - Loss of amine solvent due to evaporation - No co-removal of O_2, N_2 and H_2

TABLE B.2: Pros and cons of chemical scrubbing (Andriani et al. 2013, Hoyer et al. 2016, Hjuler & Aryal 2017, Angelidaki et al. 2018).

B.1.3 Membrane Separation

The most common technology for membrane separation is using membrane fibers. The fibers are built to only let certain molecules penetrate to the permeate side, while the other molecules leave the fibers at the retentive side. The molecules entering the fibers have different permeation rates depending on the size and the hydrophilicity of molecules. CO_2 has a high permeation rate, while methane has a low rate, leading to a low CO_2 level in the stream at the end of the fibers (Bauer et al. 2013).

One membrane is often not enough to make the gas pure enough for the natural gas grid. To increase the purity, membranes are placed in series, as shown in Figure B.3. The placement of membranes in series can both be used to reduce the amount of CO_2 in the retentate, but it can also be used to reduce the amount of methane that is lost by putting an extra membrane on the permeate side (DMT Environmental Technology 2019). The advantages and disadvantages of a membrane separation plant are shown in Table B.3.

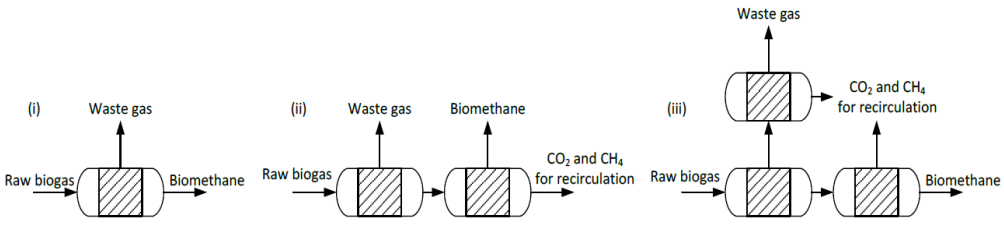

FIGURE B.3: Illustration of a membrane separation plant. Source: (Bauer et al. 2013).

Technology	Pros	Cons
Membrane Separation	- Fast installation and start up - Production output is flexible - Biogas purity and flow rate can be varied - Low energy requirements - High CH_4 purity (96-98%) and low CH_4 loss (<0.6%) - Possibility of NH_3 removal - Relatively pure CO_2	- Low membrane selectivity so more membranes are needed - Corrosion problems with H_2O and H_2S if not pre-removed - Short membrane lifetime (5-10 years) - Does not fully remove O_2, N_2 and H_2 - No co-removal of VOCs

TABLE B.3: Pros and cons of membrane separation (Andriani et al. 2013, Hoyer et al. 2016, Hjuler & Aryal 2017, Angelidaki et al. 2018).

B.1.4 Organic Physical Scrubber

An organic physical scrubber works in the same way as a water scrubber and the plant is structured in approximately the same way. A simple illustration of a plant is shown in Figure B.4.

In organic physical scrubbers the solubility of CO_2 in the solvent is much larger than the solubility of CO_2 in water, which means the scrubber requires a much lower volume flow. The higher the solubility of CO_2 into the solvent is, the better it works. However the main disadvantage of the organic physical scrubber is that the solvent is harder to recover (Hjuler & Aryal 2017). The advantages and disadvantages of an organic physical scrubber are shown in Table B.4.

Technology	Pros	Cons
Organic Physical Scrubbing	- Higher absorption than water - High CH_4 purity (96-98%) - Smaller column volume necessary than in water scrubbing - Moderate amounts of H_2S can be co-removed - Can co-remove moderate concentrations of VOCs and NH_3	- CH_4 loss (2-4%) - Complex regeneration of solvent without H_2S pre-removal - High energy demand to regenerate solvent - No co-removal of O_2, N_2 and H_2

TABLE B.4: Pros and cons of organic physical scrubbing (Andriani et al. 2013, Hoyer et al. 2016, Hjuler & Aryal 2017, Angelidaki et al. 2018).

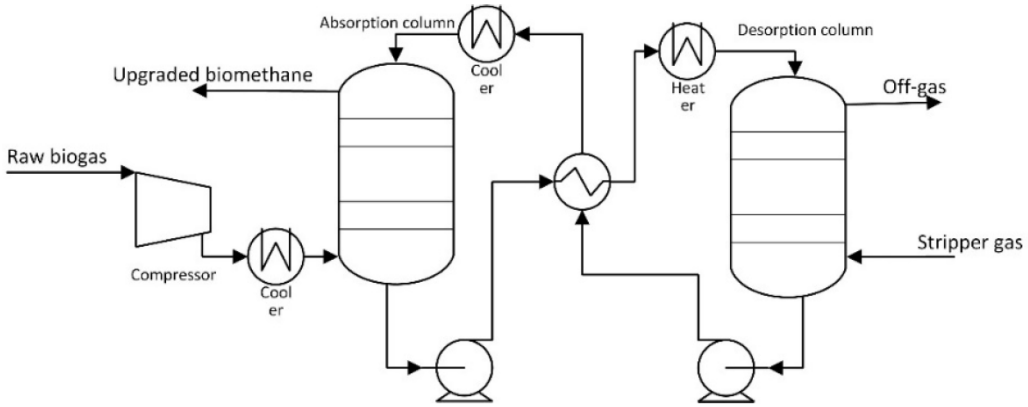

FIGURE B.4: Illustration of an organic physical scrubbing plant. Source: (Hoyer et al. 2016).

B.1.5 Pressure Swing Adsorption

Pressure swing adsorption (PSA) takes advantage of the fact that CO_2 is easier retained by some adsorbents than methane. A pressure swing adsorption plant contains several process columns, usually four, in parallel where the adsorption of CO_2 is performed. The reason for multiple columns is that each column works as a batch process, thus enough columns have to be implemented to secure a continuous flow (Hoyer et al. 2016). A simplification of the plant is illustrated in Figure B.5.

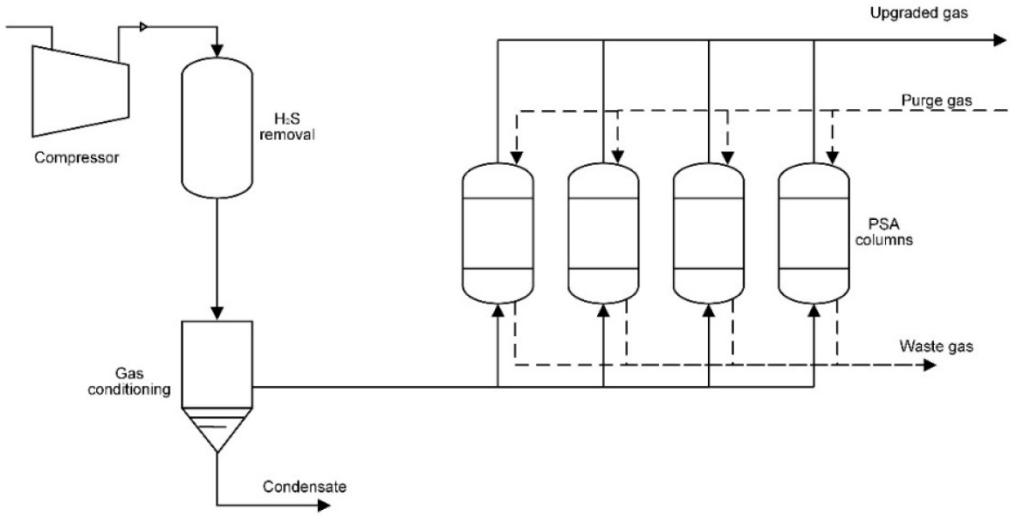

FIGURE B.5: Illustration of a pressure swing adsorption plant. Source: (Hoyer et al. 2016).

The biogas is compressed, purified for H_2S and conditioned before going into the process columns. The biogas separation in the columns consists of four phases, which are pressurization, feed, blow down and purge. An illustration of the four phases is shown in Figure B.6 containing both a depiction of the phases as well as their respective pressures. The four phases start with an initial pressurization of the column. Then biogas is fed into the column, with the upgraded biomethane leaving in the top, until

the bed is saturated and the biogas feed is stopped. Hereafter the column is emptied during the blow down phase. This is done by decreasing the pressure in the column which desorbs the CO_2 from the adsorbent. When the pressure is at its lowest, the purge phase starts and the column is blown through with upgraded gas to empty it of any remaining CO_2. The column is once more at its initial state and the process can be repeated (Bauer et al. 2013). The advantages and disadvantages of PSA are shown in Table B.5.

Technology	Pros	Cons
Pressure Swing Adsorption	- Capital cost share is moderate - Relatively quick start up and installation - High CH_4 purity (96-98%) - Possibility of O_2 and N_2 co-removal	- CH_4 loss can be up to 4% - Risk of valve malfunction leading to a larger CH_4 loss - Problems with irreversible adsorption of H_2S - No co-removal of VOCs, NH_3 and H_2

TABLE B.5: Pros and cons of PSA Separation (Andriani et al. 2013, Hoyer et al. 2016, Hjuler & Aryal 2017, Angelidaki et al. 2018).

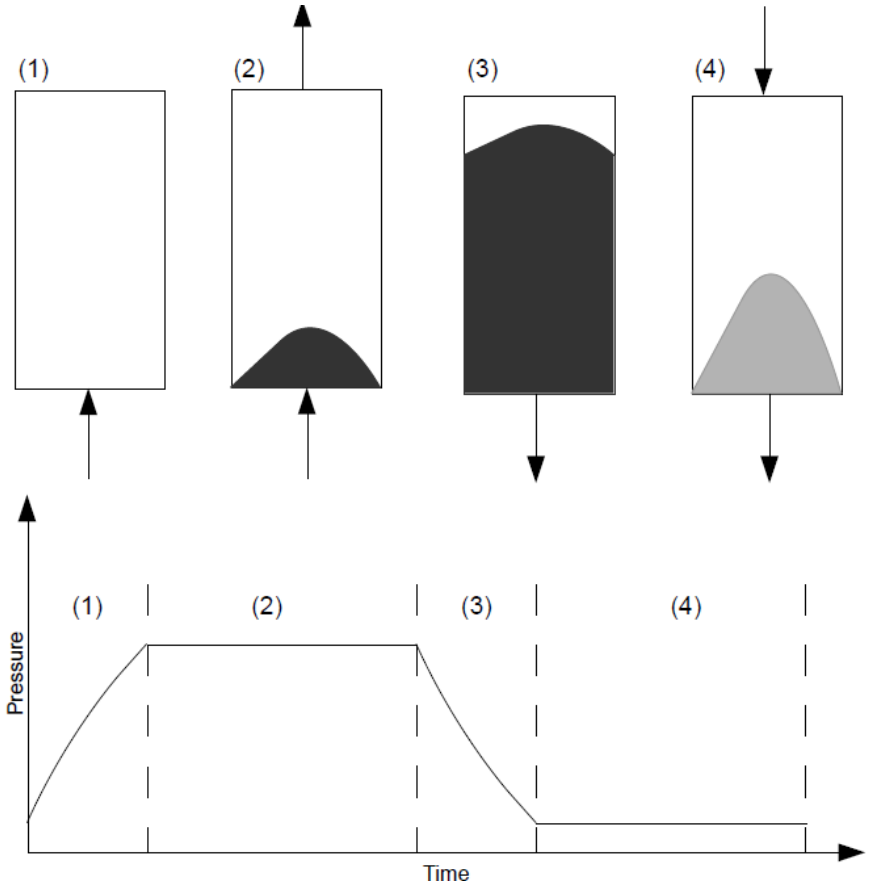

FIGURE B.6: The four phases of a pressure swing adsorption plant. Source: (Bauer et al. 2013).

B.1.6 Cryogenic Separation

The most used technologies for biogas separation are the ones that have already been screened, but another technology that might be relevant for the future is cryogenic separation.

Cryogenic separation exploits the fact that CO_2 condenses at higher temperatures than methane under certain pressures. The level of pressure used determines how low the temperature has to be to condense the CO_2. So when lowering the temperature, the CO_2 condenses while the methane stays as a gas. The technology has the advantage of achieving pure CO_2 in liquid form and cooled high purity methane that can be pressurized into bio-LNG (Cryo Pur 2019, Zabava et al. 2017). The advantages and disadvantages of cryogenic separation are shown in Table B.6.

Technology	Pros	Cons
Cryogenic Separation	- High CH_4 purity (97-98%) and low CH_4 loss (2%) - Relatively pure CO_2 - Easy to make LNG from cooled CH_4 - Possibility of H_2S co-removal - Can co-remove moderate to high concentrations of VOCs and NH_3	- Requires many devices e.g. compressors, heat exchangers and coolers - High operation and maintenance cost - No co-removal of O_2, N_2 and H_2 - Very little market experience

TABLE B.6: Pros and cons of cryogenic separation (Andriani et al. 2013, Hoyer et al. 2016, Hjuler & Aryal 2017, Angelidaki et al. 2018).

B.2 Methanation

B.2.1 Chemical Methanation

Chemical methanation utilizes catalysts to highly increase the reaction rate of carbon monooxide (CO) or CO_2 together with H_2 to produce methane and H_2O.

Chemical methanation was initially done by Sabatier and Senderens in 1902 using a nickel catalyst. Now, more than 100 years later, other metals have been found to work as catalysts for methanation as well, but nickel is still the catalyst that is applied the most for commercial methanation. Nickel has the advantage of being relatively cheap, while still having high activity and selectivity towards methane (Rönsch et al. 2016).

Other usable catalysts for methanation are ruthenium and cobalt. Ruthenium is the most active metal for methanation but it is also around 650 times more expensive on a weight basis than nickel as of May 2019. Cobalt is similar to nickel regarding its methanation activity but it is about 3 times more expensive (InvestmentMine 2019, Rönsch et al. 2016) .

The temperature of chemical methanation has to be below 225 °C and 300 °C for process pressures of 1 bar and 20 bar respectively to get a conversion rate of above 98% (Götz et al. 2016).

The most widely used type of reactor for CO_2 methanation is fixed-bed reactors. These can be either adiabatic or polytropic. The adiabatic variant has multiple adiabatic reactors in series to obtain a high conversion of CO_2. The polytropic version is with a number of tubes in parallel, where the number of tubes depends on the production rate. Other reactor types are: fluidised bed, monolith, foam, micro-channel, membrane, sorption enhanced, slurry and non-thermal plasma reactors (Ghaib et al. 2016).

While some reactor types can be used with CO_2 for methanation, many of the reactors are developed with the prospect of having CO as the input and not CO_2. The fixed-bed reactors have been developed with the purpose of converting CO_2 by companies such as Outotec, Etogas, and MAN (Ghaib et al. 2016).

B.2.2 Biological Methanation

Microorganisms are used in many industrial processes for biological conversion of inputs to higher value outputs. One of such conversions happens in a digestion plant where biogas, as mentioned in Section 1.2, is produced through anaerobic digestion of waste products. Biological methanation also takes advantage of biological conversion, using microorganisms to obtain a methane output from a CO_2 input. One way to convert the CO_2 is by using hydrogenotrophic methanogens, to convert H_2 and CO_2 into methane and H_2O directly, as seen in Equation (2.1) (Voelklein et al. 2019). Another way to convert CO_2 is by using homoacetogenic bacteria that through the Wood-Ljungdal pathway produce methane, see Equation (B.1) and Equation (B.2) (Angelidaki et al. 2018).

$$4\,H_2 + 2\,CO_2 \longrightarrow CH_3COOH + 2\,H_2O \tag{B.1}$$

$$CH_3COOH \longrightarrow CH_4 + CO_2 \tag{B.2}$$

Biological methanation can be done either directly inside the biogas plant, which is referred to as an *in-situ* process, or subsequently at an external plant, which is referred to as an *ex-situ* process. Both versions are shown in Figure B.7 and here the benefits and problems of both methods are further discussed. In general the major problem for biological methanation is that when achieving a high volumetric methane production, it is difficult to also achieve a high methane purity (Lecker et al. 2017).

A technically possible solution to this problem, but also more expensive, is combining the methanation plant with one of the separation units described in Section 2.1.1.

The *ex-situ* process is where an external methanation plant is built for the conversion of the CO_2 and H_2 into methane. This method can also be used, when the CO_2 is from another source than biogas.

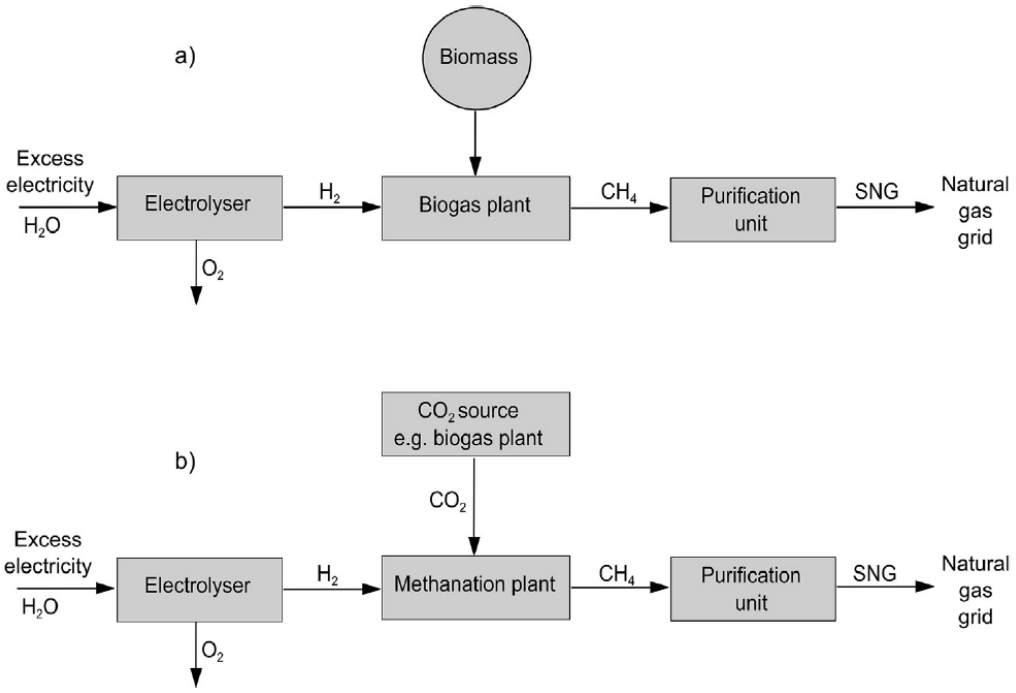

FIGURE B.7: The two different methods of doing biological methanation. One method is performing methanation *in-situ* and is shown in figure a), while the other is where methanation is performed *ex-situ* as shown in figure b). Source: (Lecker et al. 2017).

In the *in-situ* process hydrogen is added inside the biogas plant (Lecker et al. 2017). This gives the opportunity of getting a high methane purity directly out of the biogas plant and a calorific value of the gas that is high enough for it to enter the natural gas grid straight away. An *in-situ* plant has the advantage of low investment costs for the plant, as there is no need for an additional reactor used for methanation. However, *in-situ* needs cost intensive measurement equipment as the H_2 entering the plant has to match the produced CO_2 stoichiometrically as often as possible to produce an optimal amount of methane. If too much H_2 is added there will be an increase in the partial pressure of H_2 in the plant, causing microbial inhibition. Another disadvantage of *in-situ* is that in conducted research projects *in-situ* plants have had a lower volumetric methane production than *ex-situ*. The volumetric methane production has for *in-situ* plants been between 0.08 L L_{reac}^{-1} day^{-1} and 0.39 L L_{reac}^{-1} day^{-1}, while for *ex-situ* plants it has been between 0.37 L L_{reac}^{-1} day^{-1} and 688.6 L L_{reac}^{-1} day^{-1} according to Lecker et al. (2017). Even though the volumetric methane production of *ex-situ* plants have been high, it has been uncommon achieving both a high volumetric methane production and purity. The volumetric methane production decreases with higher methane purity (Lecker et al. 2017).

Appendix C

Synthesis Gas Production Technologies

C.1 Steam (Methane) Reforming

Steam Methane Reforming is the most mature of the technologies, and is largely used commercially to produce hydrogen (Maitlis & de Klerk 2013). The process produces a syngas consisting of H_2, CO and CO_2 from methane, with some slip of unconverted methane (Bertau et al. 2014).

$$CH_4 + H_2O \longrightarrow CO + 3\,H_2 \tag{C.1}$$

$$CO + H_2O \longrightarrow CO_2 + H_2 \tag{C.2}$$

The main reaction of the steam methane reforming process can be seen in Equation (C.1) whilst also Equation (C.2) is important to balance the ratio of H_2, CO and CO_2 in the product (Bertau et al. 2014). Equation (C.2) is the water gas shift reaction, and is the reverse of Equation (2.2) as seen in Appendix B.2.

The process is endothermic and takes place over a nickel catalyst, usually at a temperature of roughly 800-900 °C and 20-30 atm of pressure (Maitlis & de Klerk 2013). Theoretically, the syngas produced has a H_2:CO ratio of 3 as can be seen from the stoichiometry of Equation (C.1). However, in practice several more reactions than just Equation (C.1) occur, such as Equation (C.2), leading to a different H_2:CO ratio in the output. Additionally, the steam methane reforming reactor is not fed with the inputs in exact accordance with the stoichiometry of the reaction equations.

The steam methane reforming reactor is usually fed with steam at a ratio of 2.5-5.0 H_2O:C on a mole basis, whilst the product usually has a H_2:CO ratio of 4-7 and a CO_2:CO ratio of 0.5-1. Additionally, the methane slip is at roughly 3-5% (de Klerk 2011*a*). The process is an equilibrium reaction, and the pressure, temperature, H_2O:C ratio and feed composition are the main parameters influencing the output.

C.2 Autothermal Reforming

Autothermal reforming is similar to steam methane reforming, but the main difference is that the heat provided to the endothermic reactions in Equation (C.1) and Equation (C.2) is provided by an internal combustion in the reactor, as shown in the exothermic oxidative reactions in Equation (C.3) and Equation (C.4) (Maitlis & de Klerk 2013).

$$\mathrm{CH_4} + 2\,\mathrm{O_2} \longrightarrow \mathrm{CO_2} + 2\,\mathrm{H_2O} \tag{C.3}$$

$$\mathrm{CH_4} + \frac{1}{2}\,\mathrm{O_2} \longrightarrow 1\,\mathrm{CO} + 2\,\mathrm{H_2} \tag{C.4}$$

The process is usually based on a nickel catalyst, and the temperature and pressure in the reactor is typically at 1100-1300 °C and 20-40 bar respectively, with the odd exception using a higher pressure (Bertau et al. 2014). There are several advantages and disadvantages compared to the steam methane reforming process, which are discussed in Section 2.2.1.

The autothermal reforming reactor is typically fed with oxygen at a ratio of 0.55-0.6 O_2:C on a mole basis, steam at a ratio of 1.5-2.5 H_2O:C, whilst the output typically has ratios of 2.5-3.5 H_2:CO and 0.2-0.3 CO_2:CO. The methane slip is roughly 0.5-1% (de Klerk 2011*a*).

C.3 Partial Oxidation

Partial Oxidation is a variant of autothermal reforming. The process is noncatalytical and converts a methane input into clean synthesis gas, based mainly on the reaction in Equation (C.4) (Maitlis & de Klerk 2013, Bertau et al. 2014).

The process is usually operated at between 1200-1450 °C and 30-70 bar of pressure (Bertau et al. 2014). The partial oxidation reactor is typically fed with oxygen at a ratio of 0.55-0.6 O_2:C on a mole basis, steam at a ratio of 0-0.15 H_2O:C, whilst the output typically has ratios of 1.6-1.9 H_2:CO and 0.05-0.1 CO_2:CO. The methane slip is down to 0.1% (de Klerk 2011*a*).

Appendix D

Fischer-Tropsch Technology

In this section a short introduction to FT synthesis is given, before the technology is screened. The main factors that influence the product of the FT synthesis are discussed, especially in regards to the production of jet fuel.

D.1 Fischer-Tropsch Synthesis

FT synthesis is named after the Germans Franz Fischer and Hans Tropsch, who in 1925 synthesized longer hydrocarbons over catalysts of Cobalt and Nickel at atmospheric pressure. Development of the process continued in the following years, especially in Germany in the years 1939-1945 to produce vehicle fuels during the Second World War. After the war interest died down with the discovery of new oil fields, until it was revitalized in the 1970's in South Africa due to sanctions on oil exports to the country. This encouraged SASOL (Suid Afrikaanse Steenkool en Olie, the South African Coal and Oil company) to expand its interest in Coal-to-Liquid (CTL) plants to make the country self suppliant in liquid fuel products. Since then, SASOL has been leading the development of especially GTL and CTL-technology along with Shell (Maitlis & de Klerk 2013).

FT synthesis is usually utilized along with an integrated syngas production gas loop and product refining in a X-to-liquid (XTL) plant. The X denotes that the input to the syngas production can come from a variety of sources, including but not limited to Coal-to-Liquids (CTL), typically natural gas in Gas-to-Liquids (GTL), Waste-to-Liquids (WTL), Biomass-to-Liquids (BTL) and Biogas-to-Liquids (BgTL) (Maitlis & de Klerk 2013).

FT synthesis is not a single process but refers to the overall process of catalytically converting syngas into a mixture of primary products, mainly linear hydrocarbons, and secondary products, including branched chain and cyclic aliphatic hydrocarbons as well as some aromatics and oxygenates. The mixture of products produced by FT synthesis is collectively known as Synthetic Crude Oil, or syncrude, due to its comparability to conventional crude oil. The FT process can to a satisfactory degree be described by the following reaction equations (Spivey et al. 2010).

- The formation of alkanes:

$$(2\,\mathrm{n}+1)\,\mathrm{H_2} + \mathrm{nCO} \longrightarrow \mathrm{C}_n\mathrm{H}_{2n+2} + \mathrm{nH_2O} \tag{D.1}$$

- The formation of alkenes:

$$2\,\mathrm{nH_2} + \mathrm{nCO} \longrightarrow \mathrm{C}_n\mathrm{H}_{2n} + \mathrm{nH_2O} \tag{D.2}$$

- The formation of oxygenates:

$$2\,\mathrm{nH_2} + \mathrm{nCO} \longrightarrow \mathrm{C}_n\mathrm{H}_{2n+2}\mathrm{O} + (n-1)\,\mathrm{H_2O} \tag{D.3}$$

- The formation of aldehydes and ketones:

$$(2\,n-1)\,\mathrm{H_2} + \mathrm{nCO} \longrightarrow \mathrm{C}_n\mathrm{H}_{2n}\mathrm{O} + (n-1)\,\mathrm{H_2O} \tag{D.4}$$

- The formation of carboxylic acids and esters:

$$(2\,n-2)\,\mathrm{H_2} + \mathrm{nCO} \longrightarrow \mathrm{C}_n\mathrm{H}_{2n}\mathrm{O}_2 + (n-2)\,\mathrm{H_2O} \tag{D.5}$$

The value of n can be be from one to over 100 and denotes that the reactions occur to produce hydrocarbons of many different lengths. FT synthesis processes produce hydrocarbons with a distributed carbon length.

D.1.1 Catalysts for Fischer-Tropsch Synthesis

The FT process is catalytical, and can utilize several different catalysts along with a variety of promoters and supporters. The promoters and supporters can have a big effect on the selectivity and durability of the catalyst. The most common catalysts are based on Iron (Fe), Cobalt (Co), Ruthenium (Ru), Thorium dioxide (ThO_2) and Nickel (Ni), but industrial FT processes most frequently use Fe- or Co-based catalysts. The most important aspects to consider when selecting the catalyst are (Spivey et al. 2010):

- Sensitivity to promoters
- Water Gas Shift activity
- Handling conditions

- Hydrogenation activity

FT synthesis over a Fe- or Co-based catalyst yields vastly different results as illustrated in Table D.1, which shows differences in a low-temperature FT (LTFT) process depending on the catalyst.

Catalysis Property	Fe-LTFT	Co-LTFT
Extensive Methanation	No	At increasing temperature and decreasing CO partial pressure
Alkali Promoters	Essential	No
Water Gas Shift Activity	Yes	No
Branching Reaction	Static, increases with time	Dynamic, decreased with time
Alkene Hydrogenation	No (little)	Extensive
Alkene Isomerisation	No (little)	Extensive

TABLE D.1: Comparison of low-temperature Fischer-Tropsch Synthesis over potassium-promoted iron- and cobalt-based catalysts (Spivey et al. 2010)

Based on the important aspects to consider when choosing a catalyst, which were previously mentioned, a few comments can be made. The Co-based catalyst is not sensitive to promoters though they can be used, whereas the Fe-based catalyst requires alkali promotion in order to increase the amount of CO absorbed on its surface and increase chain growth probability. Regarding water gas shifting activity, it can be seen that the Fe-based catalyst is active whereas the Co-based catalyst is not. Therefore, CO_2 and H_2O in the Co-LTFT process are inert gasses, whereas they can still participate in the Fe-LTFT process. Regarding the handling conditions, the Fe-based catalyst is more easily prepared, cheaper and more robust to impurities than the Co-based catalyst. On the other hand, the Co-based catalyst has a longer catalyst lifetime, has a higher conversion rate (depending on the syngas) and more activity for hydrogenation, increasing the amount of saturated hydrocarbons in the syncrude, but reducing the amount of unsaturated hydrocarbons, oxygenates and aromatics (Spivey et al. 2010). The difference in hydrogenation activity and syncrude composition mainly affects the design of the refining process, which must be designed based on the syncrude composition and desired end products (de Klerk 2011*b*).

D.1.2 Operating Conditions for Fischer-Tropsch Synthesis

The operating conditions of the FT synthesis have a big impact on the product selectivity of the process. The impact of the operating conditions are summarized in Table D.2.

Selectivity parameter	Temperature	Pressure	Space Velocity	H_2:CO ratio
Carbon Number Distribution	Lower a-value	Higher a-value	No change	Lower a-value
Methane Selectivity	Increases	Decreases	Decreases	Increases
Alkene Selectivity	-	-	Increases	Decreases
Oxygenate Selectivity	-	Increases	Increases	Decreases
Aromatic Selectivity	Increases	-	Decreases	Decreases
Syngas Conversion	Increases	Increases	Decreases	-

TABLE D.2: An overview of the operating conditions' effect on the FT process. The table shows the effect of an increase in the conditions. The empty spaces denote that the relationship is more complex (de Klerk 2011*a*).

The temperature of a LTFT process is generally at 170-230 °C, whilst the HTFT process is usually at a temperature of 250-340 °C. The temperature affects the desorption of the product on the surface of the catalyst. Increasing the temperature increases the desorption rate, thus lowering the possibility of chain growth of longer hydrocarbons on the surface of the catalyst. Additionally, higher temperatures favor hydrogenation, increasing the possibility of chains breaking down into shorter alkanes. As such, HTFT generally favors lighter products and shorter hydrocarbon chains, sometimes producing only gases and never waxes, whilst LTFT favors heavier products and longer chain hydrocarbons, with the product to a large degree being waxes.

The pressure of a typical FT process is between 1.0-3.0 MPa. An increase in the pressure of a FT process increases the concentration of CO on the catalyst surface, which promotes chain growth of longer hydrocarbons. Additionally, a higher concentration of CO also increases the production of oxygenates.

An increase in the space velocity, which is the amount of reactor volumes that are treated in a given time, reduces the time the products of the FT process are in contact with the catalyst, reducing the probability of readsorption and reaction. This reduces hydrogenation of alkenes and oxygenates, increasing the production of these compounds.

An increase in the H_2:CO ratio of the syngas increases the driving force for hydrogenation, favoring the production of shorter chain hydrocarbons as the possibility of chain growth is decreased. This is examplified by looking at alkanes. The shortest alkane, methane, has a H:C ratio of 4, whilst an infinitely long alkane would approach a H:C ratio of 2. The shorter hydrocarbons are favored by a higher H_2:CO ratio, whilst longer hydrocarbons are favored by a smaller H_2:CO ratio. The H_2:CO ratio of the syngas should ideally match the usage ratio of the FT process, as there will otherwise be a build-up of the surplus reactant in the FT reactor which may influence the product distribution of the FT process (de Klerk 2011*a*).

D.2 Fischer-Tropsch Synthetic Crude Oil Refining

The choice of FT catalyst and operating conditions to get a specific syncrude composition has to be made with the syncrude refining process in mind. Both syncrude from a LTFT or HTFT process with either an iron or cobolt catalyst can to a large degree be refined to a desired product, but the ease of refining and simplicity of the refining design may favor one over the other for a specific product.

As the focus of this project is the production of jet fuel, the syncrude must be refined to meet jet fuel specifications. Some jet fuel specifications related to the chemical properties of hydrocarbons are described in Appendix D.2.1. Afterwards, the most important techniques for jet fuel refining are presented in Appendix D.2.2.

D.2.1 Jet Fuel Chemical Specification

The syncrude produced from a FT process is usually characterized by its carbon number distribution, which depends on the alpha value of the process. The alpha value can be from 0 to 1, and the higher the alpha value is, the heavier the carbon distribution of the product syncrude will be. That is, the higher the alpha value is, the longer the average hydrocarbon in the syncrude will be. Hydrocarbon chains in the syncrude can vary in length from C_1 to C_{100+}. A table of generic FT syncrude compositions on a mass basis can be seen in Table G.1 in Appendix G.

The carbon number interval of jet fuel is set by the properties required of the fuel components. The upper limit of the carbon number interval is set by the final boiling point specification which is 300 °C. As such, hydrocarbons with a boiling point that is higher than 300 °C are not suitable for jet fuel. This is the case for hydrocarbons which are longer than n-C_{16}. The lower limit of the carbon number interval is set by the density and viscosity specifications. Hydrocarbons with a carbon number smaller than C_{10} typically have a too low density for jet fuel. In general hydrocarbons for jet fuel are in the C_{10}-C_{16} range, also known as the kerosene range. The wide range allows for a wide cut of hydrocarbons that can be used without further upgrading or refining. The jet fuel yield is further maximized by refining lower or higher carbon number products into products in the kerosene range through the refining processes. Additionally, some products must be upgraded for the fuel to meet the required specifications. For instance, cyclic hydrocarbons are essential to meet the lower density limit. As seen in Table G.1, syncrude from a LTFT process is generally high in low density paraffins and low in high density aromatics. Therefore, the refining of syncrude from a LTFT process must include a step to produce aromatics for the fuel to meet the specifications (de Klerk 2011*b*).

D.2.2 Syncrude-to-Jet Fuel Refining Techniques

The products from the FT process syncrude must be upgraded and refined to maximize the fuel yield, and to ensure that the fuel meets the specifications. There are numerous technologies and techniques that can be employed, but there are mainly five that are needed for jet fuel refining (de Klerk 2011*a*):

- Aromatic Alkylation - Aromatic alkylation is the addition of an alkylating agent, e.g. an alkene, to an aromatic. Combining otherwise undesirable alkenes with e.g. aromatics, can increase their density making them usable in fuel production.
- Oligomerization - Oligomerization is one of the most important refining steps for a FT refining process. In an oligomerization process, one or more alkenes react in addition reactions to form longer hydrocarbons. The most important application of this, is to turn the shorter gaseous hydrocarbons into longer liquid hydrocarbons, thereby increasing the overall syncrude yield. The length can be increased all the way up to the desirable kerosene range, where it can be further hydrotreated. Duo to branching of the product, which is a consequence of the oligomerization, this product is the desirable iso-paraffinic kerosene for jet fuel blending.
- Hydrotreating - Hydrotreating is an upgrading step where atoms that are not carbon or hydrogen are replaced with hydrogen. Hydrotreating is further split into separate processes, where especially hydrogenation of alkenes and hydrodeoxygenation are important process for FT syncrude refining.
- Aromatization - Aromatization is the process of refining components of the syncrude into aromatics, which are essential for jet fuel. Aromatics are needed both to increase the density of the FT derived jet fuel, but also due a swelling effect on seals in jet engines, preventing leakages in the fuel delivery system.
- Hydrocracking/Hydroisomerization - Hydrocracking is the second of the most important refining steps in the FT refining process. In hydrocracking, the heavy hydrocarbons are cracked to produce shorter hydrocarbons. This is especially needed for LTFT syncrude, as a large part of the product is heavy waxes above the usable kerosene range. In addition to a shortening of the long hydrocarbons, both hydrotreating and hydroisomerization also naturally occurs in the process. In the hydrotreating, alkenes are hydrogenated into alkanes as well as generally removing heteroatoms, increasing the quality of the product. And in the hydroisomerization, the structure of the molecules are altered without changing the carbon number. This can improve one or more properties of the product, where the main benefit for jet fuel is that branched hydrocarbons have a lower freezing point than linear hydrocarbons, allowing the product to pass the specifications for the jet fuels cold flow properties.

In general, the hydrocarbons smaller than C_{10} are either oligomerized to produce longer hydrocarbons, or they are aromatized to produce the essential aromatics to increase the density of the fuel. Meanwhile the hydrocarbons larger than C_{16} are hydrocracked to produce shorter hydrocarbons in the kerosene range. Usually, hydroisomerization is done in association with the hydrocracking (de Klerk 2011*a*).

Appendix E

Methanol Pathway Technologies

E.1 Methanol Introduction

The production of methanol is a very old process and the first commercial process was a destructive distillation of wood in 1830. The process was used for about a century, until a synthetic route for methanol production through the use of syngas was suggested by Paul Sabatier in 1905, leading to the first commercial synthetic methanol plant in 1923 by Badische Anilin-und-Soda-Fabrik (BASF). The following half century introduced many improvements to the process, including the introduction of improved catalysts to ease the operating conditions of the process. Interest in the technology increased in the 1970's, partly due to the Arab Oil Embargo, which paved the way for further innovations relating to the production and use of methanol (Wu-Hsun 1994).

The Methanol-to-Gasoline (MTG) process was first introduced by Mobil in the 1970's, where syngas is catalytically converted to methanol and dimethyl ether (DME). The mixture of methanol and DME is further dehydrated and the product refined to give a desirable output. With the development of different process configurations, the process was specified to the previously mentioned MTG process, a Methanol-to-Olefin (MTO) process and a Methanol-to-Ethylene (MTE) process, with a further refining process called Mobil Olefin to Gasoline/Diesel (MOGD) (Tabak & Yurchak 1990).

The first commercial plant using Mobil's technology was put on stream on the 17th of October, 1985 in New Zealand. The plant included both methanol and fuel producing segments, but the fuel producing segment was later shut down, due to unfavorable relations between the price of methanol and the price of the produced fuel (Engineering New Zealand n.d., Bertau et al. 2014). Today, ExxonMobil are still pioneers in fuel production through the methanol pathway with their EmoGas technology, alongside Haldor Topsøe with their technology, Topsoe Improved Gasoline Synthesis (TIGAS), and Lurgi (Bertau et al. 2014).

E.2 Methanol Synthesis

As mentioned, the first step in the production of jet fuel from syngas through the methanol pathway, is the production of methanol. The production of methanol from syngas can be described by the following reaction equations:

$$CO + H_2 \longrightarrow CH_3OH \tag{E.1}$$

$$CO_2 + 3\,H_2 \longrightarrow CH_3OH + H_2 \tag{E.2}$$

$$CO + H_2O \longrightarrow CO_2 + H_2 \tag{E.3}$$

The reactions in E.1 and E.2 are exothermic and are accompanied by a decrease in pressure. Therefore, methanol formation is generally favored by decreasing the temperature and increasing the pressure. Removing heat from the reactor and keeping the reactor at its ideal temperature is especially important to avoid the production of byproducts (Bertau et al. 2014). Commercial methanol plants typically operate at 220-280 °C and 50-100 bars of pressure, although the benefit from raising the pressure to above 80 bar is rather small (Wu-Hsun 1994, Bertau et al. 2014).

The production of methanol is a catalytic process. The main properties to consider regarding the catalysts are the activity, selectivity and stability. The activity of the catalyst determines how much syngas can be converted per pass in the reactor, the selectivity of the catalyst determines how much of the converted syngas is synthesized to methanol, and the stability of the catalyst determines its robustness against impurities. Today, almost all catalysts for methanol synthesis are based on a composition of mainly copper, some zinc and a few additives, mainly aluminium. The components are typically found in the following mass-% ranges; 60-70% Copper oxide, 20-30% Zinc oxide, and 5-15% alumina (Wu-Hsun 1994). The study of catalysts, and why some are better than others, is still a heavily researched area which is not comprehensively understood (Bertau et al. 2014).

The production of methanol over CuO/ZnO-based catalysts have a trade-off between the activity and the selectivity of the process. Commercial processes generally run with a selectivity of over 99% for methanol, but the per pass conversion is also typically down towards 10-25% depending on the type of reactor employed. Higher per pass conversion rates, whilst still retaining the high selectivity, have been achieved on a laboratory scale, but not in ways that could be scaled up for commercial purposes. Commercially, the per pass rate could be increased, but this lowers the selectivity for methanol and increase the production of unwanted products such as some acids, esters and higher alcohols (Bertau et al. 2014).

Commercially, a high selectivity for methanol and a low per pass conversion rate is preferred. Therefore, methanol plants are very integrated facilities with huge recycle loops. As previously mentioned in Section 2.2.1, the reaction to synthesize methanol occurs optimally with an input with a stoichiometric number of roughly 2.0-2.1, and as the recycle loop is the main input to the reactor, the design of a recycle loop with a make-up gas with a stoichiometric number of 2.0-2.1 is one of the most important parts of a methanol plant (Bertau et al. 2014).

E.3 Dehydration of Methanol to Light Olefins

Methanol, and other alcohols such as ethanol and various isomers of butanol, can be used to produce jet fuel through a refining process where it is first dehydrated to light olefins, then oligomerized to heavier olefins, and finally hydrogenated to paraffins mainly in the jet fuel range.

The process of dehydrating methanol is most commonly known as a Methanol-to-Olefins (MTO) process. As mentioned previously, the process of converting methanol to hydrocarbons was discovered by Mobil, now ExxonMobil, in the 1970's, and through efforts to improve the selectivity for different products, different technologies were developed, hereamongst the MTO process (Bertau et al. 2014). Apart from being usable in further refining towards jet fuel, the light olefins from the MTO process can be used as a base feedstock for countless processes in the chemical industry. The demand for ethylene and propylene countinues to grow, and the MTO process is considered as an important alternative to the traditional production of olefins through naptha cracking, due to a lower CO_2 footprint amongst other benefits (Bertau et al. 2014).

Overall, the process of converting methanol to olefins can be described by the following reactions:

$$2\,CH_3OH \longrightarrow CH_3OCH_3 + H_2O \longrightarrow (CH_2)_2 + 2\,H_2O \tag{E.4}$$

The reaction usually takes place in a two-step process, where methanol is first dehydrated to dimethyl ether (DME) in one reactor and then further dehydrated to light olefins in another reactor. Usually, mainly ethylene and propylene is produced with small yields of up to C_6 olefins, as well as small amounts of paraffins and aromatics.

The MTO process is catalytical, and much research has been and is still being conducted to understand and improve on the catalysts and the process as a whole (Bertau et al. 2014). Mobil first developed the process over their ZSM-5 catalyst, short for Zeolite Socony Mobil-5 (Tabak & Yurchak 1990). The MTO process is usually conducted in a fixed or fluidised bed process, at temperatures between 400-550 °C and 1-5 bar depending on the reactor type (Tabak & Yurchak 1990, Bertau et al. 2014).

The MTO process can be designed to improve the selectivity of a desired olefin, but higher selectivity of a specific olefin will usually also result in a lower overall conversion and yield of olefins. Producing

a mix of light olefins in the MTO process should not be a problem for the further refining towards jet fuel though, as mixtures of light olefins can be oligomerized without having to separate the light olefins first (Tabak et al. 1986, Tabak & Yurchak 1990).

E.4 Refining and Upgrading of Light Olefins to Fuel Products

In the production of fuels from light olefins, the light olefins are first oligomerized to produce heavier olefins and then hydrotreated to create final products. The oligomerization process was briefly descriped in Appendix D.2.2, and that description will here be slightly expanded upon.

The oligomerization process is a catalytical process. It was originally developed to convert gaseous byproducts from crude oil cracking into liquid products, and was put into commercial use based on a solid phosphoric acid catalyst in 1935 (de Klerk 2011*a*, Tabak et al. 1986). Since then, several other catalysts have been developed, and are still being developed, for the process. Especially ExxonMobil has been a pioneer in fuel production from olefins in the last decades with the use of their ZSM-5 and ZSM-22 catalysts in the Mobil Olefins to Gasoline and Distillate (MOGD) technology and EmoGas technology (Bertau et al. 2014, Tabak et al. 1986).

The conversion of light olefins to higher olefins using the ZSM-5 catalyst in the MOGD process can happen at different temperatures and pressures, depending on which distribution of olefins that is desired (Wang & Tao 2016). High temperature and low pressure favors the production of olefins with a lighter distribution than low temperature and high pressure (Tabak et al. 1986). When targeting the production of distillate range hydrocarbons (C_{10}-C_{20}), the process should ideally run at between 220-270 °C and 2-5 bar (Tabak et al. 1986). In contrast, processes utilizing solid phosphoric acid catalysts usually run at the same temperature, but at 10-50 bars of pressure (de Klerk 2011*a*).

As the oligomerization process gives a distributed product with hydrocarbons of various lengths, the olefins produced could theoretically be separated, and those too short for the kerosene range should be recycled for oligomerization, whilst those too long for the kerosene range, should be cracked down into the kerosene range or for recycling. However, this complicates the refining process and may not be technically and economically feasible. Instead, olefins in both the gasoline, kerosene and diesel range are produced. The MOGD technology does not include this further complicated refining, and thus produces a mixture of olefins which are separated and hydrotreated to produce final gasoline, jet fuel and diesel products.

Appendix F

Additional Sankey Diagrams

F.1 The Methanol Pathway with Methane from Biogas Methanation

Here is the methanol pathway with methane from biogas methanation. As was the case for the example of the FT based pathways with methanation as presented in Figure 3.4 in Section 3.3.4, the difference is the larger amount of methane available for the GTL plant. The Sankey diagram for this pathway can be seen in Figure F.1.

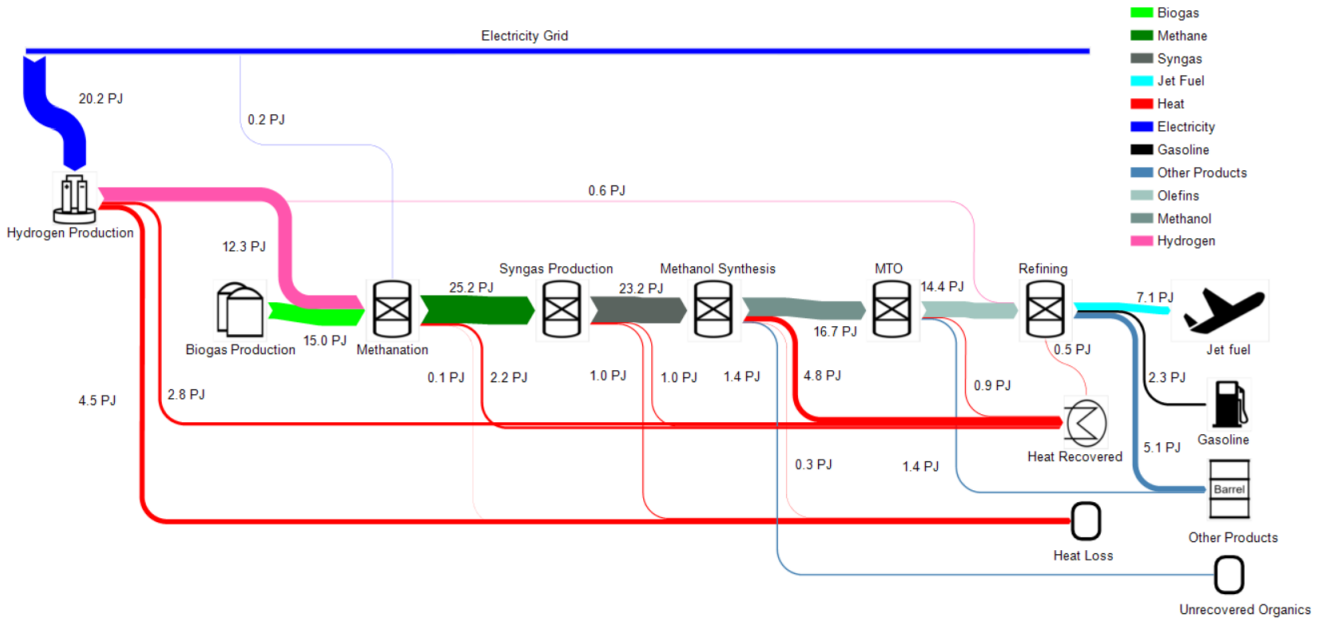

FIGURE F.1: The Sankey diagram of a methanol based GTL plant with methane from biogas upgraded by methanation.

For this pathway, the biogas is upgraded by methanation. The methane is led through the natural gas grid to the GTL plant, where it is reformed to syngas, the syngas is converted to methanol in the

methanol synthesis process, the methanol is dehydrated to light olefins, and the light olefins are refined to final fuel products.

With a 15 PJ input to the methanol pathway with methane from biogas upgrading by methanation there is a yield of 7.08 PJ of jet fuel, 2.26 PJ of gasoline and 5.11 PJ of other products where roughly 4.7 PJ is diesel.

F.2 The OCM Pathway with Methane from Biogas Methanation

Here is the OCM pathway based on methane from biogas methanation.

The Sankey diagram of the OCM pathway with biogas upgrading through methanation can be seen in Figure F.2.

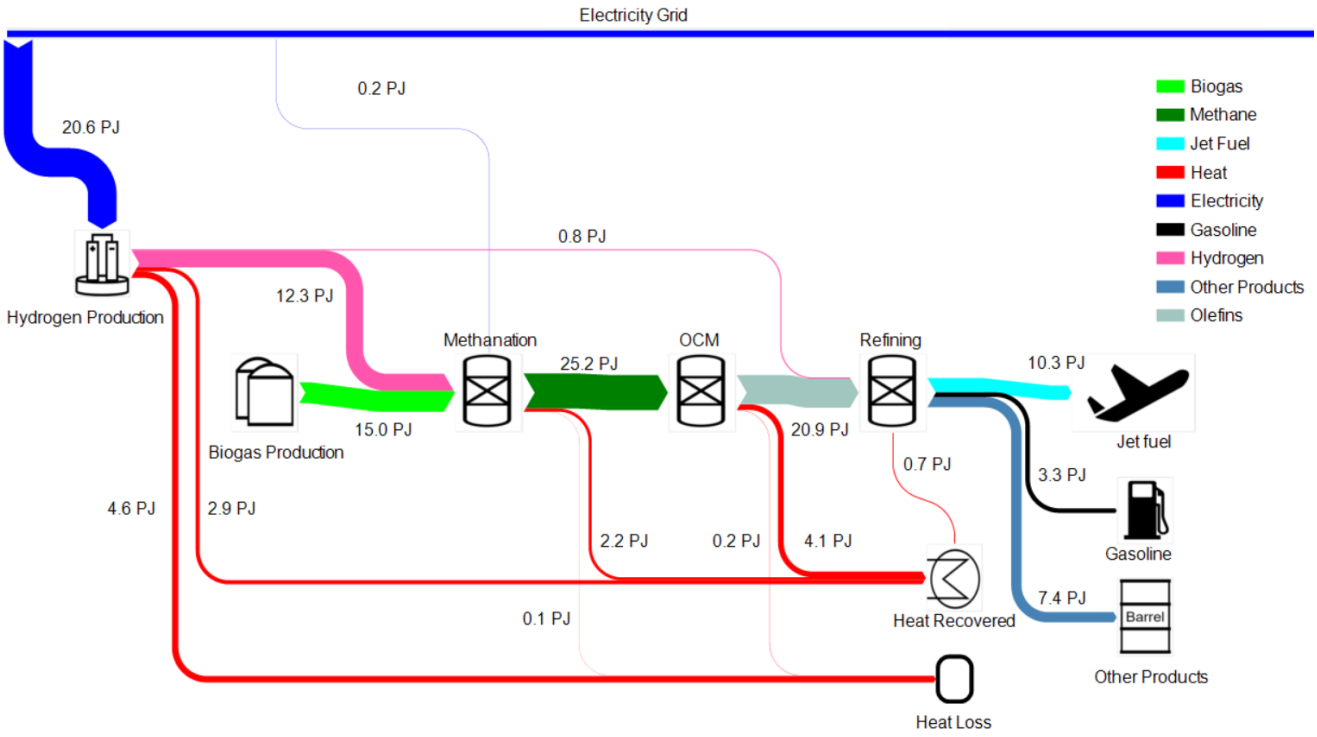

FIGURE F.2: The Sankey diagram of a OCM based GTL plant with methane from biogas upgraded by methanation.

For this pathway, the biogas is upgraded by methanation. The methane is led through the natural gas grid to the GTL plant, where it is used to produce light olefins which are refined to final fuel products.

With a 15 PJ input to the OCM pathway with methane from biogas separation, there is a yield of 10.29 PJ of jet fuel, 3.28 PJ of gasoline, roughly 7.43 PJ of diesel.

F.3 Decentral Fe-LTFT based GTL Plants

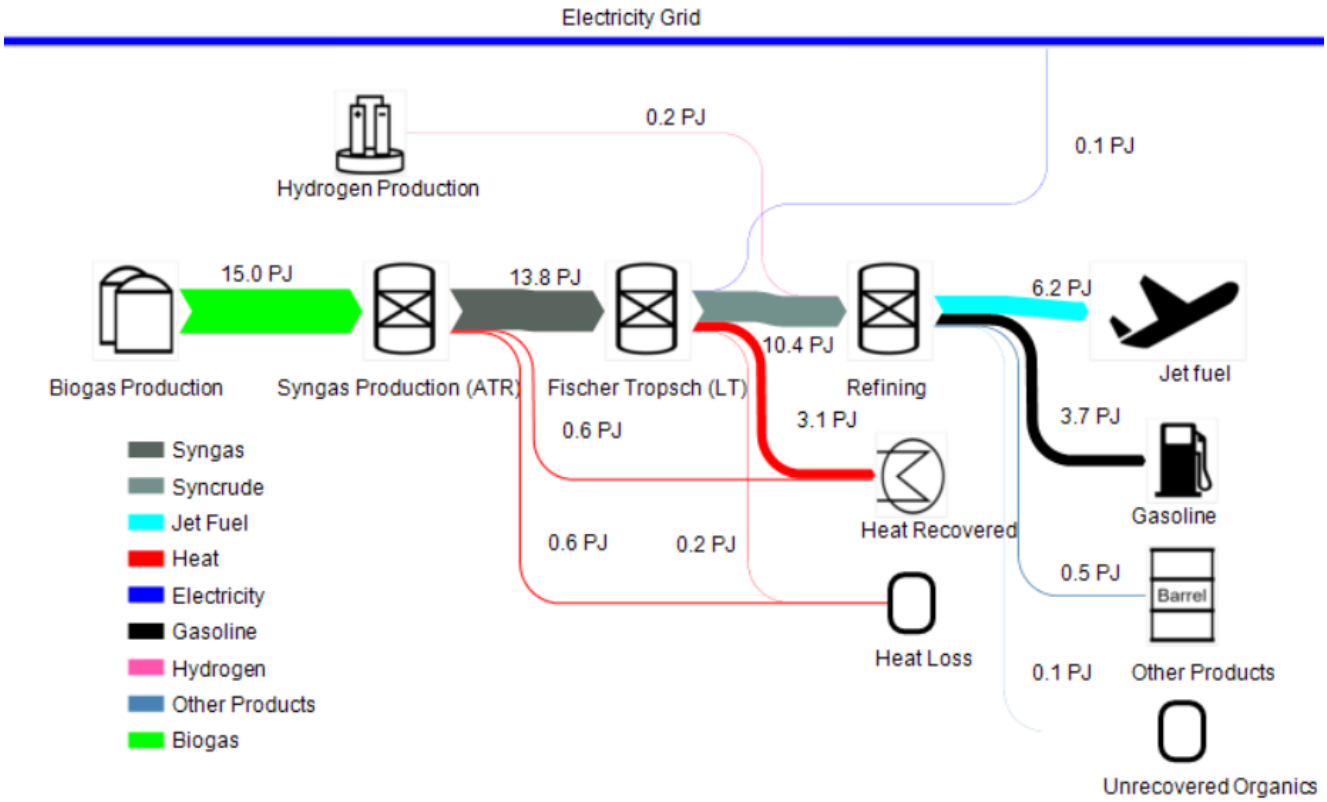

FIGURE F.3: The Sankey diagram of decentral Fe-LTFT based GTL plants.

Appendix G

Syncrude Composition

Compound	Fe-HTFT	Fe-LTFT	Co-LTFT
Gaseous product (C_1-C_4)			
Methane	12.7	4.3	5.6
Ethylene	5.6	1.0	0.1
Ethane	4.5	1.0	1.0
C_3-C_4 olefins	21.2	6.0	3.4
C_3-C_4 paraffins	3.0	1.8	1.8
Naphta (C_5-C_{10})			
Olefins	25.8	7.7	7.8
Paraffins	4.3	3.3	12.0
Aromatics	1.7	0	0
Oxygenates	1.6	1.3	0.2
Distillate (C_{11}-C_{22})			
Olefins	4.8	5.7	1.1
Paraffins	0.9	13.5	20.8
Aromatics	0.8	0	0
Oxygenates	0.5	0.3	0
Residuel wax (C_{22+})			
Olefins	1.6	0.7	0
Paraffins	0.4	49.2	44.6
Aromatics	0.7	0	0
Oxygenates	0.2	0	0
Aqueous product			
Alcohols	4.5	3.9	1.4
Carbonyls	3.9	0	0
Carboxylic acids	1.3	0.3	0.2

TABLE G.1: Generic FT syncrude compositions on a %mass basis, excluding inert gases and water gas shift products (H_2O, CO, CO_2 and H_2). A zero may indicate a very low value, and not necesarily a total absence (de Klerk 2011*b*).

Appendix H

Overview of the Funish District Heating Grids

District Heating Area	Yearly Heat Production [GJ]
Assens District Heating	360,000
Bogense District Heating	141,400
Davinde District Heatin	10,600
Ejby District Heating	64,800
Ferritslev District Heating	n.D.
Faaborg District Heating	205,200
Gelsted District Heating	n.D.
Glamsbjerg District Heating	108,000
Kerteminde District Heating	n.D.
Haarby District Heating	81,533
Kværndrup District Heating	17,598
Lohals District Heating	35,642
Marstal District Heating	160,608
Nyborg District Heating	754,718
Nørre Broby District Heating	35,280
Nørre-Aaby District Heating	93,600
Odense District Heating	8,300,000
Ringe District Heating	237,390
Rudkøbing District Heating	n.D.
Skårup District Heating	44,416
Stenstrup District Heating	48,096
St. Rise/Dunkær District Heating	n.D.
Svendborg District Heating	658,800
Sydlangeland District Heating	n.D.
Tommerup District Heating	45,000
Tullebølle District Heating	n.D.
TVIS District Heating	442,800
Vissenbjerg District Heating	72,397
Ærøskøbing District Heating	n.D.

TABLE H.1: The Funish district heating areas and their yearly heat demand (EMD International A/S 2014).

Appendix I

Odense DH Transmission Lines

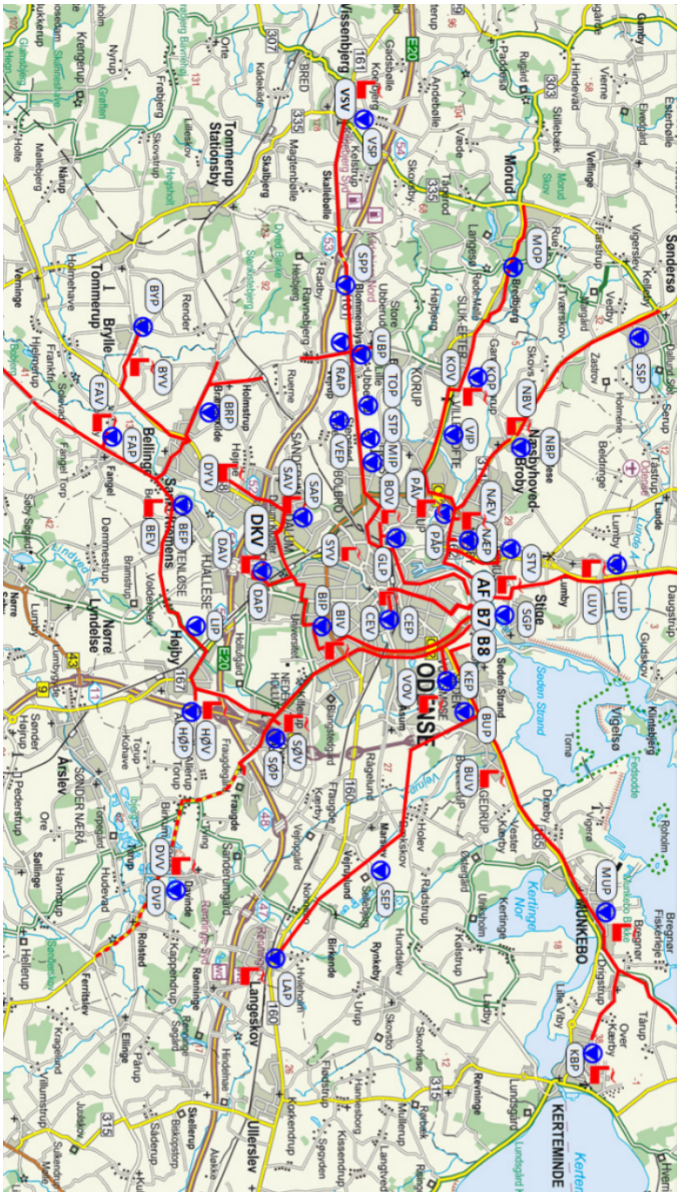

FIGURE I.1: A map of Odense and the transmission lines and pump stations of the DH grid. Rotated 90 degrees right. Source: (Fjernvarme Fyn 2018)

Appendix J

Funish Gas Grid

FIGURE J.1: A map of Funen and the transmission lines of the natural gas grid. Source: (Center 2018)

Appendix K

Excel Model Values

Energy Types	Separation (1 biogas input)									
	Water Scrubber		Chemical Scrubber		Organic Physical Scrubber		Membrane Separation		PSA	
	In	Out	In	Out	In	Out	In	Out	In	Out
Heat			0.11	0.10	0.07	0.00		0.02		0.03
Electricity	0.05		0.02		0.04		0.03		0.04	
Methane (CH4)		0.97		0.98		0.97		0.97		0.97
Hydrogen (H2)										
Biogas	**1.00**		**1.00**		**1.00**		**1.00**		**1.00**	
Unrecoved Organics		0.03		0.03		0.03		0.03		0.03
Syngas										
Syncrude										
Jetfuel										
Gasoline										
Other Products										
Methanol										
Olefins										
Heat Losses		0.05		0.02		0.11		0.01		0.01

TABLE K.1: An overview of the relative input and output values of all of the reviewed technologies. Part 1/5.

Energy Types	Methanation (1 biogas input)				Syngas Production (1 biomethane input)					
	Biological		Chemical		Steam Reforming		ATR		Partial Oxidation	
	In	Out	In	Out	In	Out	In	Out	In	Out
Heat		0.14		0.15		0.04		0.04		0.04
Electricity	0.17		0.01							
Methane (CH4)		1.68		1.68	**1.00**		**1.00**		**1.00**	
Hydrogen (H2)	0.82		0.82							
Biogas	**1.00**		**1.00**							
Unrecoved Organics										
Syngas						0.92		0.92		0.92
Syncrude										
Jetfuel										
Gasoline										
Other Products										
Methanol										
Olefins										
Heat Losses		0.17		0.01		0.04		0.04		0.04

TABLE K.2: An overview of the relative input and output values of all of the reviewed technologies. Part 2/5.

Energy Types	Fischer-Tropsch (1 syngas input)						Methanol Synthesis (1 syngas input)		Ethylene (1 methane input)	
	Fe-LTFT		Fe-HTFT		Co-LTFT		Syngas → Methanol		Oxidative Coupling of Methane	
	In	Out	In	Out	In	Out	In	Out		
Heat		0.23		0.23		0.23		0.21		0.16
Electricity		0.01		0.01		0.01				
Methane (CH4)									**1.00**	
Hydrogen (H2)										
Biogas										
Unrecoved Organics								0.06		
Syngas	**1.00**		**1.00**		**1.00**		**1.00**			
Syncrude		0.75		0.75		0.75				
Jetfuel										
Gasoline										
Other Products										
Methanol								0.72		
Olefins										0.83
Heat Losses		0.01		0.01		0.01		0.01		0.01

TABLE K.3: An overview of the relative input and output values of all of the reviewed technologies. Part 3/5.

Energy Types	FT Refining (1 syncrude input)					
	Fe-LTFT refining		Fe-HTFT refining		Co-LTFT refining	
	In	Out	In	Out	In	Out
Heat						
Electricity						
Methane (CH4)						
Hydrogen (H2)	0.02		0.00		0.02	
Biogas						
Unrecoved Organics		0.01		0.02		0.003
Syngas						
Syncrude	**1.00**		**1.00**		**1.00**	
Jetfuel		0.60		0.53		0.65
Gasoline		0.36		0.31		0.33
Other Products		0.04		0.14		0.04
Methanol						
Olefins						
Heat Losses		0.00		0.00		0.00

TABLE K.4: An overview of the relative input and output values of all of the reviewed technologies. Part 4/5.

Energy Types	Methanol Refining (1 methanol or 1 olefins input)				Electrolysis	
	Methanol → Olefins (MTO)		Olefin Refining (MOGD)		Alkaline EC	
	In	Out	In	Out	In	Out
Heat		0.05		0.03		0.14
Electricity					**1.00**	
Methane (CH4)						
Hydrogen (H2)			0.04			0.64
Biogas						
Unrecoved Organics						
Syngas						
Syncrude						
Jetfuel				0.49		
Gasoline				0.16		
Other Products		0.08		0.36		
Methanol	**1.00**					
Olefins		0.86	**1.00**			
Heat Losses		0.0		0.0		0.22

TABLE K.5: An overview of the relative input and output values of all of the reviewed technologies. Part 5/5.